UNIVERSITY OF
LIVERPOOL

Through Water Electromagnetic Communications

Thesis submitted in accordance with the requirements of the University of Liverpool for the degree of

Doctor of Philosophy

by

Apostolos Goudevenos

Department of Electrical Engineering and Electronics

The University of Liverpool

August 2008

ABSTRACT

Underwater communications at high frequencies have a wide variety of applications including diving, military equipment, oil and gas exploration in offshore fields as well as oceanographic mapping. Wireless communications are much more practical than hardwire communications due to the nature of the ocean environment. Currently the most commonly applied method for underwater communications is acoustic communications but have some serious disadvantages. These include low data rate, shadowing and reflections. Optical fibre communications have been offered as a viable alternative but their use is limited to small distances.

Currently the use of electromagnetic communications in the ocean environment is restricted due to high attenuation. The current study aims to demonstrate that with improved antenna design suitable for generating sub-sea electromagnetic waves for the frequency range 1 to 100MHz electromagnetic propagation suitable for underwater communications can occur. The new design consists of a two parallel rod antenna immersed in tap water, inside a PVC barrel, that has lower conductivity than salt water and operates by electrically exciting the water molecules to emit dipole radiation. A theoretical model of the antenna impedance was also formulated that matched the actual impedance scans. The distance scans performed in the laboratory tank showed that the barrel antenna produces up to 40dB increase in emitted signal when compared with a coated double loop antenna placed directly in the seawater suitable for video signal propagation for up to 25 frames per second.

In order to minimise the size of the barrel antenna and make it more compact and practical for different applications different designs are also considered in this study with a coaxial antenna immersed in different liquids in order to improve dipole excitation.

ACKNOWLEDGEMENTS

This study could not have been performed without the help of the following people, who I would like to express my gratitude.

First of all, my supervisor Professor James Lucas for his invaluable help, guidance and patience throughout the study.

Professor Jeremy Smith for his help throughout the study.

The members of the RF and Microwave group of the University of Liverpool, especially Dr C. K Yip for his collaboration on the project. I would also like to thank Dr P. Mavromatidis and Dr M. Houghton for their help in various aspect of this study.

I would also like to thank my friends past and present for their support.

Last but not least I would like to thank my family for their financial and emotional support during this study

Apostolos Goudevenos

August 2008

Contents

Contents

Contents

CHAPTER 1 INTRODUCTION

1.1 Project Overview

The development of radio technology as well as the appearance of submarines during the world wars first gave rise to the need for a viable underwater wireless communication system. Since then underwater communications have been widely employed in offshore gas and oil exploration, diving and oceanographic mapping among other applications. Hardwire communications cannot be considered as a practical option since the nature of the environment leads to great difficulties and expenses in their design and implementation. Acoustic communications are the preferred option currently since they are inexpensive and are quite easily implemented. Despite their wide use sound is easily affected by the severe ocean environment, besides they also suffer from dark zones behind large objects at the ocean bed and do not provide a high data rate. The use of underwater optical communications is often employed to provide a higher data rate but they also suffer from shallow zones.

Electromagnetic waves provide high data rates in high frequencies and do not have any problems with dark zones. Their main disadvantage is that electromagnetic waves (EM) suffer from large attenuation that increases with distance. EM propagation in water is much different to air since it has high permittivity and electrical conductivity leading to high plane wave attenuation which in turn increases with frequency. Attenuation losses in seawater are much higher than fresh water due to the much lower conductivity in the latter. There is also a large refraction angle at the air to water interface. This leads to losses due to reflection once the signal enters the water.

Despite these limitations underwater EM communications offer a large range of advantages over the other currently applied methods. EM waves are not affected by multipath propagation, they are immune to acoustic noise and they do not suffer from shadow zones or

low visibility due to marine fouling which limit the application of acoustic and optical communication systems. The system if applied at high frequencies requires small antennas so compact portable units can be used. There will be a higher propagation speed which is more efficient and will provide a higher data rate than other methods.

There is a wide range of applications by utilising this technology that include

- **Military Applications**: Communication between submarines and offshore stations
- **Diving**: Diver to diver communications including speech and texting
- **Autonomous Unmanned Vehicles (AUV)**: Communication and real time control of AUV using high data rates between AUV to unmanned service vehicles.
- **Underwater Sensors**: Data collection and transmission to the shore.
- **Oil and Gas Industry**: Location of underwater oil deposits as well as fault detection in the offshore apparatus.
- **Oceanographic mapping**: Underwater cameras will provide high quality images.
- **Environmental Applications**: Location of oil leaks or changes in the underwater environment
- **Docking systems**
- **Subsea Networks**
- **Subsea and Underwater Navigation**

The aims and objectives of the project are outlined in section 1.2. The main aim is to design and test different antennas in order to identify the most suitable for underwater propagation at different frequencies. The results obtained will lead to a theoretical explanation of transmission in the seawater.

1.2 Project Aims and Objectives

The main aims of the project are outlined below

- Design and construct different types of antennae in order to determine the most suitable for the application.
- Apply different frequencies, around the lower MHz region, to observe the most suitable frequency for transmission.
- Investigate and explain the behaviour of EM waves in the antenna near and far field in the water.
- Design and construct a transmitter and receiver circuit, which are not affected by noise and operate in the oceanic environment.
- Perform trials in the laboratory tank as well as in remote locations.
- Create a theoretical model for the transmission of EM waves underwater.
- The communication system should be able to transmit and receive different types of data like sound, video and test.

At the end of the study the objectives that should be reached include

- Improvement of the antenna performance: The signal strength should be stronger through improved antenna design and impedance matching.
- The most suitable frequency range for transmission should be identified: EM waves suffer from attenuation in the water so the frequency range should be adjusted in order to minimise the losses.
- Improvement of the receiver and the transmitter design: Apart from constructing suitable communication elements for lab trials, special consideration must be taken for their applications in remote environment
- Antenna behaviour in the water: This will demonstrate theoretically the antenna impedance measured when the antenna is surrounded by water. This will allow improved antenna design.

- Explanation of underwater EM transmission: This thesis will demonstrate that apart from conventional radiation, there is also an element of dipole radiation that contributes to transmission.

1.3 Thesis Structure

Chapter 1 deals with the rationale behind this project. It shows the benefits of using EM waves instead of optical or acoustic systems in the case of the latter the currently most commonly applied method. Some of the applications of this method are also discussed. The next part deals with the objectives set out at the beginning of this study and the deliverables that were achieved by the end.

Chapter 2 deals with the communication principles that are relevant in this project. The general aspects of a desired communication system are outlined such as the requirements for a suitable receiver and transmitter as well as the considerations for each specific medium with noise taken into account. The currently applied methods for underwater communications are also discussed with their respective advantages and limitations. Finally a literature review is present of past trials of underwater EM transmission. In general the last part is rather limited since the general consensus for many years has been that application of high frequency EM waves is not practicable in the marine environment due to high attenuation. Besides this technology was mainly restricted to military applications where there are obvious restrictions in the related literature.

In chapter 3 the general theory of EM waves is considered. This includes the propagation of EM waves in free space, in dielectrics as well as lossy media. There the complex permittivity is discussed as well as the propagation coefficient in different media. There is also a description of Debye's model which is very important in the formulation of the theoretical model in the following chapters. The dielectric properties of water are also shown as well as an observation in the nature of permittivity measurements in water as well as some of the models suggested. Then there is an introduction into transmission lines, waveguides and

resonant cavity. The equations shown there are used for the water antenna design in chapter 5. There is also a significant amount of antenna theory. The last part deals with impedance matching using transformers and lumped components.

In the methodology section there is a general description of antenna design and construction. Then the two transmitter systems are described. The first one comprises of a PIC chip whose action is controlled by an interface on a laboratory computer through optical fibres that allows placement inside the laboratory tank. The PIC chip then directs a direct digital synthesiser (DDS) that provides a sine wave output. This transmitter is used for the 1 to 10MHz range. For higher frequencies a crystal oscillator based transmitter was used. This system included four different oscillators controlled by a rotary switch. The output is then turned into a sine wave by applying a low pass RF filter. The main disadvantage of this design despite the strong output is that the frequency change needs to be performed manually and so is more time consuming. The latter part deals with the setup for the laboratory trials like the placement of the electronics and the antenna inside a specially designed box in order to insert the whole apparatus in the laboratory tank. Then there is a description of the matching applied in order to improve the power transfer. The last part describes the coaxial antenna used in chapter 7.

Chapter 5 is the beginning of the result section. There is an analysis of the antenna used with the equivalent circuit shown. The next part deals with the theoretical aspects associated with the losses when the antenna comes into contact with saltwater. All the equations shown in these sections are used to form a theoretical model of the antenna in different types of water. Then the results from the theoretical model are compared to the actual impedance measurements. There is also a presentation of the theoretical values for the antenna power and transmission coefficients. The final part deals with the effect of the bucket on transmission and the electric field of the antenna.

Chapter 6 deals with the propagation of the signal inside the laboratory tank. There is a short introduction that examines the theoretical aspects of the signal transmission with the tank being filled with tap and salt water. Then the distance scans are shown with the double loop

antenna as well as the two rod antenna act as transmitter antenna with different receivers. Then matching is performed between the transmitter and the antenna in order to improve the performance of the antenna. The distance scans are shown as well as the theoretical measurement of the effect of matching. The last part deals with the focusing effect that the barrel provides that enhances transmission.

In chapter 7 a coaxial antenna is tested by using a similar model to the one shown in chapter 5. The actual impedance measurements are performed and then compared to those provided by the impedance model. In this case different liquids were tested in addition to tap and distilled water with very low conductivity in order to observe whether an improved match is provided compared to salt and tap water. This is required in this case since the effective area of the liquid is restricted since the cylindrical tube that surrounds the antenna is limited compared to the bucket for the two rod antenna. This section also includes theoretical measurements of power transfer as well as the transmission coefficients for the different liquids.

The last chapter provides the conclusions from this study on antenna design for underwater transmission as well as further research required to formulate these ideas.

The appendix shows the MATLAB codes used in order to provide the models.

CHAPTER 2 COMMUNICATION SYSTEMS

2.1 Introduction

Communications play a very important role in everyday life so there is a general great deal of research into rapidly improving its demands now as well as the foreseeable future. Most modern communication systems require radio frequency and microwave signals for wireless transmission of information. Typically these systems include various others components such as oscillators, mixers, filters and amplifiers in order to produce and process the signal. The main challenge facing modern communication systems is the transmission of vast amounts of information over large distances without losses associated with noise interference.

A typical communication system [1], although very general, is shown below

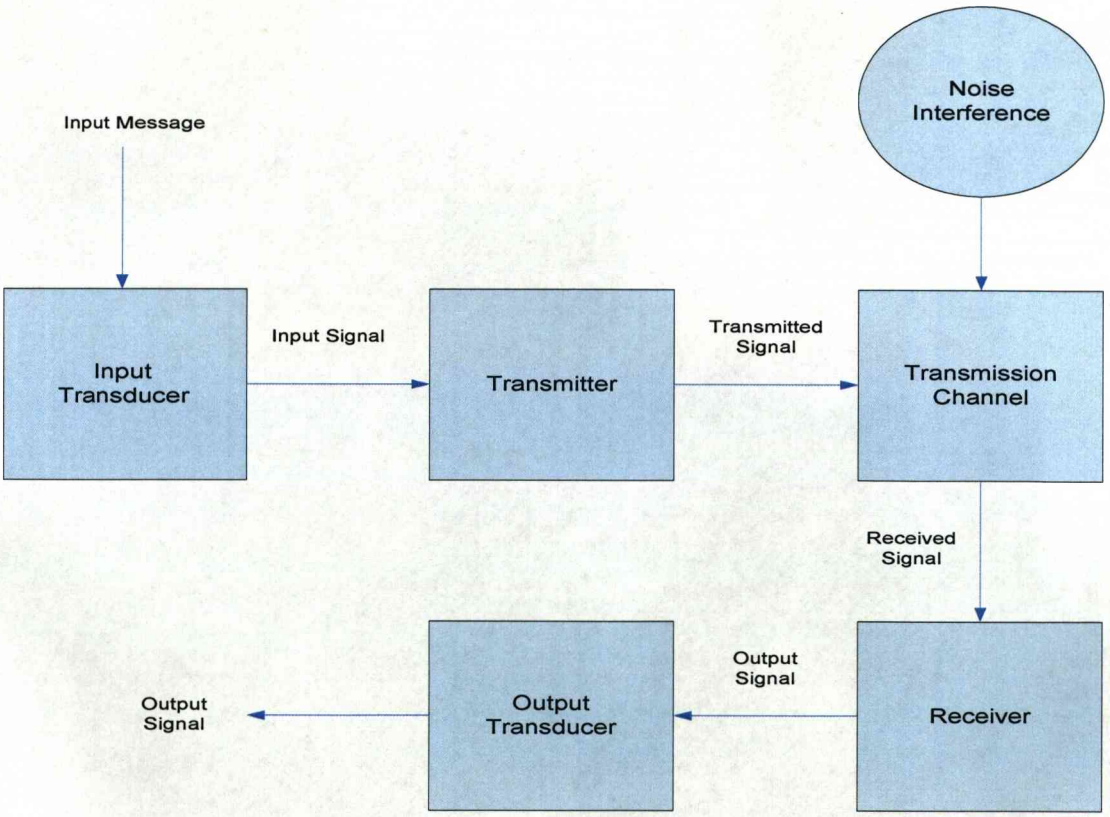

Figure 2.1 Typical communication system

The origin of the message is the source. If the data that needs to be sent is nonelectrical it is then converted by the input transducer into the message signal that is essentially an electrical waveform. The source so acts as an interface between the outside world and the communication system and so provides the message signal that is processed by the transmitter. The four main classes of input devices are audio, video and data input devices or sensors.

The next stage in the communication system is the modification of the received signal by the transmitter making it much more suitable for transmission. The source of the signal is the frequency synthesiser and further amplification takes place before the transmission. The way in which the transformation is performed depends on the type of the information source, the nature of the transmission medium and the type of the communication system. The transmitter is modified in such a way in order for transmission to occur in the authorised frequency band and at the permitted power level, in many cases to minimise the cost as well as the requirement of the minimum processes. These include source coding such as lower pass filtering, multiplexing, analogue to digital conversion, then there is also encryption, channel coding, carrier or spread spectrum modulation or radiation.

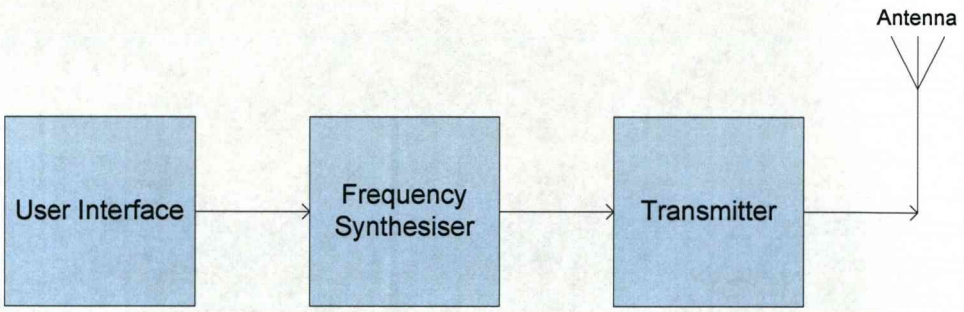

Figure 2.2 Transmitter Block diagram

The transmitter output reaches the receiver after it passes through the transmission medium. There are two types of transmission media, termed closed and open media. The former allows communications between a transmitter and a specifically connected receiver. These include twisted wire pairs, coaxial cable, optical fibre and the metallic waveguide. Open media

provide broadcast as well as mobility in telecommunications [2]. This category includes all types of electromagnetic wave propagation. The transmission medium will be dealt in more detail below.

Once the signal passes through the transmission medium it is picked up by an antenna and is then passed to the receiver that is the destination where the signal is processed and delivered to the output transducer. The signal that arrives at the receiver has been processed twice, once intentionally by the transmitter while it has also been corrupted by noise and dispersion in the transmission medium. The receiver reverses the processing performed by the transmitter by performing the following steps in reverse steps compared to the transmitter, these steps include radio reception, spread spectrum demodulation in order to remove carrier spreading as well as carrier demodulation to bring the signal back to baseband frequencies. Clock extraction and synchronisation occur in order to use the same timing intervals for operations at transmitter and receiver. Then there is also channel decoding, decryption and source decoding to recover the original message. The main requirements for the receiver are that it should match the dynamic range of the received signal at the receiver input to the dynamic range of the signal processor. The problems most commonly associated with this function are interfering signals that can either be generated externally or internally conducted and electromagnetic coupling.

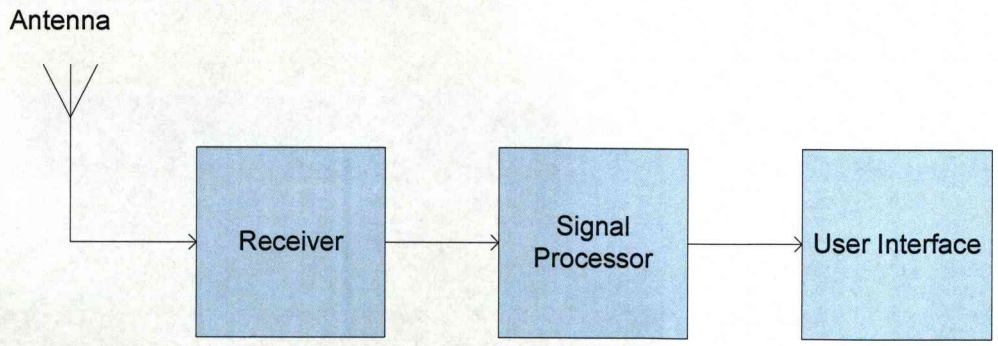

Figure 2.3 Receiver Block Diagram

2.2 Transmission Medium

Apart from providing the link between transmitter and receiver, the transmission medium partly acts to attenuate the signal and distort its waveform. Ideally, the communication channel should lead to safe passage of the signal from source to destination without any external or internal interference for all signal frequencies. Besides if the signal would reach the receiver without any attenuation there would be no need for amplification. This is not the case since the signal always suffers some degree of attenuation. The bigger the length of the transmission medium, the higher the amount of signal attenuation and waveform distortion occur due to different amounts of attenuation and phase shift suffered by different frequency components. Distortion does not only occur by the channel, but it is also contaminated along the propagation path by noise that consists of random and unpredictable signals inflicted by internal or external factors. The latter include noise from nearby channels or equipment in close range. A typical example of internal noise is the one that arises from the thermal motion of electrons in conductors.

One of the most frequently used transmission medium are the twisted wire pairs that are commonly used in digital communication channels as well as local area network connections in modern communications. There are many limitations to the use of twisted wire pairs since the attenuation suffered by the signal is frequency dependent and in order to achieve the required bandwidth some form of frequency sensitive compensating network usually in the form of an equaliser is required. Another major limiting factor is crosstalk between wires. This is caused by magnetic fields which in turn are formed by currents in nearby conductors, which in turn induce currents in other wire pairs in the same cable. Crosstalk can also be induced due to capacitance in two different conductors.

Another commonly used medium is the coaxial cable. Structurally the outer conductor has the shape of a tube and is covered by plastic, with another conductor placed into the centre of it that is kept into place by polyethylene discs [3].

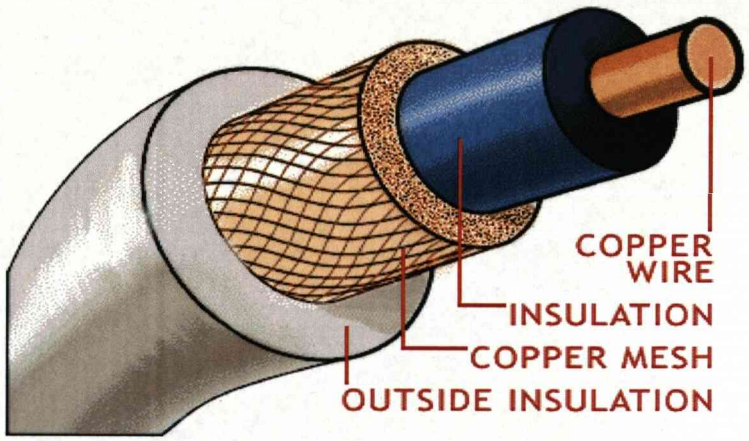

Figure 2.4 Coaxial Cable

If the outer conductor is earthed it leads to a decrease in interference, radiation loss and crosstalk, since the electric and magnetic fields are almost constrained within the cable, compared to twisted pair cables as well as providing a larger bandwidth. On the other hand the attenuation for such a cable increases with the square root of frequency and equalisation is also required. Their most common applications include high bandwidth analogue systems, frequency-division multiplexing (FDM) telephone as well as data terminal equipment interconnection with buildings.

The development of the optical fibre has led to a decrease in the use of the coaxial cable for long distance links. Essentially the optical fibre is a dielectric waveguide consisting of silica glass and the signals inside it are carried as light waves. Its main advantages include transmission frequencies of up to 200GHz while more recent designs show less attenuation and since the signal is optical there is no interference even in extremely noisy environments. Besides there is no occurrence of crosstalk while the fibre acts as an electrical insulator and so acts as a barrier between the transmitter and the receiver. It is also a very cost-efficient means of communication since the fibre is cheap and abundant raw material as well as being small in diameter. Finally, since the fibre can act as an electrical insulator it does not conduct electrical energy. Its main drawbacks are the special connections required between the optical source and the fibre as well as between fibres to decrease the losses. Another major disadvantage is that any technical problems are hard to locate and fix.

2.3 Modulation

In order for a signal to contain different types of information an element of the signal must be changed relating to the information that will be transmitted, this is termed modulation. It improves the efficiency of the transmission line by imposing message information on the carrier frequency most suitable for that particular transmission channel. This also helps avoiding many hardware limitations as well as decreasing the size of the antennas required. The more efficient exploitation of the transmission channel can also be achieved by using more than one user in the same medium at the same time. It also allows the use of higher bandwidths. Besides, some types of modulation decrease noise and interference by making the transmission bandwidth much greater than the signal bandwidth. This permits an exchange of increased bandwidth for decreased signal strength.

There are three basic types of modulation. A general expression for a sinusoidal signal is

$$v_c(t) = A_c \cos(2\pi f_c t + \varphi) \quad (2.1)$$

There are three parameters that are varied in modulation. If the amplitude A_c is varied, this leads to amplitude modulation (AM), by varying the frequency f_c or phase φ we get frequency (FM) and phase (PM) modulation respectively. Due to the similarities between the last two types of modulation they are usually termed as angle modulation In the case of applying a digital signal, modulation will cause the varying parameter to shift in discrete steps.

2.4 Demodulation

The demodulation process requires the receiver to selectively pick up the correct signal and remove the modulation to get the original baseband signal back. Once the signal has been received amplification is performed to increase the level strength so the demodulator circuit

can operate properly. The main type of receiver used is the superheterodyne whose principle of operation is the translation of the carrier signal, regardless of the value, to an intermediate frequency where the majority of the required selectivity and amplification take place.

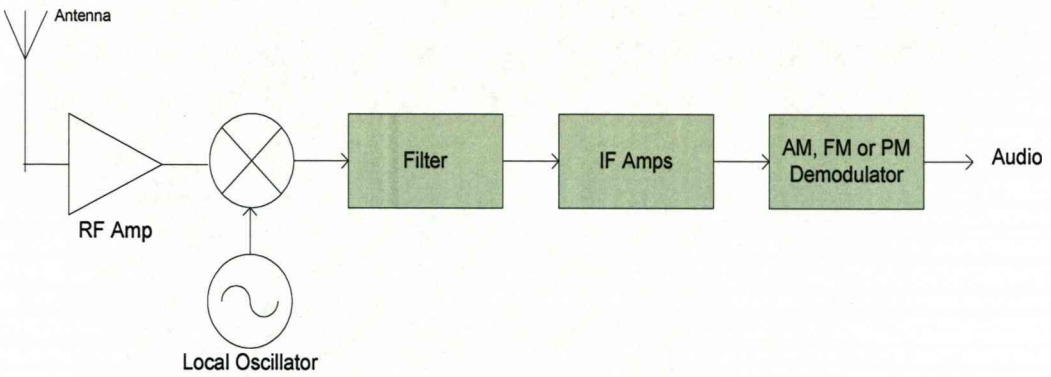

Figure 2. 5 Superheterodyne Receiver

Conversion of the RF signal from one part of the spectrum to another is accomplished by combining the RF signal with a locally generated signal in a non linear device. This requires a local oscillator and a non-linear device in the circuit.

2.5 Noise

Noise can be broadly described as the effect of any unwanted signal that tends to interfere with the desired signal. Noise occurs in every communication system and all signals arriving at the receiver have a certain amount of noise. Noise causes severe limitations in the lower power regions and it is of critical importance that most of it is removed from the system.

The ratio of the signal power to the noise power at any point in a transmission medium is the signal to noise ratio (SNR) and defined as

$$SNR = {}^{S_p}/_{N_p} \quad (2.2)$$

where S_p= average signal power

N_p=average signal power

The SNR can also be defined in dB

$$\text{SNR}=10\log\left[{}^{S_p}/_{N_p}\right] \quad (2.3)$$

The minimum acceptable level for SNR is around 10dB [4], although for many systems this requirement can only be met with sophisticated and expensive arrangements at the receiver.

As mentioned above noise is present in every communication system and so the lowest level of the SNR will be seen at the receiver. In order to determine the amount of noise in the system a quantitative measure is used, termed the noise factor F. The latter is defined as the ratio of the SNR value at the input over the SNR value at the output

$$F = \frac{SNR_{in}}{SNR_{out}} \quad (2.4)$$

Ideally the noise factor should have a value close to unity although this is not always the case

2.5.1 Sources of noise

Noise in each communication system can be subdivided into random and artificial noise. The latter can be attributed to electronic sparks or crosstalk between different communication channels. Random noise on the other hand can be both external to the system caused by

natural phenomena like lightning discharge that the designer has no control over, it can also be internal to the system like thermal and active device noise

2.5.2 Thermal Noise

Thermal or Johnson noise arises from the random thermal motion of electrons in any resistive material [5]. It is independent of the nature of any resistance as well as of any applied voltage.

The value of the root mean square voltage (V_T) of thermal noise generated in an impedance Z over a frequency interval Δf [5] is given by

$$\bar{V}_T^2 = 4KTR\Delta f \quad (2.5)$$

where R = the resistive component of the impedance

T = Absolute temperature in Kelvins

K = Boltzmann's constant=1.38×10^{-23} Joules/Kelvin

As it can be seen from the above equation the real part of the impedance is frequency dependent, leading to thermal noise being frequency dependent.

2.5.3 Active-Device Noise

Apart from the resistors that give rise to thermal noise, other devices like diodes and transistors give rise to another type of random noise termed active device noise. The two main types are flicker and shot noise. The former usually occurs in the lower frequency regions [4]. Its main characteristic is that the power density follows a $1/f^{\alpha}$ curve, where the value of α is close to unity.

Shot noise on the other hand occurs when electrons pass through a barrier like the semiconductor pn junction or the cathode of a vacuum tube. This leads to random emission due to thermal motion. The noise barrier can be represented by applying a current source and a dynamic resistance in parallel.

2.6 Underwater Communications

This part of the report deals with different types of communication systems employed for undersea communications. These include acoustic, optical and electromagnetic (EM) communication systems.

2.6.1 Acoustic Communications

Acoustic communication systems have been shown to be the most versatile and are currently the most widely used technique for underwater communications. Their basic principle of operation is by applying a diaphragm submerged in water that vibrates by electrical means leading to mechanical energy of motion. By placing another diaphragm in the water close to the first one it will collect the acoustic energy leading to vibrations that can be recorded by electrical means. The first diaphragm is referred to as the source or the transducer and the second as the receiver or hydrophone. In some cases only one diaphragm is used that acts as both transducer and receiver.

Despite their wide applications there are many limitations to the use of acoustic communications. As the acoustic wave propagates through water there is energy absorption, attenuation as well as scattering due to fish in the sea. The sound intensity also depends inversely to the square from the distance of the source. There is also sound reflection from various objects or the bottom of the seabed that will lead to larger recordings as well as

interference with the signal. Especially in shallow zones the effects of absorption and multipath propagation are exacerbated. Another parameter that affects transmission is the inhomogeneous nature of the ocean environment. An important factor is the temperature of the seawater, which under normal conditions changes at a fixed rate between different layers of the ocean. An increase in the temperature will lead to a higher sound velocity, while a decrease in temperature will have the opposite effect. Variations in the water density have a similar effect. Another limiting factor in the use of acoustic systems is the slow speed of acoustic propagation in water, around 1500m/sec that can lead to a slow data rate. Finally, behind large objects shadow zones are created through which sound cannot penetrate.

2.6.2 Optical Communications

Fibre-optic systems are used in a wide variety of applications and are steadily replacing cable connections. Their main difference is that fibre-optics in general transmit information using light pulses instead of electronics. The data arriving in the transmitter is translated into coded light pulses and picked up by the receiver through optics [6].

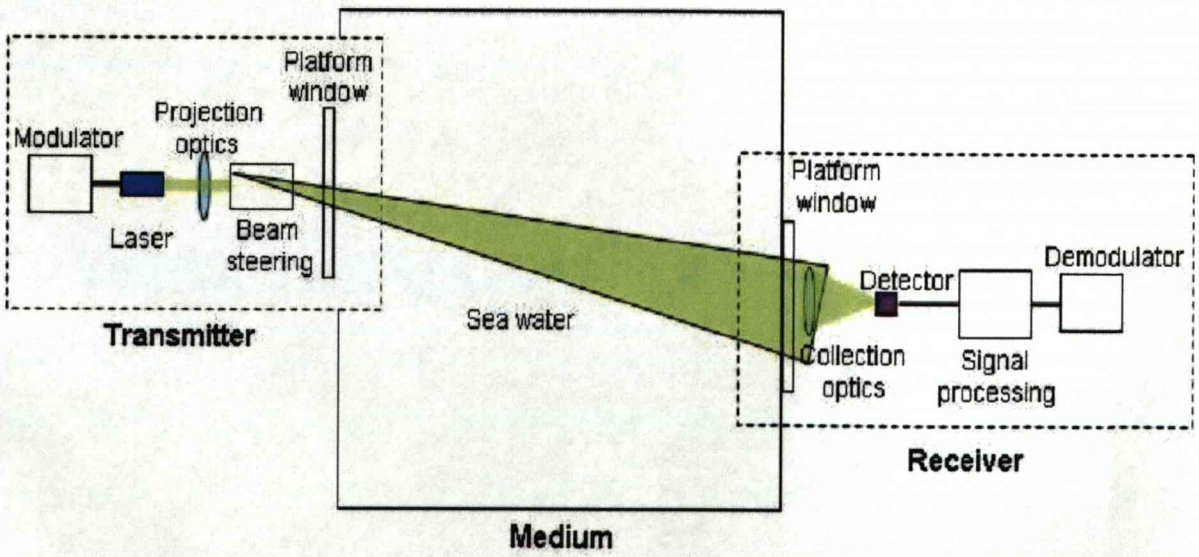

Figure 2.6 Typical Optical Underwater System

Despite having shorter ranges compared to acoustic systems due to increased attenuation of light in water they provide higher bandwidth, a higher data rate as well as covertness [6]. This has lead to them being a more effective means in underwater communications than sound especially in short range applications.

The main disadvantage of optical systems is that they also suffer from shadow zones since light cannot penetrate through large objects. Although effective in short range applications, use in larger distances is restricted by backscatter and absorption. Another disadvantage is that the visibility of water in many cases is close to zero.

2.6.3 Electromagnetic Communications

Despite the many advantages of EM communications their use in underwater communications is restricted due to the large attenuation that EM waves suffer in water. In general propagation in sea water follows a similar pattern to propagation through a lossy medium. This section provides a literature review of the work performed in this area which is rather limited.

As mentioned above the primary use of underwater communications was for military applications mainly submarines. The main frequency region used is the ELF (3-300Hz), where waves are able to penetrate sea water with reasonable attenuation, about 0.3dB/m at 76Hz [7]. In fact this is believed to be one of the rare successful deployment of underwater EM communications as it allowed limited transmission of characters [8]. A major disadvantage is that the ELF communication channel can operate only in one direction due to the impractability of adding a transmitter to the submarine. Besides the ELF signal suffers attenuation until it reaches the receiver in the shore [9]. This has necessitated the use of very large antennas and the construction of large transmitting stations at a considerable cost. Due to this disadvantage the use of EM waves in the very low frequency (VLF) region and at higher frequencies was promoted [10].

Measurements at higher frequency regions, as used in this study, are scarce. Propagation in seawater at 7MHz [11] produced a transmission distance of 460m at a depth of 76m. King [12] used frequencies of 14 and 100MHz in a laboratory tank as well as in remote locations, similar to this study, and demonstrated rapid attenuation of the signal strength in the vicinity of the transmitter. A later theoretical attempt, based on these results, used a 1.8MHz frequency and concluded that underwater propagation was only possible when the antennae were placed at a depth of less than 0.5m and that propagation was partially through an air path as shown below. The maximum transmission path with air loss was 18.7m and by eliminating the water to air interface was 28m [13].

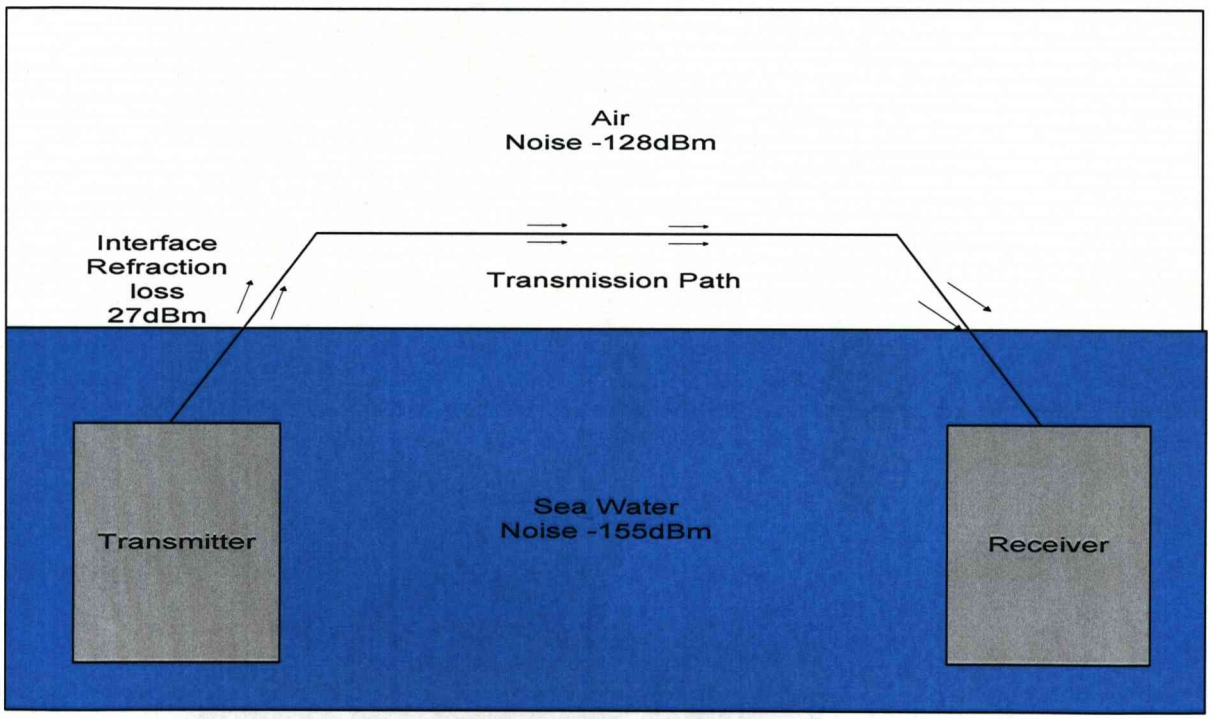

Figure2.7 Suggested Transmission Path

Earlier trials from Al-Shamma'a et al [14] have shown that signal propagation up to a distance of 85m is possible by using a different range of frequencies [14]. The signal attenuation was found to be 80dB over 85m. It was also shown that after that distance the signal attenuation decreases and all losses are comparable to diffraction losses.

Further trials from J.Lucas et al [15], apart from improving the current levels of signal strength also aim to create a clear theory of how transmission occurs in the underwater environment. The main accomplishment has been to be able to clearly demonstrate that by surrounding the antenna with tap water instead of leaving it directly exposed to salt water increases the signal strength and propagation distance. Besides it has been shown that an additional part of the radiation is caused by dipole excitation.

This thesis will try to build on the work of the previous research mentioned above in improving the signal strength in underwater communications and will also try to explain in more detail the underlying mechanism of signal transmission in the sea water.

CHAPTER 3 ELECTROMAGNETIC THEORY

3.1 Electromagnetic Waves

EM waves are formed when an electric and magnetic field are perpendicular to each other. Both fields oscillate at right angles to the direction of wave propagation while both fields oscillate at right angles to each other. The waves transfer energy and when there is neither electric nor magnetic field in the direction of propagation [16], they propagate in the transverse electromagnetic mode (TEM).

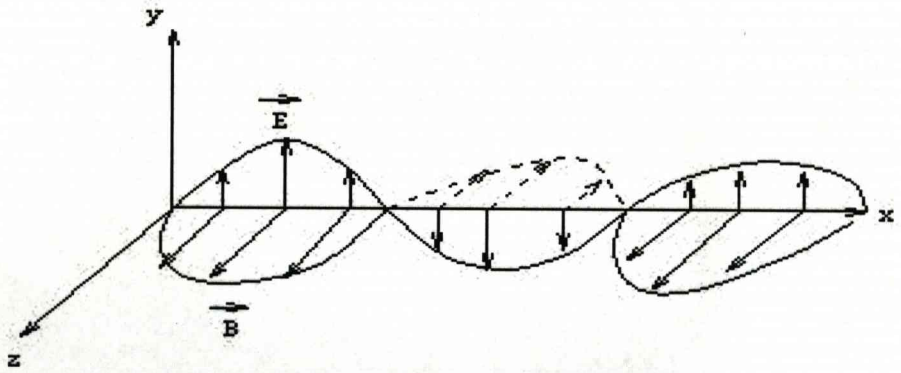

Figure 3.1 Electromagnetic Wave in Space

The electromagnetic spectrum is the distribution of EM radiation according to energy. Alternatively by using the wave equation

(3.1)

where c = speed of light = 3×10^8m/sec

f = frequency (Hz)

λ = wavelength (m)

EM waves can be arranged according to frequency and wavelength. As it can be derived the higher the frequency the shorter the wavelength, since the speed of propagation is always constant and equals the speed of light [17].

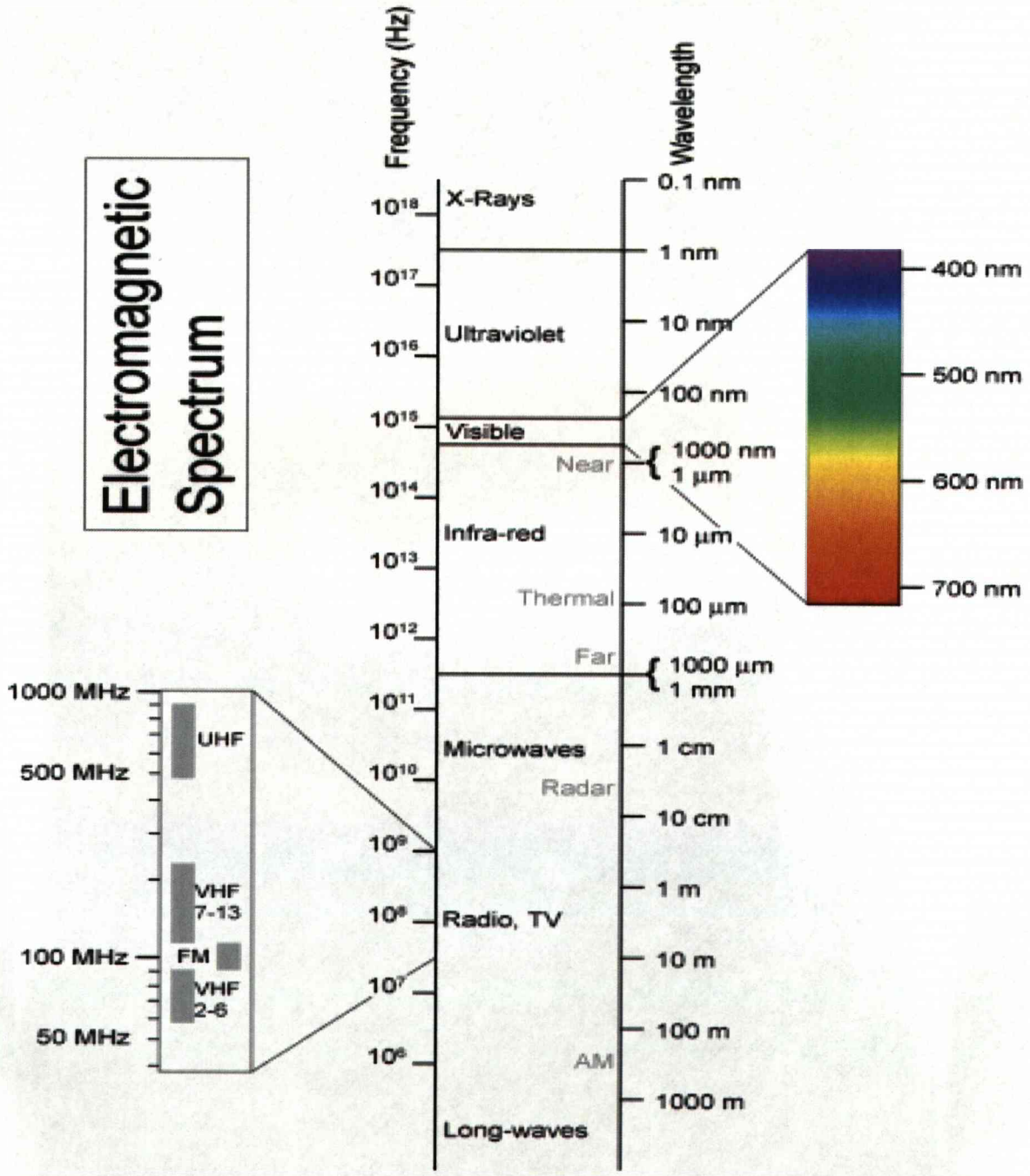

Figure 3.2 Electromagnetic Spectrum

3.2 Maxwell's laws

These laws present a unified EM theory and represent the fundamentals of electricity and magnetism. They consist of the laws of Ampere, Faraday and Gauss for magnetic and electric fields. These equations have been defined in both integral and differential forms as shown below. The former have line, surface and volume integrals while the differential equations involved, consist of divergence and curl and apply at a point.

- **Amperes law:** This law states that the magnetic field around a closed loop in space is proportional to the net current flowing through the loop

  Integral Form $\oint H \cdot dl = \int_s \left(J + \frac{dD}{dt}\right) \cdot ds = I_{TOTAL}$ (3.2)

  where H = Magnetic field (ampere per meter)

  l = Length of the vector (meter)

  J = Free Current Density (ampere per square meter)

  D = Electric Flux Density (coulomb per square meter)

  s = Vector element of surface area S (square meters)

  I = Net electrical current enclosed (ampere)

  Differential Form $\nabla \times H = J + \frac{dD}{dt}$ (3.3)

  This law is mainly used for the calculation of the magnetic field for simple geometries

- **Faradays Law:** The interpretation of this law is that any disruption in the magnetic field of a coil of wire will cause a voltage induction across the coil. The integral form of the law is shown below

Integral Form $\oint E \cdot dL = -\int_s \frac{dB}{dt} \cdot ds = V$ (3.4)

where E = Electric field (Volts per meter)

B = Magnetic Flux density (Tesla)

V = Volume enclosed by surface S (cubic meters)

Differential Form $\nabla \times E = -\frac{dB}{dt}$ (3.5)

- **Gauss Law for electric field:** This law states that the charge enclosed in any closed surface is equal to the integral of the flux density D.

Integral Form $\oint_s D \cdot ds = \int_v \rho \cdot dv = Q$ (3.6)

where ρ=free electric charge density (coulomb per cubic meter)

Q=the charge enclosed (Coulombs)

Differential Form $\nabla \cdot D = \rho$ (3.7)

- **Gauss Law for magnetic field:** The total magnetic flux exiting any closed surface is equal to zero.

Integral form $\oint_s B \cdot ds = 0$ (3.8)

Differential Form $\nabla \cdot \mathrm{B} = 0$ (3.9)

Some constitutive relations that arise

$$D = \varepsilon \cdot E \quad (3.10)$$

$$B = \mu \cdot H \quad (3.11)$$

$$J = \sigma \cdot E \quad (3.12)$$

where ε is the electrical permittivity of the material

μ is the magnetic permeability of the material

σ is the electrical conductivity of the material

3.3 Complex Permittivity

The dielectric constant or permittivity is a measure of the electrostatic line concentration in any material. It is defined as the ratio of the electrical energy stored in the material over the permittivity of free space, $\varepsilon_o = 8.8542 \times 10^{-12}$F/m.

The complex permittivity can be defined as

$$\varepsilon = \varepsilon' + j\varepsilon'' \quad (3.13)$$

Where ε is the complex permittivity

ε' is the real part of the complex permittivity

ε'' is the imaginary part of the complex permittivity.

The real part of the complex permittivity refers to the ability of the dielectric to store energy. The imaginary part is related to the losses of the material that arise mainly from the movement of free charge carriers, in this case electrons and ions, space charge polarization, and dipole orientation. Figure 3.3 shows the different absorption regions in different

frequencies. It must also be mentioned that absorption also depends on the nature of the material which will be dealt with more detail below [18]

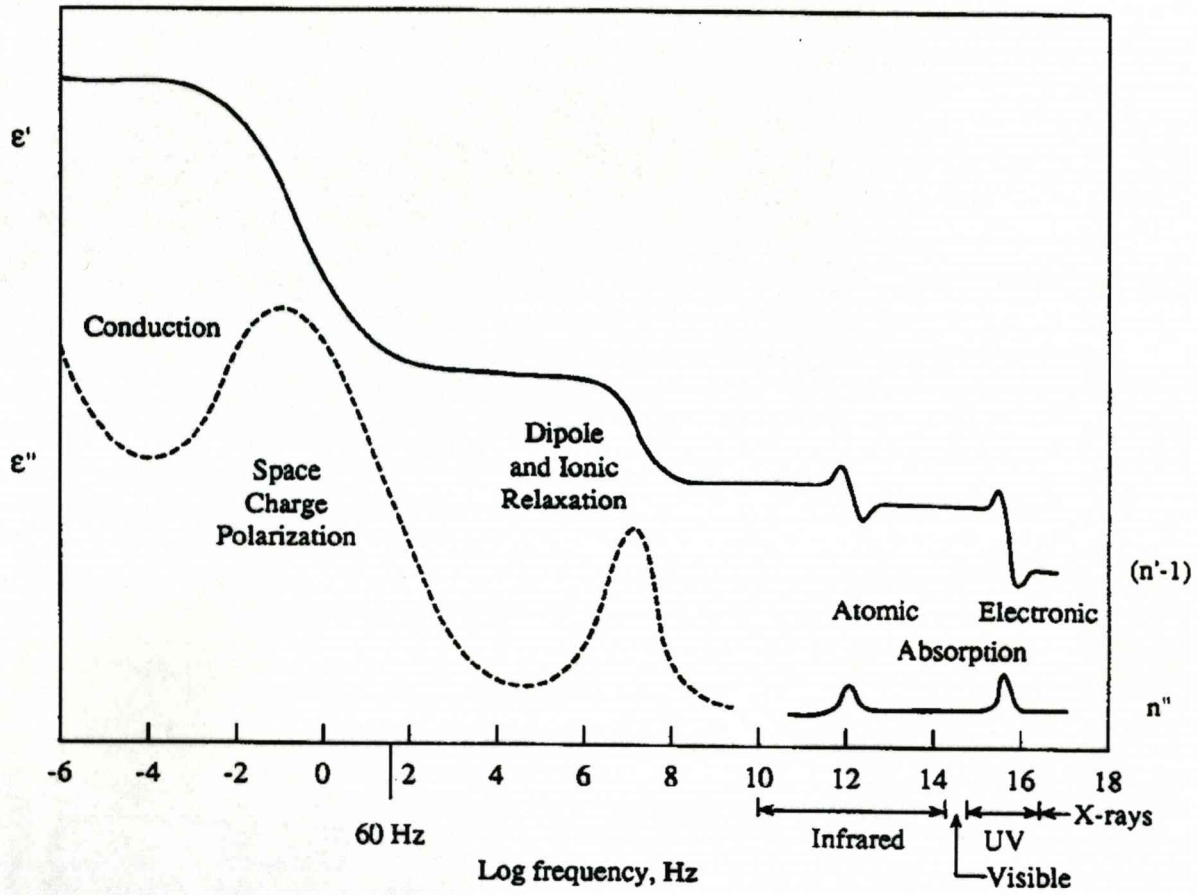

Figure 3.3 Different absorption regions

The dielectric loss behavior is described by the Debye equations described in this chapter.

3.4 Polarization

Placement of any dielectric material into an applied field, leads to charge displacement of the positive and negative ions against the force of atomic and molecular attractions. Polarization depends on the nature of the material as well as the frequency of the external applied field. There are four different types of polarization that occur at different frequencies [19].

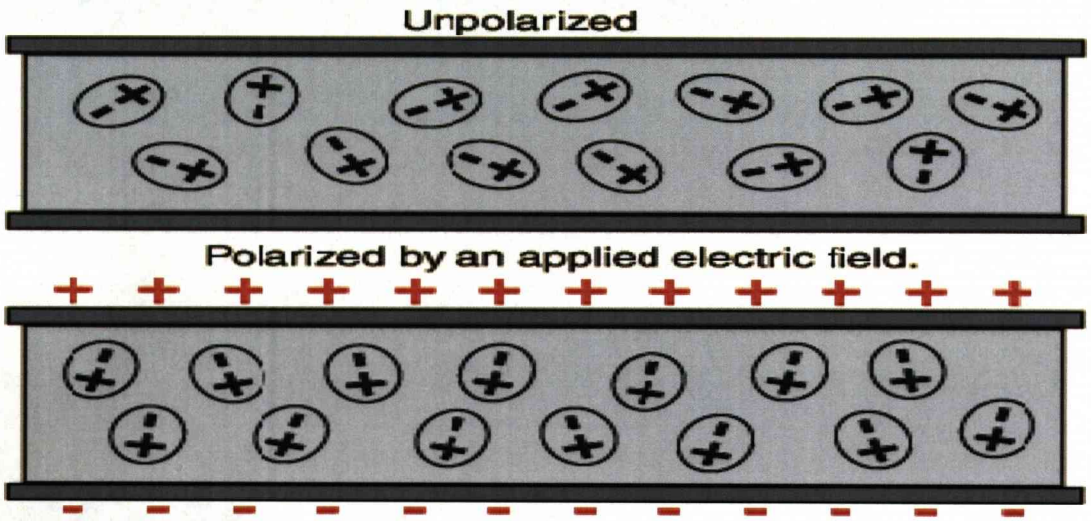

Figure 3.4 Polarization of molecules

Space charge polarization occurs at very low (VLF) or low frequency (LF) regions. This is predominantly seen at materials that contain free electrons whose movement is restricted by barriers. Application of an external electric field leads to accumulation of charge on the barriers. This leads to charge separation, where the electron in the atom is exited to a higher energy level and leaves the atom for an acceptor, which leads to polarization of the material.

Another type of polarization is caused by dipole alignment when an electric field is applied. In a polar dielectric, the constituent molecules are neutral but their centers of positive and

negative charges do not coincide geometrically. This form is usually observed at high frequency (HF) and microwave regions.

Ionic polarization occurs at infrared frequencies due to the relative displacement of positive and negative charges of the dielectric.

At very high frequencies (VHF) electrical polarization takes place. This is caused by the displacement of the negative electronic cloud surrounding the positive charged nucleus. The direction of the displacement is in the same direction as the direction of the applied field. In practice the different types of polarization overlap and are usually very hard to distinguish.

3.5 Electromagnetic Wave Propagation

3.5.1 Propagation in Free Space

In an EM wave, a varying electric field produces a changing magnetic field, which in turn produces an electric field and so on, with a resulting propagation of energy.

The simplest case is a plane wave in free space where the electric and magnetic fields lines are perpendicular to each other (fig 3.1), as well as to the wave direction and are in phase. The wave equation is given by

$$\frac{\partial^2 E_y}{dt^2} = \frac{1}{\mu\varepsilon}\frac{\partial^2 E_y}{\partial x^2} \quad (3.14)$$

The wavenumber in free space is defined as

$$k_0 = \frac{\omega}{c} \text{ rad/m} \quad (3.15)$$

The wavenumber k_0 is essentially the phase constant for a lossless propagation of a uniform plane wave in free space. The wavelength in free space is the distance over which a 2π spatial phase shift occurs or

$$\lambda = \frac{2\pi}{k_0} \quad (3.16)$$

The impedance Z is defined as the ratio of E_y to H_z

$$Z = \frac{E_y}{H_z} = \sqrt{\frac{\mu}{\varepsilon}} \quad (3.17)$$

In free space $\mu = \mu_0 = 4\pi 10 \times 10^{-7}$ NA^{-2} and $\varepsilon = \varepsilon_0$ so

$$Z_0 = \sqrt{\frac{\mu_0}{\varepsilon_0}} = 377\Omega \text{ Intrinsic impedance of free space}$$

The velocity u in air or vacuum is a function of constants μ and ε of the medium

$$u = \lambda \times f = \frac{1}{\mu\varepsilon}(ms^{-1}) \quad (3.18)$$

$$\text{In free space } u = \frac{1}{\sqrt{\mu_o \varepsilon_o}} = 3 \times 10^8 = c \rightarrow speed\ of\ light$$

A uniform plane wave is an ideal case and cannot exist physically as it extends to infinity in two dimensions at least and represents an infinite amount of energy. In this study the far field of the transmitting antenna can be essentially described as a uniform plane wave in some limited region.

3.5.2 Propagation in Lossy Media

In contrast to EM propagation through lossless media, in a source-free lossy medium the homogenous vector, Helmhotz's equation, is used similar to that through a vacuum with the only difference being the wavenumber [20].

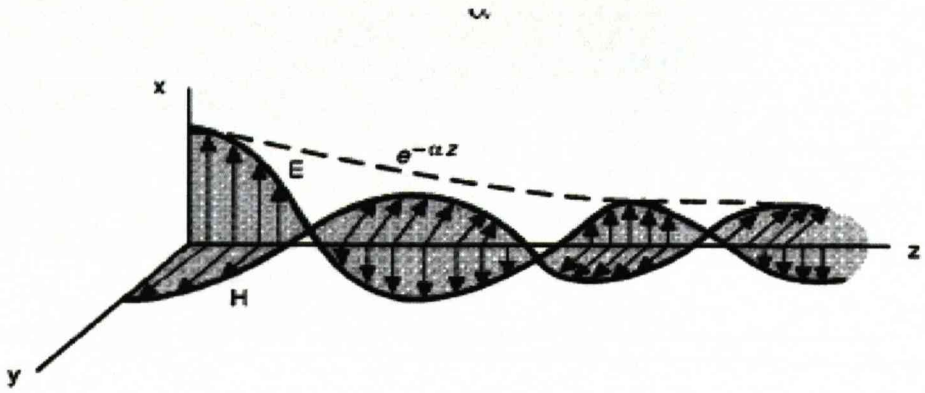

Figure 3.5 Wave Propagation in a lossy medium

The wave equation in lossy media is given by

$$\nabla^2 E + k_c^2 E = 0 \quad (3.19)$$

The wavenumber is $k_c = \omega\sqrt{\mu\varepsilon_c}$ (3.20)

and the permittivity of the medium

$$\varepsilon_c = \varepsilon - j\frac{\sigma}{\omega} \quad (3.21)$$

The propagation constant γ is defined as

$$\gamma = jk_c = j\omega\sqrt{\mu\varepsilon_c} \quad (3.22)$$

Since γ is complex and ε_c is given from equation (3.21), by substituting into the previous equation we obtain

$$\gamma = \alpha + j\beta = j\omega\sqrt{\mu\varepsilon}\left(1 + \frac{\sigma}{j\omega\varepsilon}\right)^{1/2} \leftrightarrow$$

$$\gamma = \alpha + j\beta = j\omega\sqrt{\mu\varepsilon'}\left(1 + j\frac{\varepsilon''}{\varepsilon'}\right)^{1/2} \quad (3.23)$$

where α is the real part and β the imaginary part of γ. For a lossless medium, $\sigma = 0$ ($\varepsilon'' = 0$ and $\varepsilon' = \varepsilon$), $\alpha = 0$ and $\beta = k = \omega\sqrt{\mu\varepsilon}$

So by substituting into (3.19)

$$\nabla^2 E - \gamma^2 E = 0 \quad (3.24)$$

3.5.3 Propagation in Dielectrics

The next case considered is of a uniform plane wave propagating in a dielectric. The latter show their insulating properties due to the high energy gap between the highest filled valence band and the conduction band and are used to isolate electrical components. The medium is assumed homogenous, the values for μ and ε are constant in each position, and isotropic, μ and ε are not affected by the field orientation.

The Helmhotz equation is given as

$$\nabla^2 E_s = -k^2 E \quad (3.25)$$

The wavenumber is a function of the material properties and the dielectric constant are given as

$$k = \omega\sqrt{\mu\varepsilon} = k_0 = \sqrt{\mu_r\varepsilon_r} \quad (3.26)$$

$$\varepsilon = \varepsilon' - j\varepsilon'' = \varepsilon_o(\varepsilon_r' - j\varepsilon_r'') \quad (3.27)$$

The attenuation and phase constants of γ become

$$\alpha = Re\{\gamma\} = \omega\sqrt{\frac{\mu\varepsilon'}{2}}\left(\sqrt{1+\left(\frac{\varepsilon''}{\varepsilon'}\right)^2} - 1\right)^{\frac{1}{2}} \quad (3.28)$$

$$\beta = Im\{\gamma\} = \omega\sqrt{\frac{\mu\varepsilon'}{2}}\left(\sqrt{1+\left(\frac{\varepsilon''}{\varepsilon'}\right)^2} + 1\right)^{\frac{1}{2}} \quad (3.29)$$

The phase velocity is defined as $u_p = \omega/\beta$ (3.30)

This leads to the fundamental definition of the wavelength $\lambda = 2\pi/\beta$ (3.31)

The intrinsic impedance is shown as

$$\eta = \sqrt{\frac{\mu}{\varepsilon' - j\varepsilon''}} = \sqrt{\frac{\mu}{\varepsilon'}}\frac{1}{\sqrt{1 - j(\varepsilon''/\varepsilon')}} \quad (3.32)$$

An ideal case is that of a lossless dielectric in which $\varepsilon'' = 0$ and so $\varepsilon = \varepsilon'$ or $\alpha = 0$. The propagation coefficient equals

$$\beta = \omega\sqrt{\mu\varepsilon'} \quad (3.33)$$

This can be interpreted as a wave moving in the z direction with a velocity v_p

$$v_p = \frac{\omega}{\beta} = \frac{1}{\sqrt{\mu\varepsilon'}} = \frac{c}{\sqrt{\mu_r\varepsilon_r'}} \quad (3.34)$$

The wavelength is found to equal

$$\lambda = \frac{2\pi}{\beta} = \frac{\lambda_o}{\sqrt{\mu_r\varepsilon_r'}} = \frac{c}{f\sqrt{\mu_r\varepsilon_r'}} \quad (3.35)$$

λ_o is the wavelength of free space.

Another case of particular interest is the propagation of EM waves through conductive materials, were currents are formed due to the movement of free electrons or from holes under the influence of an externally applied electric field. The relation that dictates the action of these materials is $J = \sigma E$. The conductivity of a material determines the power losses in a material due to resistive heating. So, in a conductive medium the loss factor becomes

$$\varepsilon'' = \frac{\sigma}{\omega} \quad (3.36)$$

The level of the loss for a wave is proportional to the magnitude of the loss tangent $\varepsilon''/\varepsilon'$. This parameter has a direct effect on the attenuation coefficient. In the case of a conducting medium to which $\varepsilon'' = \sigma/\omega\varepsilon'$, the wave equation equals

$$\nabla \times H_s = (\sigma + j\omega\varepsilon')E_s = J_{\sigma s} + J_{ds} \quad (3.37)$$

This shows the equation in terms of conduction current density to displacement current density. The ratio equals

$$\frac{J_{\sigma s}}{J_{ds}} = \frac{\varepsilon''}{j\varepsilon'} = \frac{\sigma}{j\omega\varepsilon'} \quad (3.38)$$

The angle θ can be identified as the angle by which the displacement current density leads the current total density

$$\tan d = \frac{\varepsilon''}{\varepsilon'} = \frac{\sigma}{\omega\varepsilon'} \quad (3.39)$$

If the loss factor is small then approximations can be made such that $\varepsilon'' > \varepsilon'$ or $\sigma/\omega\varepsilon \ll 1$. In a good dielectric γ becomes

$$\gamma = \alpha + j\beta \cong j\omega\sqrt{\mu\varepsilon'}\left[1 - j\frac{\varepsilon''}{2\varepsilon'} + \frac{1}{8}\left(\frac{\varepsilon''}{\varepsilon'}\right)^2\right] \quad (3.40)$$

The attenuation and phase constant equal

$$\alpha = Re\{\gamma\} = j\omega\sqrt{\mu\varepsilon'}\left(-j\frac{\sigma}{2\omega\varepsilon'}\right) \cong \frac{\omega\varepsilon''}{2}\sqrt{\frac{\mu}{\varepsilon'}} \quad (3.41)$$

$$\beta = Im\{\gamma\} \cong \omega\sqrt{\mu\varepsilon'}\left[1 + \frac{1}{8}\left(\frac{\varepsilon''}{\varepsilon'}\right)^2\right](rad/m) \quad (3.42)$$

The intrinsic impedance of a low loss dielectric is complex and given by

$$\eta = \sqrt{\frac{\mu}{\varepsilon'}}\left(1 - j\frac{\varepsilon''}{\varepsilon'}\right)^{-1/2} \cong \sqrt{\frac{\mu}{\varepsilon'}}\left(1 - j\frac{\varepsilon''}{\varepsilon'}\right)(\Omega) \quad (3.43)$$

It must be mentioned that the electric and magnetic field intensities in a lossy dielectric are not in time and phase between them [21].

3.5.4 Propagation in Good Conductors

A good conductor is a medium which σ/ωε>>1. So by taking the equation for a low loss dielectric and neglect 1 with the term σ/jωε

$$\gamma = j\omega\sqrt{\mu\varepsilon}\sqrt{\frac{\sigma}{j\omega\varepsilon}} = \sqrt{j}\sqrt{\omega\mu\sigma} = \frac{1+j}{\sqrt{2}}\sqrt{\omega\mu\sigma} \leftrightarrow$$

$$\gamma = \alpha + j\beta \cong (1+j)\sqrt{\pi f\mu\sigma} \quad (3.44)$$

For a good conductor the attenuation and phase constant equal

$$\alpha = \beta = \sqrt{\pi f\mu\sigma} \quad (3.45)$$

The velocity equals $v_p = \omega\delta$ (3.46)

where δ is the skin depth described in detail in section 3.8.

The intrinsic impedance of a good conductor is

$$\eta_c = \sqrt{\frac{\mu}{\varepsilon_c}} \cong \sqrt{\frac{j\omega\mu}{\sigma}} = (1+j)\sqrt{\frac{\pi f\mu}{\sigma}} = (1+j)\frac{\alpha}{\sigma} \quad (3.47)$$

3.6 Water as a Dielectric

The water molecule (H_2O) has a highly asymmetric configuration as well as an exceptionally high polarity. Its chemical structure is shown in figure 3.6.

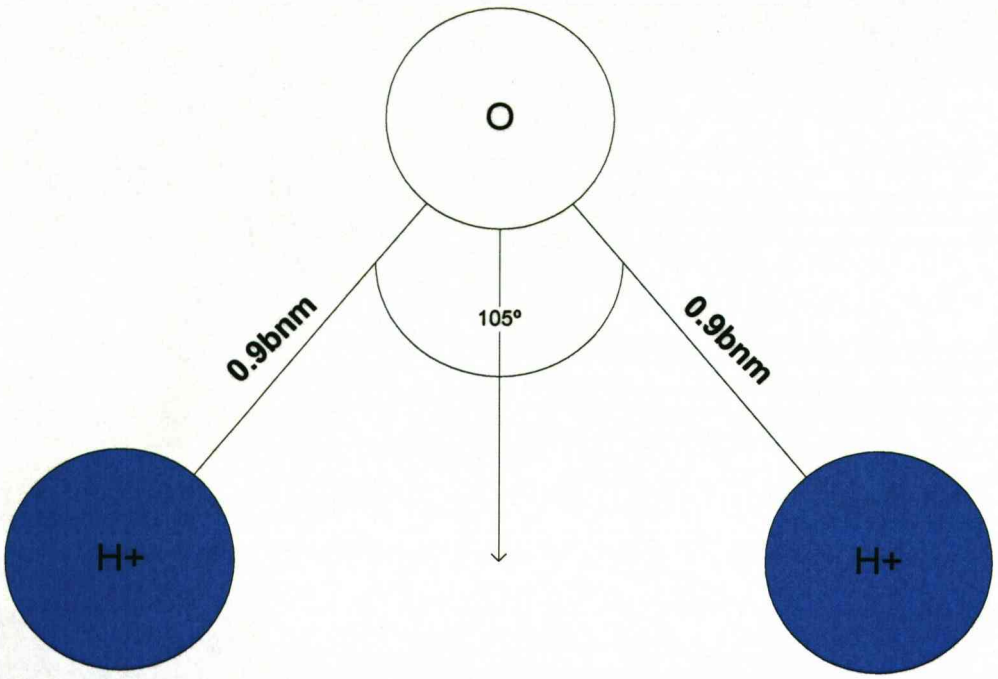

Figure 3.6 Chemical structure of water [22]

The two positive charged hydrogen atoms join the negative charged oxygen atom at an angle of 105 degrees. The distance between the oxygen and hydrogen atom is 0.09bnm, where bnm or Angstrom equal to 0.1nm, and the resulting dipole moment is estimated to be 0.62×10^{-29}Cm [22]. The charge differences between the negative oxygen atom and the positive hydrogen atoms lead to the attraction between water molecules to each other. This is known as hydrogen bonding and explains the special properties of water. Each water molecule can form a maximum of four hydrogen bonds because it can accept two and donate two hydrogen atoms. The unusual properties of water include high heat capacity, high heat of evaporation as well as boiling and freezing points and a low freezing point.

Sea water has increased conductivity, which is proportional to the number of ions present. Polarization depends also on the salinity, which is the dissolved content of salt in the water S, and the composition of sea water. The main ions are sodium (Na^+) and Chlorium (Cl^-). In seawater the density and the boiling point are increased compared to pure water while the freezing point is reduced.

3.6.1 Debye's Model

Debye's model [23] displays the relationship between relative permittivity and the frequency of EM waves in a dielectric. It is based on the assumption that there are no interactions between the molecules, so that they are free in the dielectric [24].

If the dielectric is placed in a static electric field of magnitude E, the induced component of polarization, P_1, assuming that there is no inertia equals [25]

$$P_1 = \varepsilon_0(\varepsilon_\infty - 1)E \quad (3.48)$$

where ε_∞ is the permittivity at infinite frequency.

On the other hand the orientation of polarization, P_0, shows an exponential rise [25] reaching a maximum value of

$$P_0 = \varepsilon_0(\varepsilon_s - 1)E - \varepsilon_0(\varepsilon_\infty - 1)E \text{ at } t=\infty \quad (3.49)$$

The maximum value of total polarization equals

$$P = \varepsilon_0(\varepsilon_s - 1)E \quad (3.50)$$

Debye's model is then derived

$$\varepsilon = \varepsilon_\infty + \frac{\varepsilon_s - \varepsilon_\infty}{1 + j\omega\tau} \quad (3.51)$$

where τ is the amount of time required for the dielectric to return to molecular disorder more commonly known as the relaxation time.

So by separating the real and imaginary parts

$$\varepsilon' = \varepsilon_\infty + \frac{\varepsilon_s - \varepsilon_\infty}{1 + \omega^2\tau^2} \quad (3.52)$$

$$\varepsilon'' = \frac{(\varepsilon_s - \varepsilon_\infty)\omega\tau}{1 + \omega^2\tau^2} \quad (3.53)$$

where ε_∞ is optical-frequency value of the real permittivity

ε_s is the static value of the real permittivity.

The maximum value for the loss factor occurs at frequency

$$f = \frac{1}{2\pi\tau} \quad (3.54)$$

It can be obtained that the loss factor has a maximum value of

$$\varepsilon''_{max} = \frac{\varepsilon_s - \varepsilon_\infty}{2} \quad (3.55)$$

It must be taken into account that some terms of Debye's equation are a function of temperature T and frequency, so the equation becomes

$$\varepsilon(\omega, T) = \varepsilon_\infty(T) + \frac{\varepsilon_S(T) - \varepsilon_\infty(T)}{1 + j\omega\tau(T)} \quad (3.56)$$

3.6.2 Cole-Cole model

As mentioned above Debye's model assumes that there are no intermolecular interactions. Besides in many cases dielectrics do not have a single relaxation time. This leads to the Debye formula being modified by the addition of the distribution parameter ν in the Debye formula [26].

This formula is known as the Cole-Cole model and mathematically shown as

$$\varepsilon = \varepsilon_\infty + \frac{\varepsilon_s - \varepsilon_\infty}{1 + (j\omega\tau)^{1-\nu}} \quad (3.57)$$

where ν has a value between zero and unity.

By separating the real and the imaginary parts of the Cole-Cole model we obtain

$$\varepsilon' = \varepsilon_\infty + \frac{(\varepsilon_s - \varepsilon_\infty)\left[1 + (\omega\tau)^{1-\nu}\sin\left(\frac{\nu\pi}{2}\right)\right]}{1 + 2(\omega\tau)^{1-\nu}\ sin\left(\frac{\nu\pi}{2}\right) + (\omega\tau)^{2(1-\nu)}} \quad (3.58)$$

$$\varepsilon'' = \frac{(\varepsilon_s - \varepsilon_\infty)(\omega\tau)^{1-\nu}\cos\left(\frac{\nu\pi}{2}\right)}{1 + 2(\omega\tau)^{1-\nu}\ sin\left(\frac{\nu\pi}{2}\right) + (\omega\tau)^{2(1-\nu)}} \quad (3.59)$$

The dielectrics usually have many dielectric relaxation times due to dielectrics having different polar groups whose value is around a central value τ_0 according to a function

$$f(\tau) = \frac{\sin(\nu\pi)}{2\pi\cosh\left[(1-\nu)\ln\frac{\tau}{\tau_0}\right] - \cos\nu\pi} \quad (3.60)$$

3.6.3 Models for Fresh and Sea Water Permittivity

Initially for the permittivity model of sea and fresh water a single Debye model as shown in section 3.6.2 was appropriate [27]. Later studies showed that this model was only accurate for frequency values up to 100GHz [28]. For higher frequencies a double Debye model is much more accurate. This model assumes that a second polarization process also takes place with a different relaxation time as shown below

$$\varepsilon_r(\omega,T) = \varepsilon_\infty(T) + \frac{\varepsilon_s(T) - \varepsilon_1(T)}{1 + j\omega\tau_1(T)} + \frac{\varepsilon_1(T) - \varepsilon_\infty(T)}{1 + j\omega\tau_2(T)} \quad (3.61)$$

Liebe et al [29] claim that their double Debye model can be used for frequencies up to 1THz and may be used up to 30THz by the inclusion of two Lorentzian terms. It must be mentioned that there is no clear underlying physical process for the second Debye relaxation, but is used to provide a more accurate fit for the permittivity over a wider frequency range [25].

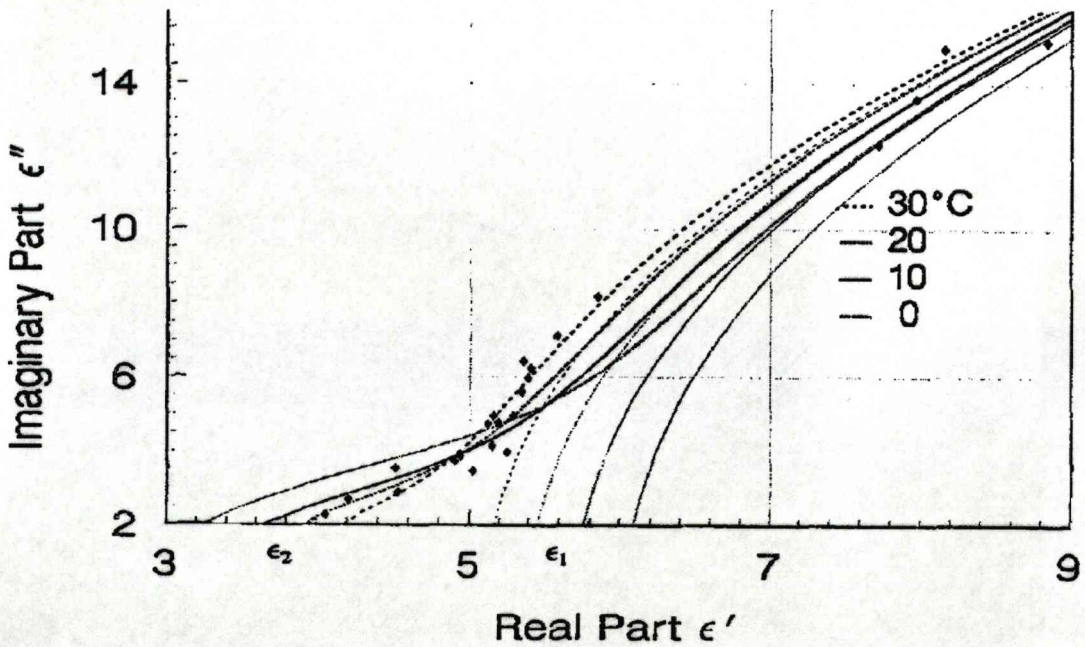

Figure 3.7 Complex Permittivity of water between 0.1 and 1THz, with a double Debye model [used from Liebe et al 29]

Similarly, a double Debye model is used for seawater. The main difference is the inclusion of the effect of conductivity of the dielectric constant and has been shown as [25]

$$\varepsilon_r(\omega,T,S) = \varepsilon_\infty(T,S) + \frac{\varepsilon_s(T,S) - \varepsilon_1(T,S)}{1 + j\omega\tau_1(T,S)} + \frac{\varepsilon_1(T,S) - \varepsilon_\infty(T,S)}{1 + j\omega\tau_2(T,S)} \quad (3.62)$$

3.7 Transmission Lines

Transmission lines are interconnections that are used in communications to transmit information from one point to another. The transmission line can be described schematically as a four terminal network that includes a series resistance R (Ω/m), a series inductance L (H/m), a shunt conductance G (S/m) and a shunt capacitance C (F/m) [30].

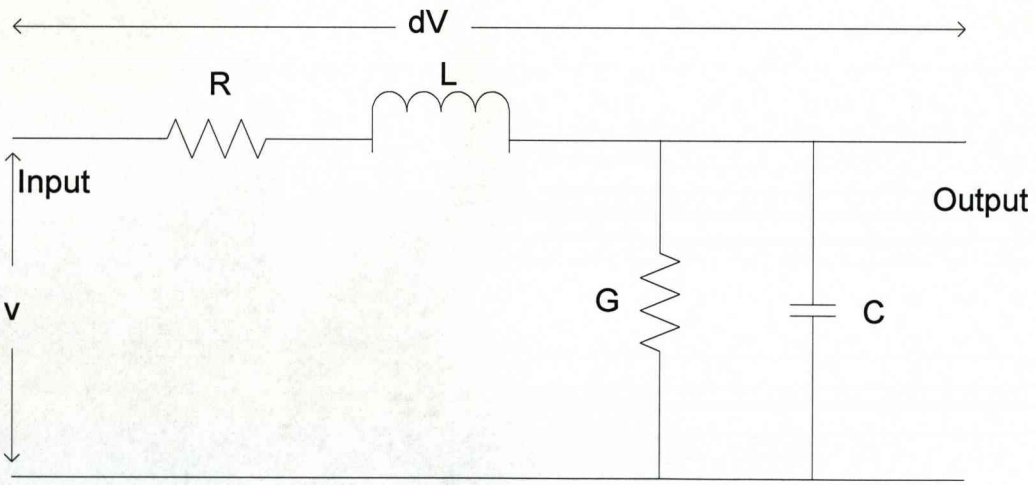

Figure 3.8 Transmission line equivalent circuit

In the ideal case of a lossless line R = G = 0, the change in voltage over the distance dx is given by [30]

$$\frac{dV}{dx} = L \cdot \frac{dI}{dt} \quad (3.63)$$

$$\frac{dI}{dx} = C \cdot \frac{dV}{dt} \quad (3.64)$$

Differentiating (3.63) with respect to distance x and (3.64) with respect to time t, the transmission line equation is obtained as

$$\frac{d^2V}{dt^2} = \frac{1}{LC}\frac{d^2V}{dx^2} \quad (3.65)$$

The velocity equals

$$v = \frac{1}{LC}\left(\frac{m}{sec}\right) \quad (3.66)$$

The characteristic impedance of the line is defined as

$$Z_{line} = \sqrt{\frac{R + j\omega L}{G + j\omega C}} \quad (3.67)$$

For a lossless line R=G=0

$$Z_{line} = \sqrt{\frac{L}{C}} \quad (3.68)$$

3.7.1 Terminated Transmission line

In this case a line of characteristic impedance Z is terminated in a load impedance Z_L. The ratio of the voltage of the incident wave traveling to the right over the voltage of the traveling reflected wave to the left equals the reflection coefficient Γ

$$\Gamma = \frac{V_I}{V_O} = \frac{Z_L - Z_O}{Z_L + Z_O} \quad (3.69)$$

The impedance Z_X at a distance x from the load equals

$$Z_X = Z_O \frac{Z_L + Z_O \tanh \gamma x}{Z_o + Z_L \tanh \gamma x} \quad (3.70)$$

If the line is open circuited then $Z_L = \infty$ and the impedance equals

$$Z_x = \frac{Z_o}{\tanh \gamma x} = Z_o coth \gamma x \quad (3.71)$$

If the line is short circuited and Z_L=0 then the impedance equation reduces to

$$Z_x = Z_o \tanh \gamma x \quad (3.72)$$

3.8 Skin Depth

Skin depth is a measure of how far electrical conduction takes place in a conductor and is a function of frequency. At DC (0Hz) the entire conductor is used and it does not depend on the thickness of the conductor. At RF frequencies, the effect of the thickness on the conductance is nonlinear.

The equation for skin depth is shown below, as it can be seen skin depth is the function of three variables frequency (f), resistivity (ρ) and relative permeability (μ_r). Typical values for skin depth in this study are shown in chapter 5.

$$\delta = \sqrt{\frac{2\rho}{2\pi f \mu_o \mu_r}} \quad (3.73)$$

3.9 Antennas

3.9.1 Introduction

An antenna can be defined as a device for radiating or receiving radio waves. The main mechanism of antenna radiation is down to accelerated free electron charges through the antenna.

The Thevenin equivalent of an antenna in a transmitting mode is shown below. In this case, the transmission line is shown as line with characteristic impedance Z_c, while the load Z_A represents the antenna which is connected to the transmission line [31]

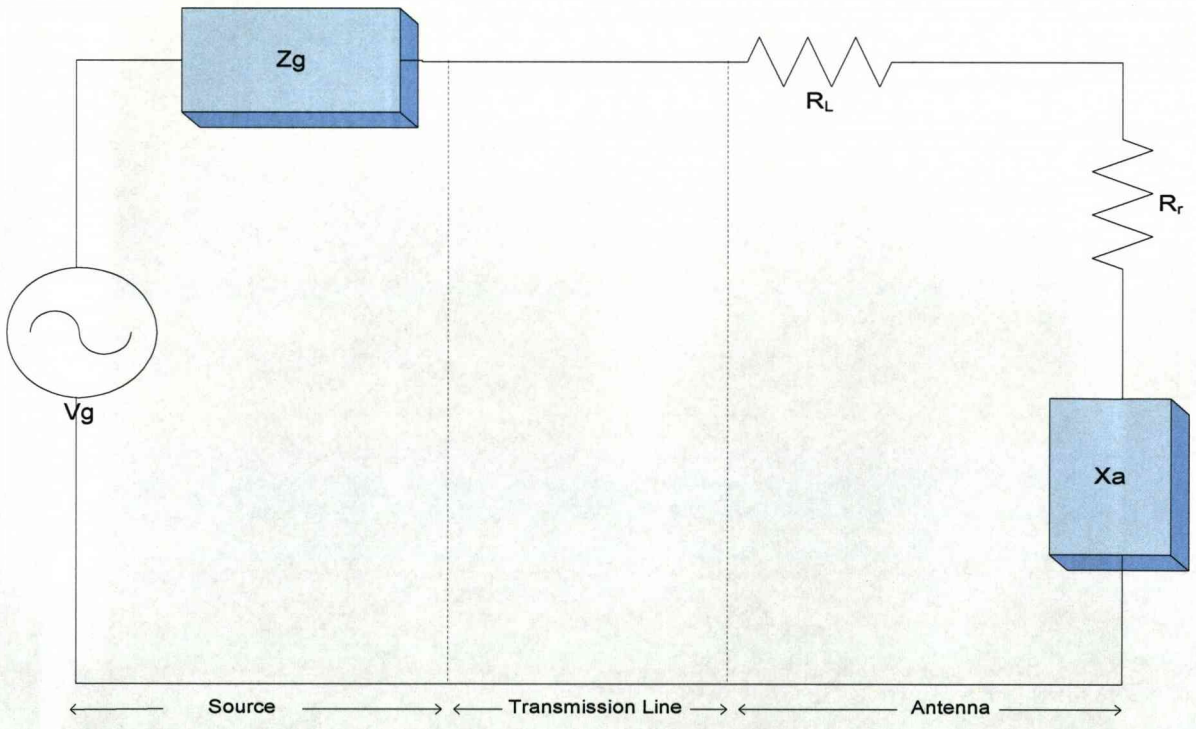

Figure 3.9 Antenna equivalent circuit

From the equivalent circuit it can be seen that

$$Z_A = (R_L + R_r) + jX_a \quad (3.74)$$

The resistance R_L is used to describe the dielectric and conduction losses associated with the antenna structure, R_r is the radiation resistance and X_a is the reactance that represents the imaginary part associated with antenna radiation. Under ideal conditions, energy generated by the source should be totally transferred to the radiation resistance R_r.

There are various types of antennas depending on the structure like monopole, dipole, loop, wire antennae among others, but these are of particular interest in this study. In order to classify the performance of an antenna there are various parameters including radiation pattern, field region, power density radiation resistance that will be now dealt with more detail.

3.9.2 Radiation Patterns

By representing graphically the radiation properties of an antenna as a function of space coordinates, usually in the far field region, the antenna pattern is obtained. The main radiation properties observed includes power flux density, radiation intensity, field strength, directivity or polarisation [32].

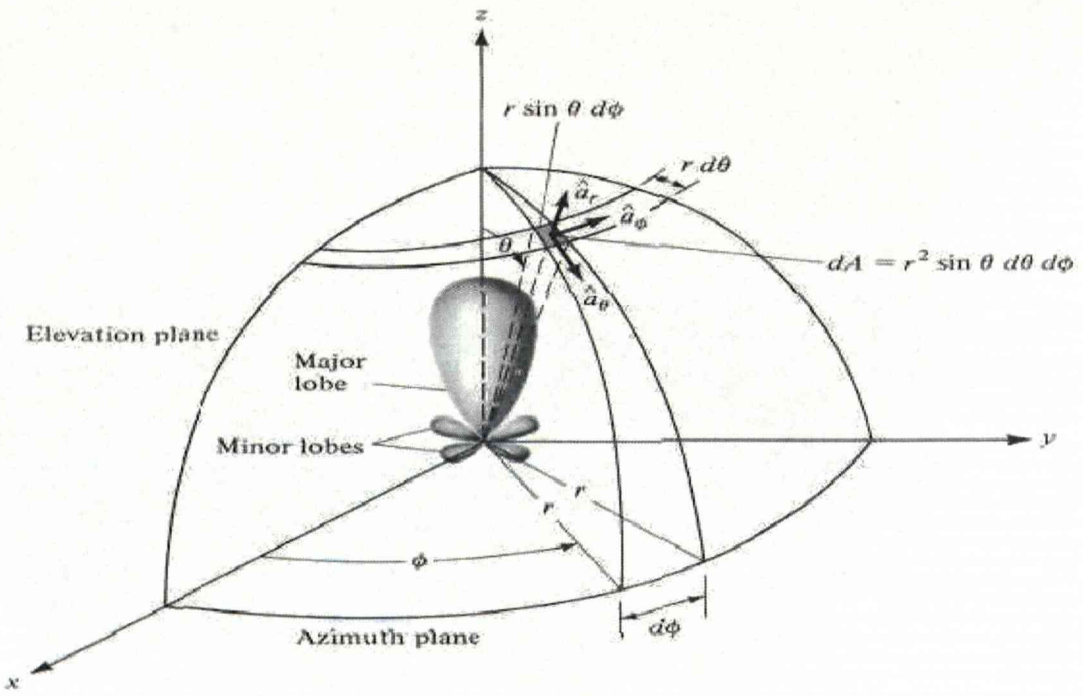

Figure 3.10 Radiation Pattern for antenna [32]

3.9.3 Antenna Field Regions

The fields surrounding the antenna can be divided into two regions the near and far field. The boundary between the two fields is at a radius R and is given by the equation

$$R = \frac{2D^2}{\lambda} \quad (3.75)$$

where D is the maximum dimension of the antenna (m).

Furthermore the near field can be divided into two sub-regions the reactive and radiating near field. Despite this difference there are no abrupt changes when leaving the one field and entering the other [33]. Immediately surrounding the antenna is the reactive near field which as the name suggests the reactive component predominates. The boundary for this antenna is shown at

$$R_1 < 0.62\sqrt{D^3/\lambda} \quad (3.76)$$

Similarly in the radiating near field, the radiating component predominates and its boundary is given between equations (3.75) and (3.76). In the far field the angular field distribution is independent of the distance of the antenna

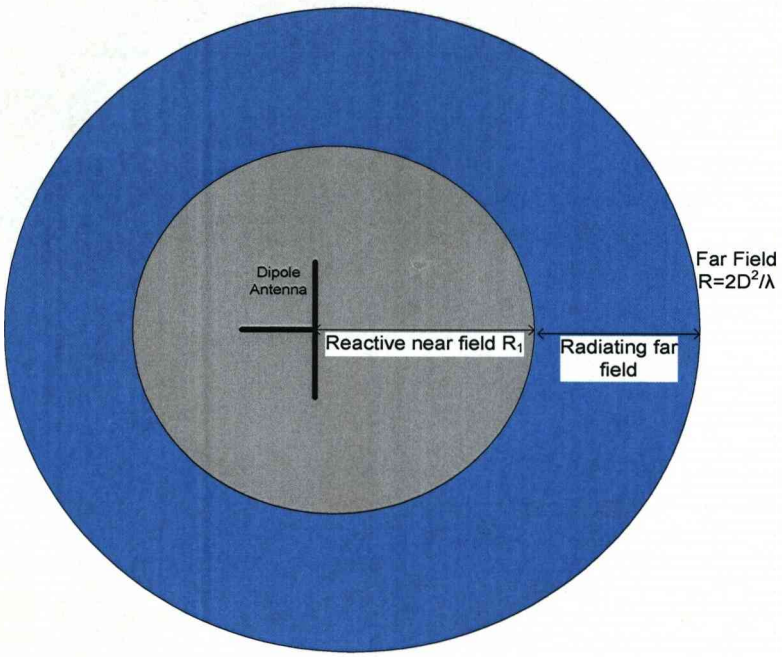

Figure 3.11 Antenna Field Regions

It must be mentioned that in the near field the energy falls as a cube of the distance while in the far field energy drops as a square of the distance [34].

3.9.4 Radiation Intensity

This term demonstrates the power radiated from an antenna per unit solid angle, it is given by the following equation.

$$U^2 = r^2 \cdot W_{rad} \quad (3.77)$$

Where r is the distance the power is radiated

W_{rad} is the radiation density (W/m^2)

By integrating the radiation intensity the total power can be obtained

$$P_{rad} = \oiint_{\Omega} U \cdot d\Omega = \int_0^{2\pi}\int_0^{\pi} U \sin\theta \cdot d\theta \cdot d\varphi \quad (3.78)$$

Where $d\Omega$ = element of solid angle = $\sin\theta \cdot d\theta \cdot d\varphi$

In case of an isotropic source

$$U_0 = \frac{P_{rad}}{4\pi} \quad (3.79)$$

3.9.5 Directivity

Directivity is defined as the ratio of the radiation intensity in a predetermined direction over the radiation intensity averaged over all other directions. So,

$$D = \frac{U}{U_0} = \frac{4\pi}{P_{rad}} \quad (3.80)$$

Similarly the direction of the maximum radiation intensity can be expressed as

$$D_{max} = D_0 = \frac{U_{max}}{U_0} = \frac{4\pi U_{max}}{P_{rad}} \quad (3.81)$$

In the case of a spherical coordinate system, the total maximum directivity D_0 for the orthogonal and spherical components can be given as

$$D_0 = D_\theta + D_\varphi \quad (3.82)$$

Where

$$D_\theta = \frac{4\pi U_\theta}{(P_{rad})_\theta + (P_{rad})_\varphi} \quad (3.83)$$

$$D_\varphi = \frac{4\pi U_\varphi}{(P_{rad})_\theta + (P_{rad})_\varphi} \quad (3.84)$$

In this case the coordinates θ, φ demonstrate the direction of the radiation intensity.

3.9.6 Antenna Gain

Another important parameter is gain that is defined as the ratio of the radiation intensity over the total input power and given by the mathematical equation below

$$Gain = 4\pi \frac{U_{(\theta,\varphi)}}{P_{in}} \quad (3.85)$$

3.9.7 Half-Power Beamwidth

This is essentially a figure of merit. It is the solid angle where

$$\frac{S_{(\theta,\varphi)}}{S_{max}} = 0.5 \quad (3.86)$$

where S is the Poynting vector

The electric field equals

$$\frac{E_{(\theta,\varphi)}}{E_{max}} = \frac{1}{\sqrt{2}} \quad (3.87)$$

3.9.8 Bandwidth

The bandwidth of an antenna is the range of frequencies of the antenna where its performance is acceptable for the required application and has units of Hz. The bandwidth of an antenna may depend on some of its characteristics (input impedance, radiation pattern, beamwidth) but not in any particular manner. This means that there is no standard definition for the operational values of the bandwidth, but are defined according to the application. It is often defined as the range over which the power gain is maintained to within 3dB of its maximum value, or the range over which the Voltage Standing Wave Ratio (VSWR, see below) is no greater than 2:1; whichever is smaller [35].

Fractional bandwidth (FB) is often used to describe bandwidth, due to the fact that it is constant relative to frequency. The FB of a signal is the ratio of the bandwidth to the centre frequency and is defined as

$$FB = \frac{f_{max} - f_{min}}{(f_{max} + f_{min})/2} \times 100\% \quad (3.88)$$

Where f_{max} and f_{min} are the effective highest and lowest frequencies of the signal.

3.9.9 Polarisation

Any waves that are transmitted by an antenna can be polarised linearly, circularly or elliptically. The type of polarisation depends on the vector that describes the electrical field. If it is directed along a line then it is linearly polarised and so on.

3.9.10 Antenna Aperture

The physical aperture of the antenna A_p is a measure of the physical size of the antenna. This depends on the characteristics of the antenna. If all the power is extracted, the total power absorbed equals

$$P = \frac{E^2}{Z} A_p = S \cdot A_p \quad (3.89)$$

In most cases the effective aperture A_e of the antenna is much smaller than the physical aperture. The aperture efficiency ε_{ap} equals

$$\varepsilon_{ap} = \frac{A_e}{A_p} \quad (3.90)$$

3.9.11 Dipole Antenna

The Hertzian dipole has a very short length of wire over which the current distribution is essentially uniform. When the antenna is energised by a high frequency current, according to Maxwell's equation, is associated with an induction field that decreases inversely at the square of the distance and a radiation field that decreases inversely against the distance. The latter is measurable at large distances and is the radiation field used in radio communications.

The magnetic field of the antenna at a distance r is shown to be

$$H_\varphi = \frac{I_o dl \sin\theta}{4\pi} \left[\frac{j e^{j\omega(t-rc)} \omega}{rc} + \frac{e^{j\omega(t-r/c)}}{r^2} \right] \quad (3.91)$$

The first term is the radiation field while the second term is the induction field. For the latter we obtain

$$H_\varphi = \frac{j I_o e^{j\omega(t-r/c)} dl \sin\theta (\omega/cr)}{4\pi} = \frac{j I_o e^{j\omega(t-r/c)} dl \sin\theta}{2\lambda r} \quad (3.92)$$

Also from Maxwell's equations we obtain

$$\frac{E_\theta}{H_\varphi} = 120\pi \quad (3.93)$$

$$E_\theta = \frac{j60\pi dl \sin\theta \, I_o e^{j\omega(t-r/c)}}{\lambda r} \quad (3.94)$$

The root mean square (r.m.s) value E_m assuming r.m.s current I,

$$E_m = \frac{60\pi I dl}{\lambda r} \quad (3.95)$$

The electric field is directional to the vertical plane but is omnidirectional in the horizontal plane [36].

The radiation resistance of a dipole antenna is defined as

$$R_r = 80\pi^2 \left(\frac{dl}{\lambda}\right)^2 \quad (3.96)$$

3.9.12 Loop Antenna

A vertical loop antenna can be created by combining the radiation from four doublets; two of them being vertical while the other horizontal. The value of E_θ in the XY plane of a loop antenna of diameter d can be found as

$$E_\theta = \frac{60j\pi I_o dl e^{j\omega(t-r/c)}}{\lambda r} \quad (3.97)$$

The resultant field is given by the phasor sum of the fields of the two doublets with a path difference dcosφ [36].

$$E_r = \frac{120\pi^2 I_o A e^{j\omega(t-rc)} \sin\varphi}{\lambda^2} \quad (3.98)$$

The power radiated from the loop equals

$$P = 160\pi^4 I_o^2 \left(\frac{A}{\lambda^2}\right)^2 \quad (3.99)$$

where A is the loop area

The radiation resistance is found to be

$$R_r = 320\pi^4 \left(\frac{A}{\lambda^2}\right)^2 \quad (3.100)$$

3.10 Waveguides

Waveguides are used to guide waves at higher frequencies usually over 2.45GHz. At these frequencies the use of the transmission line or coaxial cable is restricted due to high losses associated with power dissipation in the resistance of the conductors. Waveguide propagation is achieved by the skin effect, which leads to current density being greater at the conductor than at the core. This restricts the flow of a current to the surface. There are many modes in which the wave can propagate through the waveguide and they depend on the operating wavelength and polarization as well as the shape and size of the guide. The two main modes are the longitudinal and transverse mode. The latter is classified into different modes but are of particular importance in this study

- Transverse Electric (TE) modes where there is no electric field in the direction of propagation
- Transverse Magnetic (TM) modes where there is no magnetic field in the direction of propagation
- Transverse Electromagnetic (TEM) modes where there is no magnetic and electric field in the direction of propagation
- Hybrid modes are those where both electric and magnetic field components in the direction of propagation

As it can be seen waveguides limit the three dimensional propagation of a electromagnetic waves and guide the wave through the waveguide using a single direction.

The main types of waveguides are hollow cylindrical and rectangular. As mentioned above at low frequencies and high wavelengths there is no propagation through the guides. The lowest frequency at which transmission is possible is termed the cut-off frequency and for a rectangular waveguide is defined as

$$f_c = c\sqrt{\left(\frac{n\pi}{a}\right)^2 + \left(\frac{m\pi}{b}\right)^2} \quad (3.101)$$

where n m≥0 are the mode number

a, b are the dimensions of the waveguide

3.11 Cavity Resonators

Resonant cavities are mainly used to provide a higher quality factor Q at high frequencies. Of particular interest in this project is the circular resonant cavity that essentially consists of a section of circular waveguide of length l and radius α, with short circulating plates.

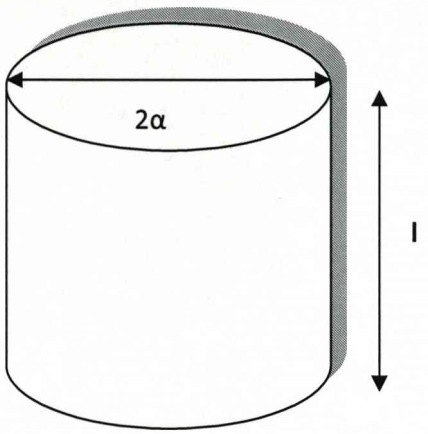

Figure 3.12 Cylindrical Resonant Cavity

For any given mode the resonant frequencies for both TE_{nml} and TM_{nml} is given as

$$f_{nml} = \frac{c}{2\pi\sqrt{\mu_r \varepsilon_r}} \sqrt{\left(\frac{q_{nm}}{\alpha}\right)^2 + \left(\frac{l\pi}{d^2}\right)^2} \quad (3.102)$$

where q_{nm} is the mode value for TE and for TM modes it is denoted p_{nm}

The mode chart shown in figure 3.13 shows over what range of frequency and 2α/d only a single mode can resonate [37].

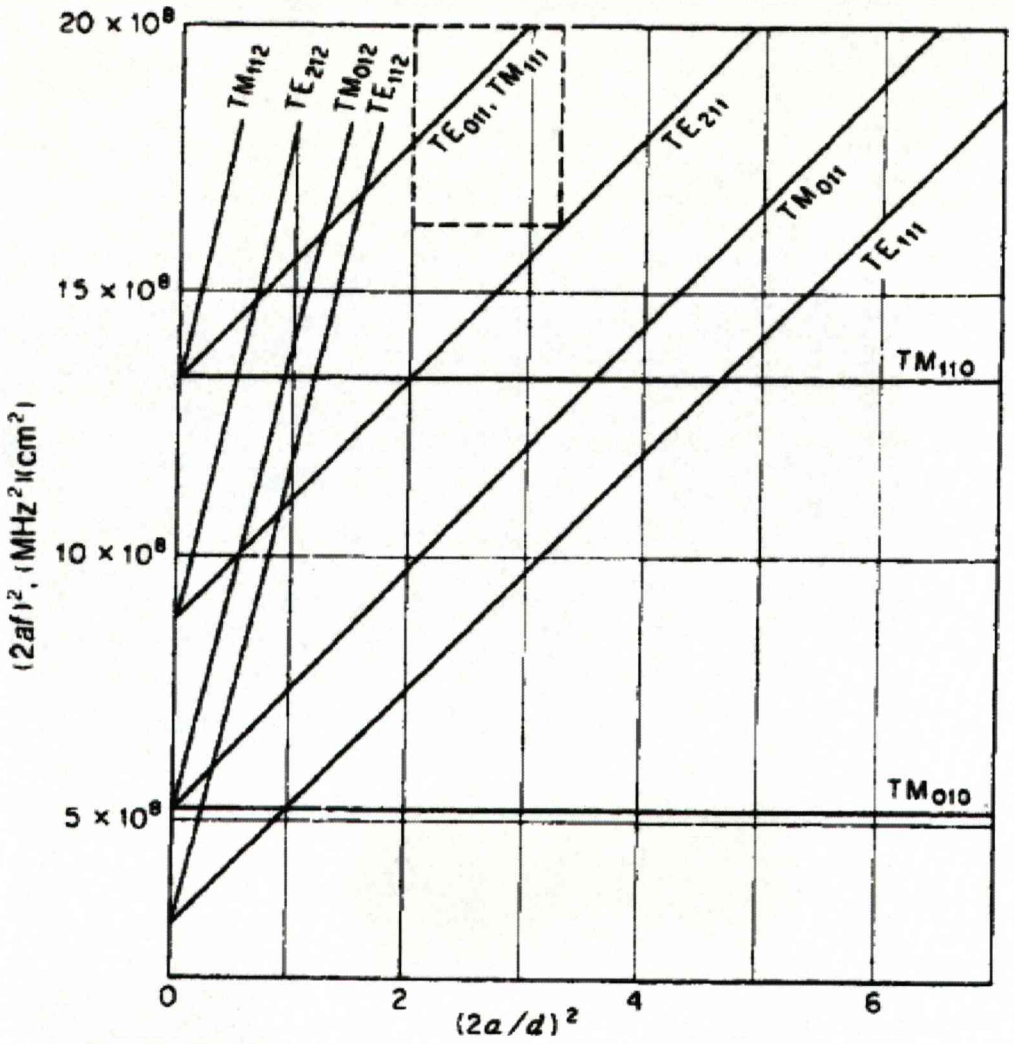

Figure 3.13 Mode chart for cylindrical resonant cavity

3.12 Impedance matching

In order for the antenna to make effective use of all its available power from the transmitter if the signal is sent or to the receiver when the antenna receives the signal, the impedance between these components must be matched.

In any communication system the transmitter or the receiver usually has impedance equal to that of the transmission line Z_O. However, the antenna impedance Z_L usually has a different value compared to that of the transmission line. To determine the level of matching between two impedances are the reflection coefficient Γ was introduced, that demonstrates the relationship between transmitted and reflected power.

The Voltage Standing Wave Ratio (VSWR), often abbreviated to SWR, can be defined as the ratio of the maximum to minimum voltage and is related to the reflection coefficient as

$$VSWR = \frac{1 + |\Gamma|}{1 - |\Gamma|} \quad (3.103)$$

If the transmission line is of high quality, these reflections represent low-dissipative losses. On the other hand it is not necessary to have a very low VSWR since a system with a VSWR value of 2 shows power transmission in the range of 89% [38]. If the VSWR has a very high value then this leads to serious problems in the system. Power travels along the transmission line in both directions leading to increased dissipative losses depending mainly on the length of the line. In high-power applications, arcing can be created due to the high voltages that occur in the conductors. Besides it can lead to variations in the impedance along a transmission line as well as variations due to frequency change. Another important factor is that both phases of the transmitted and the received signal should be in phase otherwise superimposition will occur.

3.12.1 Transformer Matching

If the impedance mismatch creates problems to the system, there are several methods for improving its performance by applying various matching circuits. A typical matching system is a quarter wave length transformer which is in essence a quarter wave long transmission line with characteristic impedance $\sqrt{Z_0 R_L}$. If there is a reactive component in the antenna impedance then other devices may be used. At low frequencies variable capacitors and coils are used preferably to tune out the reactive component because the electrical dimensions of

these lumped elements are very small compared to the wavelength. At ultrahigh and microwave frequencies, elements such as stub tuners are used in order to transform the real part of the impedance to that of the transmission line as well as removing the reactive component.

Transformers like those shown below can be used to transform one resistance to another resistance. Their main advantage is that the value of the resistance depends on the ratio of inductance on the primary and secondary coil [39]

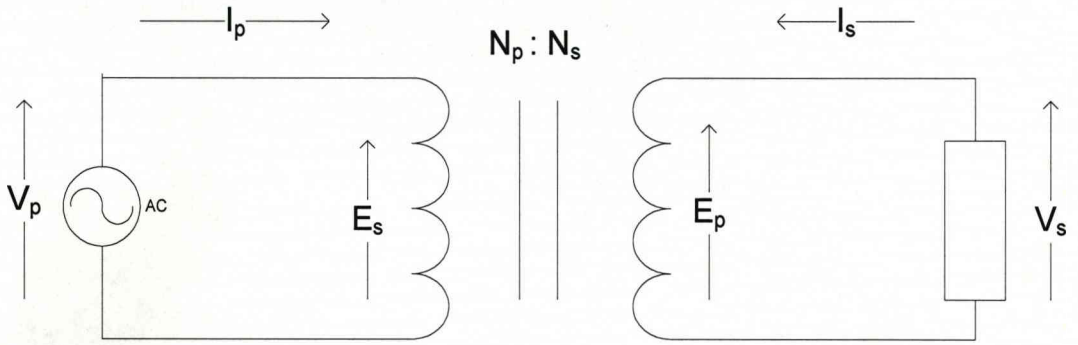

Figure 3.14 The ideal transformer for impedance matching

Taking the case that the transformer is ideal, that means that the coupling of magnetic energy is perfect, and lossless, then

$$L_p = NL_s \quad (3.104)$$

where N is the inductance ratio, L_p and L_s the inductances and I_p and I_s the currents on the primary and secondary coil respectively and by physics

$$\frac{V_p}{V_s} = \frac{I_p}{I_s} = \sqrt{N} \quad (3.105)$$

If the impedance on the secondary coil is R_s, then the impedance on the primary coil R_p will equal

$$R_p = \frac{V_p}{I_p} = \frac{V_s\sqrt{N}}{\frac{I_s}{\sqrt{N}}} = \frac{V_s}{I_s}N \leftrightarrow$$

$$R_p = R_s N \quad (3.106)$$

So the impedance ratio is related by the inductance ratio and this make it simpler to transform impedance from one value to another. On the other hand a real transformer does display losses and it may require tuning of the transformer. Besides by placing a resistor in series with the transformer rather than parallel it will lead to a creation of a voltage divider by between the resistor and the inductor that will cause problems with the impedance matching. In order to avoid this problem a capacitor is added in order to resonate the transformer and so providing an open circuit at the frequency in which the matching is required. This leads to bandwidth problems within the system.

The main disadvantages that occur with matched elements include bandwidth limitations. The closer the match the more narrow-banded the system becomes. By applying a broadbanded matching system, it will not provide an ideal match at all frequencies over the band.

3.12.2 Matching using lumped components

The main advantage of using reactive components in impedance matching is the fact that there do not absorb any power or add any interference to the system. If a parallel inductance or capacitance is added to the circuit this will allow the load impedance to equal the input impedance of the system. When adding a series component to the circuit, this will lead to movement of the impedance along a constant resistance circle on the Smith Chart, while parallel components will cause a shift in the admittance along a constant conductance circle. The main effects of lumped component matching are shown in the table below [40]

Table 1 LC matching

Component	**Impedance and Admittance result**	**Description**
Series Inductor	$z \rightarrow z + j\omega L$	Clockwise movement along a resistance circle
Series Capacitor	$z \rightarrow z - j/\omega c$	Counterclockwise movement along a conductance circle due to smaller capacitance so increased impedance
Parallel Inductor	$y \rightarrow y - j/\omega L$	Counterclockwise movement along a conductance circle due to smaller inductance, so increased admittance
Parallel Capacitor	$y \rightarrow y + j\omega c$	Clockwise Movement along a conductance circle

It must be mentioned that in any region a number of circuits may work while others will not. So, in order to choose the more suitable circuit for any particular application the following parameters may be taken into consideration include stability, component value or personal preference. Each circuit and the particular region where it acts is shown below

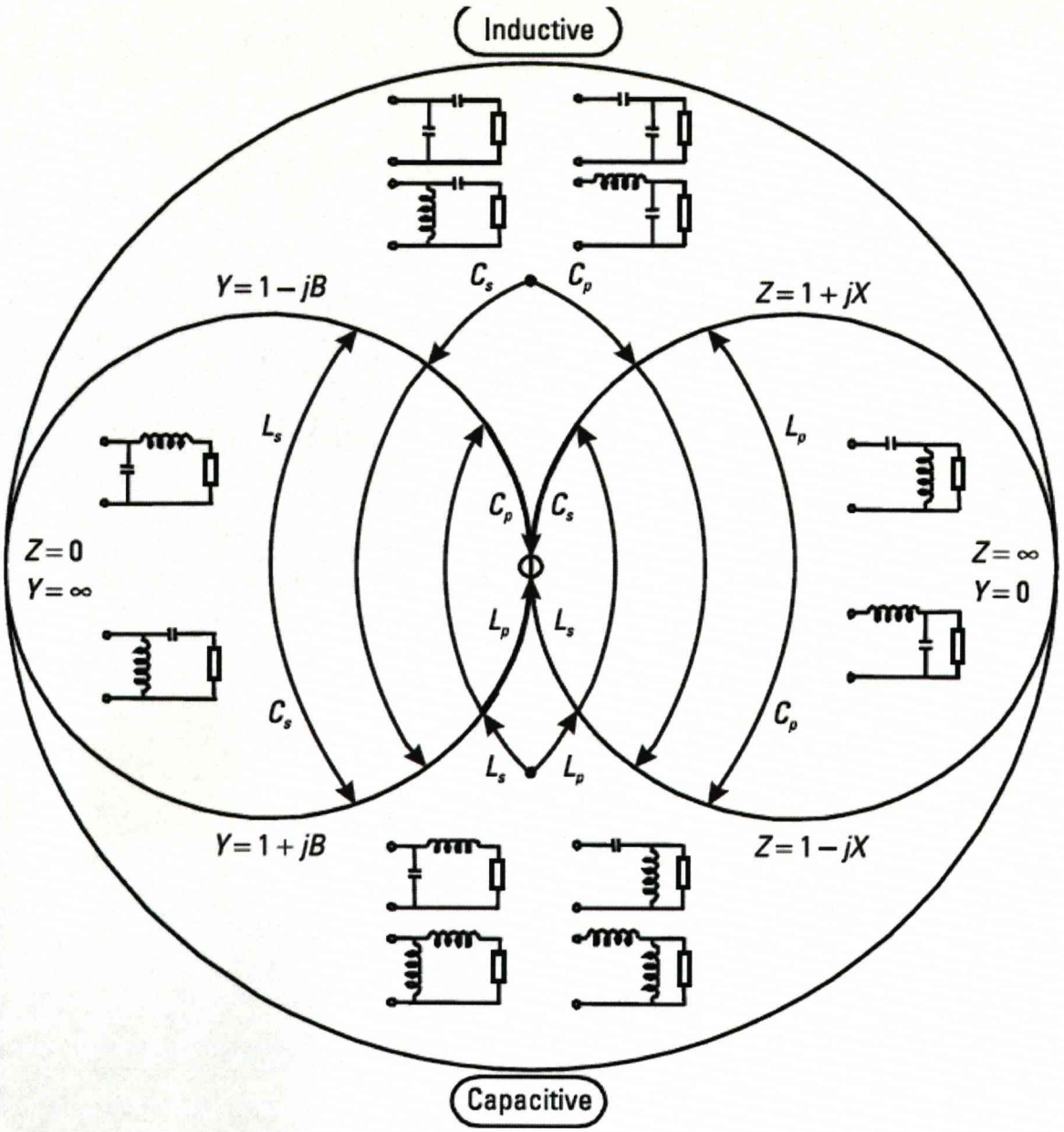

Figure 3.15 Area of each network operation

Figure 3.15 demonstrates where each LC matching circuit is required to perform an impedance match.

CHAPTER 4 METHODOLOGY

4.1 Antenna Design

The nature of the study requires the design and testing of various types of antennas in conditions that match the ocean environment. It includes measuring the antennas properties, like impedance, VSWR as well as measuring the antennae performance in a water tank with different conductivities of water in each case in order to observe the strength of the transmitted signal. The impedance is of particular importance in order to match it to the transmission line and determine the suitable antenna size for transmission.

As mentioned before antennas of different diameter and different type are applied although usually single and double loops antennas are preferred. Previous testing in the project now dictates the use of frequency region of up to 40MHz is where the propagation path with minimal attenuation in the far field has been found. The antenna diameter both for the transmitter and the receiver is usually around 30cm that is approximately the size for most applications in this frequency range.

The antennas are constructed by cooper wire and shaped accordingly to the ones required (loops, dipoles). They are usually coated to avoid losses and normalise the action of the antenna. Once the antenna has been constructed it is usually placed in a bucket of water, as large as possible in order to avoid reflections, connected to a network analyser that provides a Smith chart showing the antenna performance of an antenna over a range of frequencies up to 60MHz.

4.2Transmitter Design

In order to be able to match the conditions the system will encounter in the remote trials as well as to remove unwanted noise from the system the transmitter is placed into the water.

4.2.1 Transmitter system using DDS

This transmitter was mainly used in the 1-20MHz frequency range. The block diagram of its design is shown below.

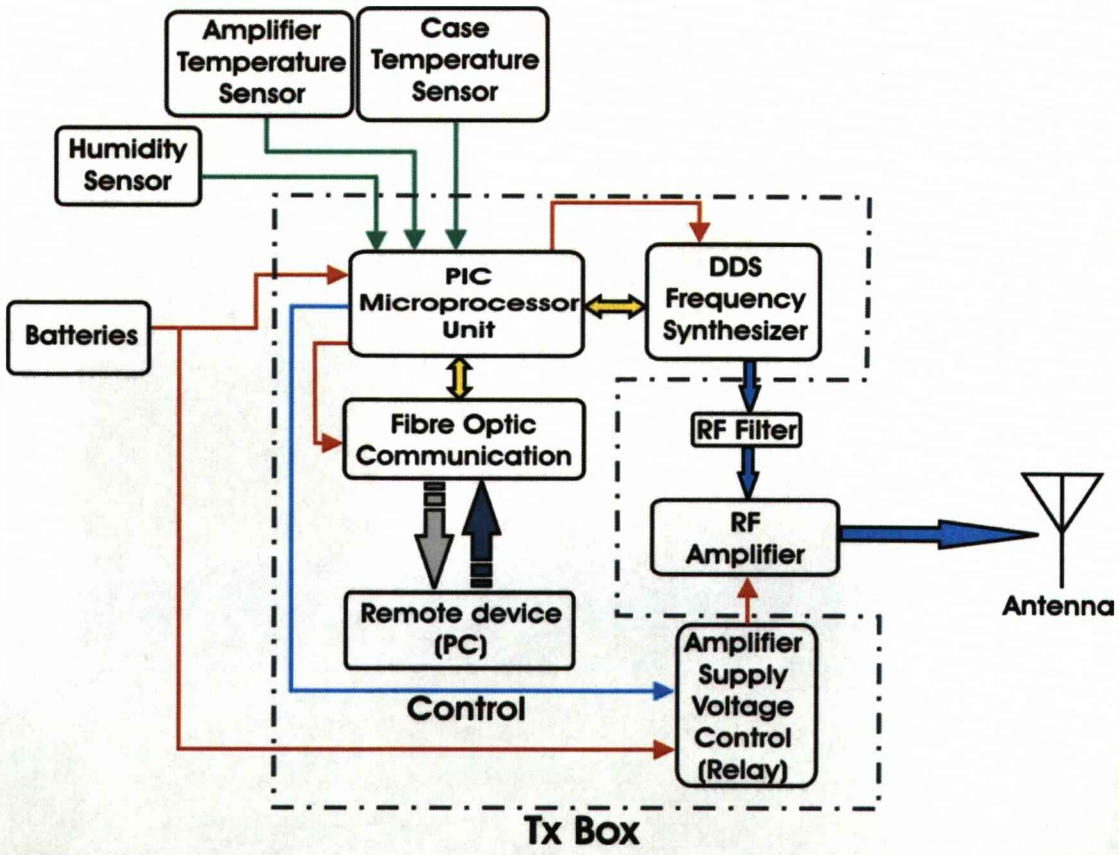

Figure 4.1 DDS transmitter block diagram

The required input is provided through the computer via the RS232 port. The latter is bidirectional, as it provides two separate communication channels for reception and transmission of the signal. The frequency selection is provided by an on screen interface shown below

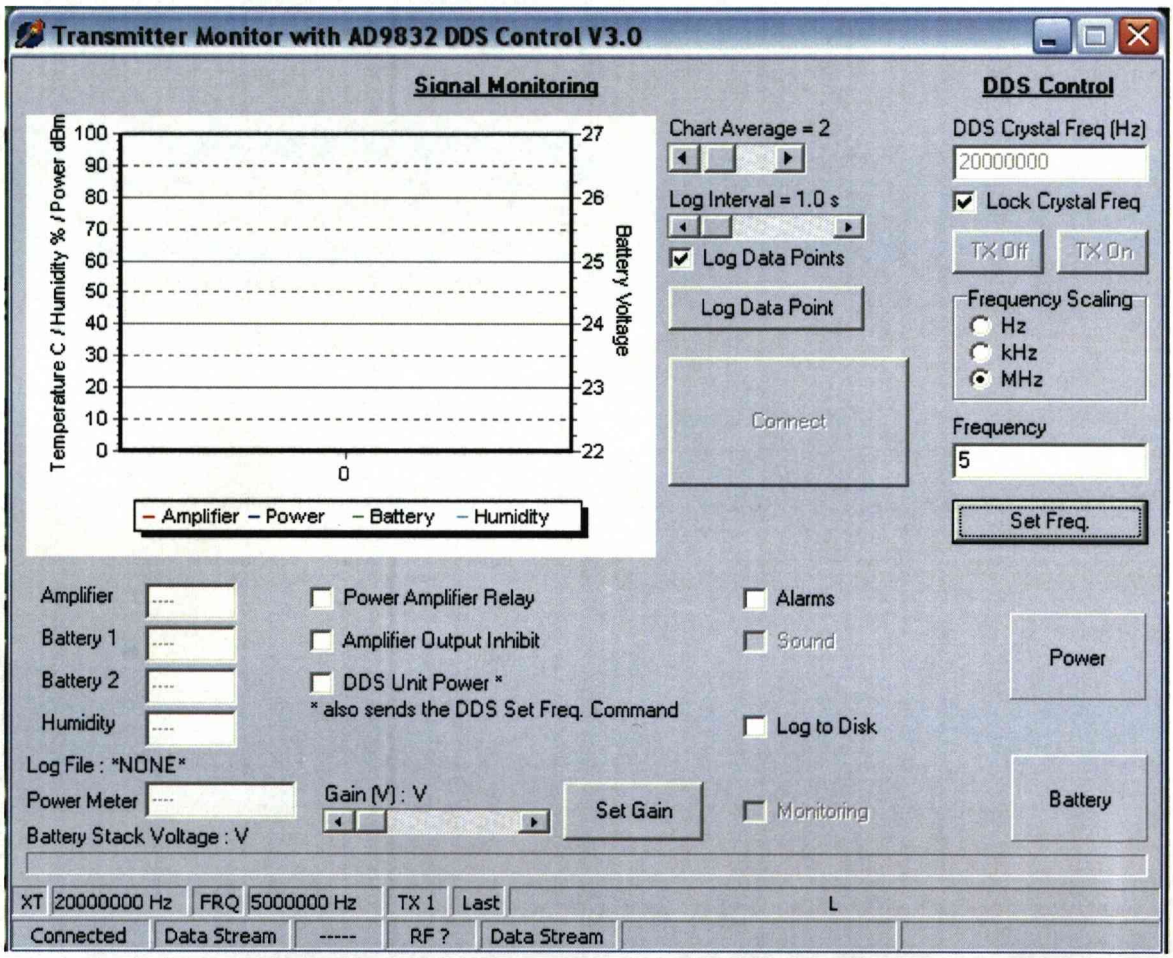

Figure 4.2 DDS Transmitter Interface

As it can be seen from fig4.2 the interface provides the frequency selection unit as well as feedback obtained from the transmitter for the state of the battery voltage and humidity. The information is then sent to the transmitter via optical fibres.

The RSS232 is connected to the transmitter via optical fibre cables. The output from the port is converted into a TTL signal. The conversion is performed by a 5V powered multichannel

RS232 receiver. As in any typical optical communication link, the light coming out of the optical source travels through the fibre and is detected by photodetectors, which in turn convert the light into a TTL signal that is used to input the PIC microcontroller. Once the frequency selection is complete the PIC sends an acknowledgement through the receiving channel in the reverse process.

The signal travels through the optical fibre and reaches the PIC microcontroller. The PIC apart from sending the confirmation message of the signals arrival, is also connected to two temperature sensors, one for the amplifier the other for the case temperature, a humidity sensor and also monitors the battery power. This information is send back to computer and displayed on the interface.

Once the signal arrives at the PIC, it is then directed to the direct-digital- synthesizer (DDS).The DDS chip applies digital data blocks as a mean to generate analogue sine waves signals referenced to a fixed clock source [41]. Originally the output signal is in a digital form before it passes through a digital to analogue (D/A) converter and so obtaining the required analogue waveform.

The basic components of a DDS include a reference block, an address counter, a programmable read only memory (PROM) and a D/A converter. Each of the PROM's memory locations, which correspond to a complete sine wave cycle, are accessed by the address counter and the contents of the locations are then sent to the D/A converter. The output frequency of the DDS chip depends on. The frequency of the reference depends on the frequency of the reference clock and the sinewave step size that is programmed into the PROM.

Once the circuit is constructed it is then placed inside a metal box to avoid radiation that is emitted from the system. The complete transmitter used is shown below

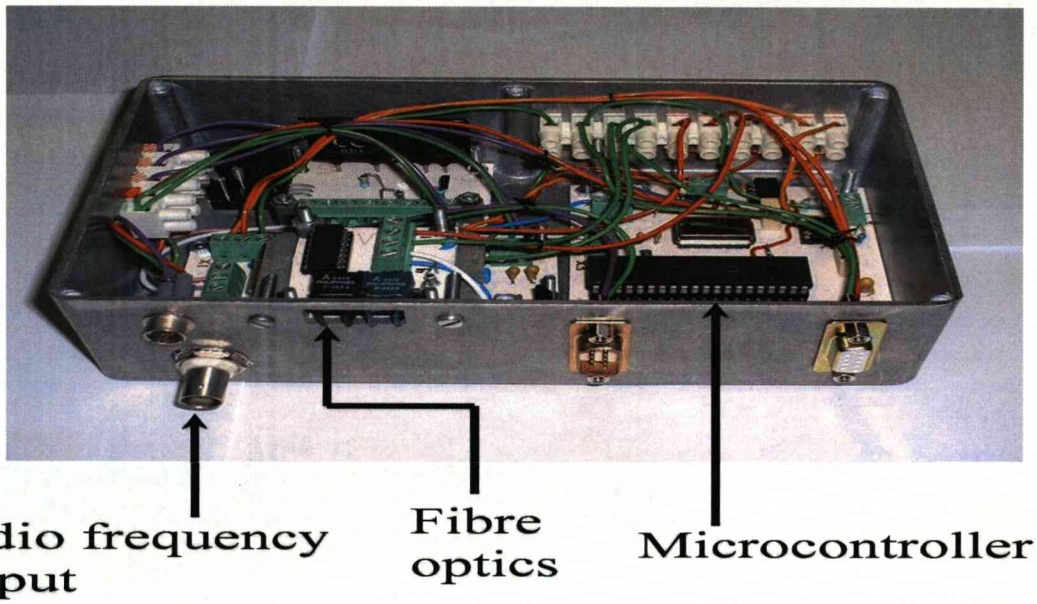

Figure 4.3 DDS based Controller

4.2.2 Crystal Oscillator design

The DDS based transmitter was optimized and mainly used for the frequency range between 1-20MHz. At higher frequencies it was unstable and so a crystal based oscillator transmitter system that provides high stability was designed whose block diagram is shown below

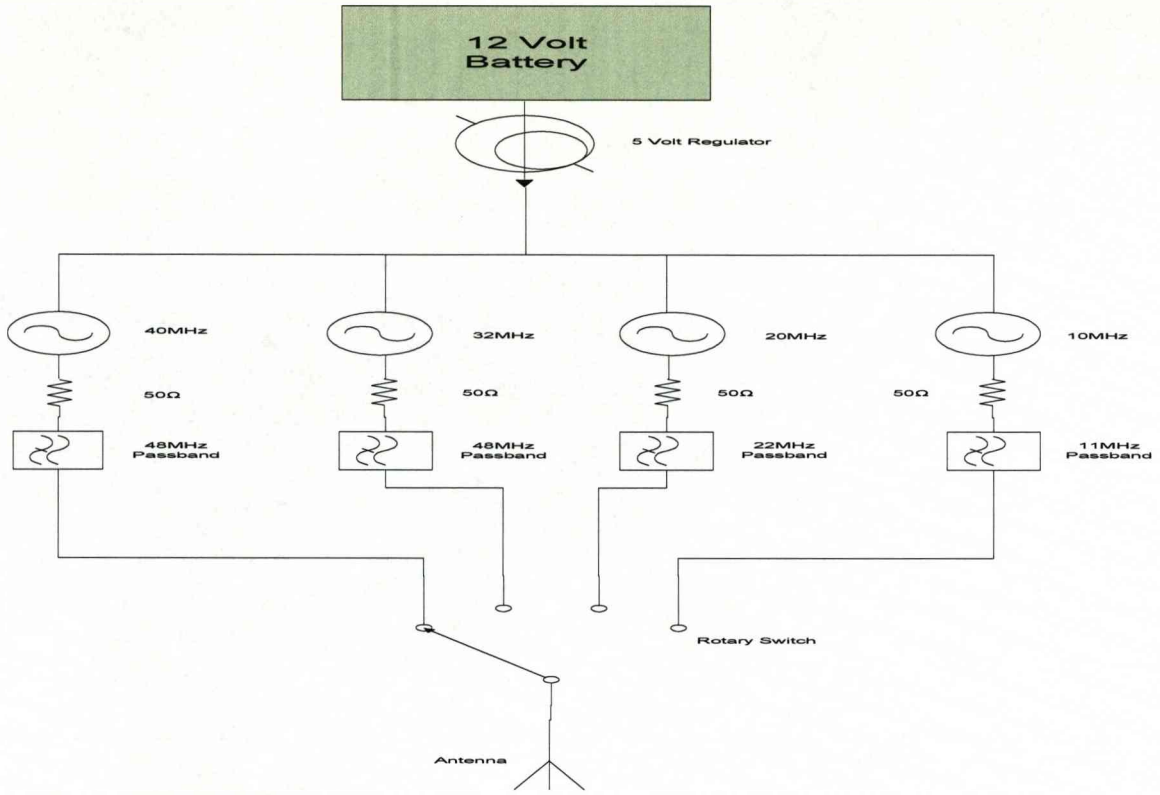

Figure 4.4 Crystal oscillator transmitter circuit diagram

The system is powered by a 12V battery, while a 5V voltage regulator ensures that the correct amount of voltage passes through the crystal. Once the signal leaves the oscillators it passes through a 50Ω resistor in order to match it to the line. The choice of the frequency is performed by a simple analogue rotary switch. The low-pass filter is added after the output to ensure the removal of unwanted harmonics. As it can be seen multiple filters are used each one for a different frequency.

As it can be seen the main component of the circuit is the crystal oscillator. Its main components are oxygen and silicon (SiO_2). It operates with the piezoelectric principle whereby an externally applied mechanical stress is converted to a voltage across the crystal. The vibration mechanism depends on the way the crystal is cut [42].

The equivalent circuit of a crystal resonator is shown below

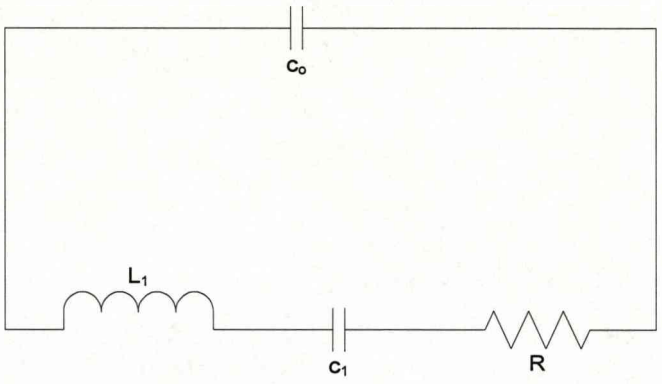

Figure 4.5 Crystal oscillator equivalent circuit

c_o represents the capacitance between the electrodes. The inductance L_1 represents the mechanical inertia of the crystal, c_1 is due to compliance and R arises predominantly due to frictional losses.

It can be seen from the equivalent circuits that there are two possible ways in which the circuit can reach resonance. The first is the series resonance of L and c which provides very low impedance. The other is a parallel resonance, when the value of c equals c_1. The latter mode provides higher impedance and is most commonly used although there are not many differences between the two modes.

The main advantage of this transmitter is that it provides higher stability and a clearer sine wave signal compared to the DDS. Its main disadvantage is that in order to change the frequency as well as change the low-pass filter, the transmitter needs to be removed and both these tasks performed manually that is more time consuming than with the DDS transmitter.

4.3 Lab Tank Trials

In order to be able to compare the theoretical results with practical ones, it is necessary to have an experimental environment that will approximate the antenna currently studied with

the required homogenous isotropic dissipative medium. The currently applied environment is within a polyethylene tank which dimensions are 2.5m length, 1.5m in height and 1.5m width. Ideally the tank must be as large as possible but this is sufficient considering size and cost. It is constructed from polyethylene of thickness about 4mm in order to avoid reflections that can lead to errors in the measurement associated with wooden tanks especially in less-dissipative media [43]. The tank in order to avoid leaks is then lined with a FLP HD (Heavy Duty) PVC with 0.5mm thickness.

The tank in the beginning is filled with tap water were the first experiments are performed. Salt is added gradually until the concentration of the whole tank reaches the normal ocean levels. Measurements are taken at each level in order to observe the effect of different concentrations of salt in water in order to determine the effects of different levels of conductivity on the signal strength.

The transmitter is placed inside a plastic box with the batteries and any matching circuit applied to the antenna. The antenna is covered by plastic to avoid damage or any leaks towards the electrical equipment. This is done to avoid any interference from radiation from the transmitter box and to be able to match the conditions that will be met in the real environment.

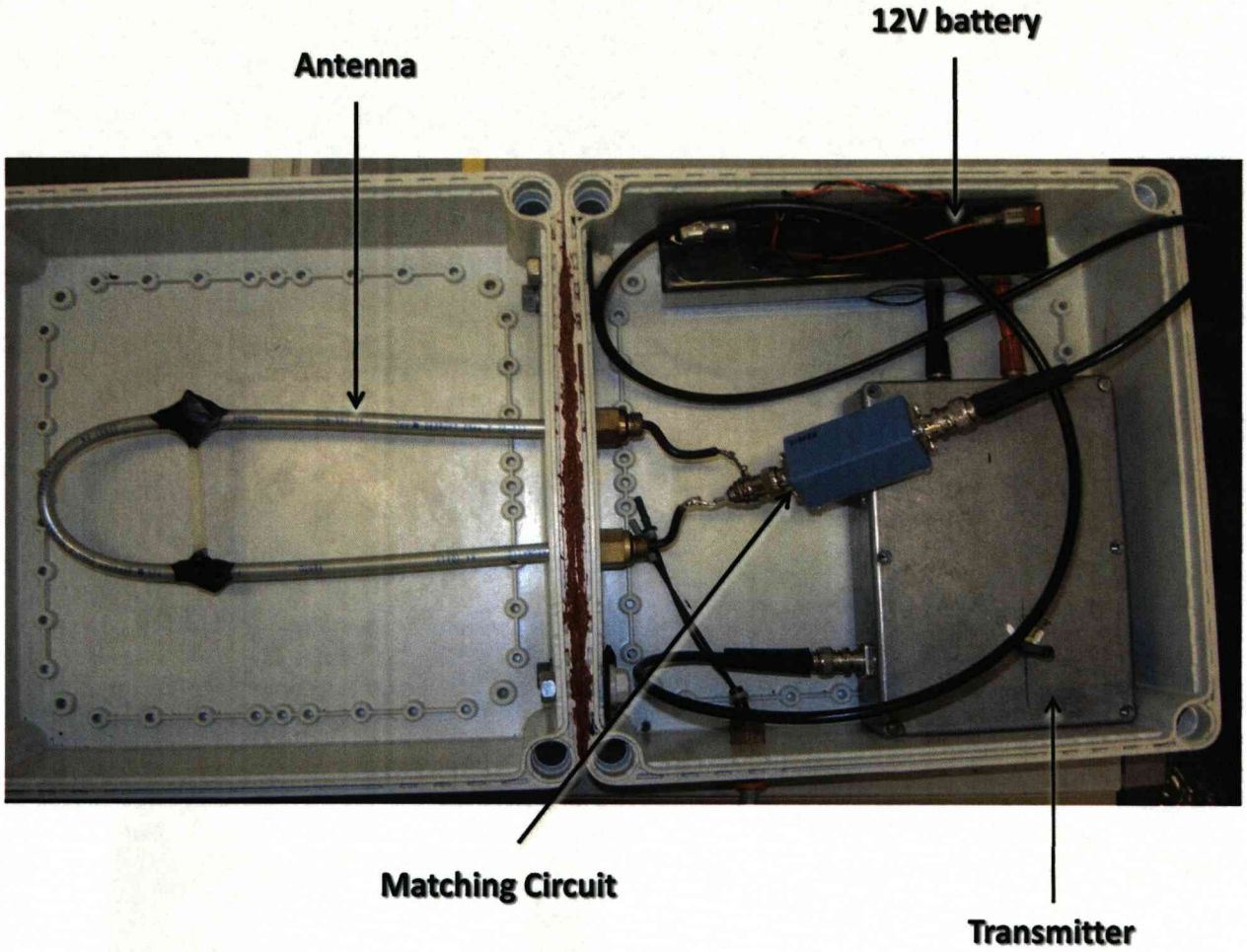

Figure 4.6 Transmitter Setup

Sea water is very harmful for the transmission signal. As mentioned before the tank will be full of seawater that will not be helpful for the trials. In order to avoid the damaging effect of seawater the antenna is placed in a barrel full of tap water, for reasons that will be explained below. The barrel dimensions shown below are 70cm (height), 47cm (diameter) and 47cm (width).

Figure 4.7 Barrel in which transmitter is placed

On the other hand the receiver usually consists of a double loop antenna connected to an Anritsu MS2711D spectrum analyser that is used to measure the signal shown in figure 4.8.

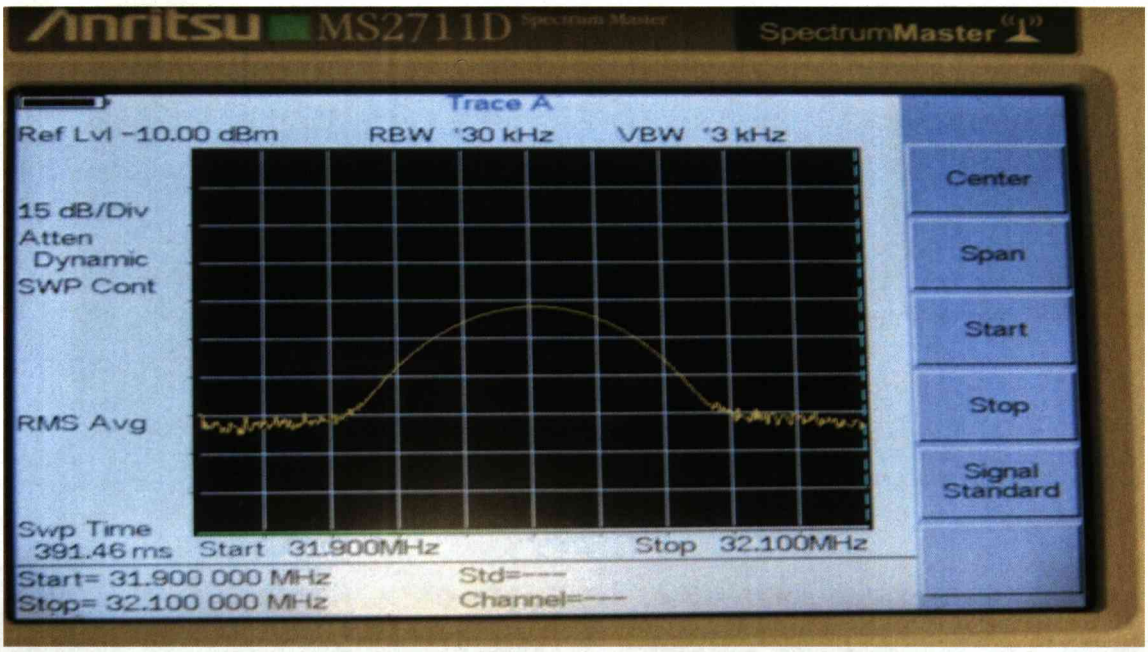

Figure 4.8 Anritsu MS2711D spectrum analyser

The next step is field trials that must be performed in a larger and most natural environment. These trials will be performed in the Liverpool dock due to its close proximity to the labs as well as the large area provided. The transmitter and receiver circuits are placed in different

larger boxes in order to be able to withstand the different conditions and different matching methods are required.

4.4 Impedance Matching

In order to improve the transmission signal, the transmitter antenna is matched to the transmission line. This is achieved by adding lumped LC circuits. The impedance is measured using the network analyser and the VSWR is calculated. The values for the appropriate frequencies are identified and the calculation for the suitable match is performed by using the program LCmatch by Radiocom shown below

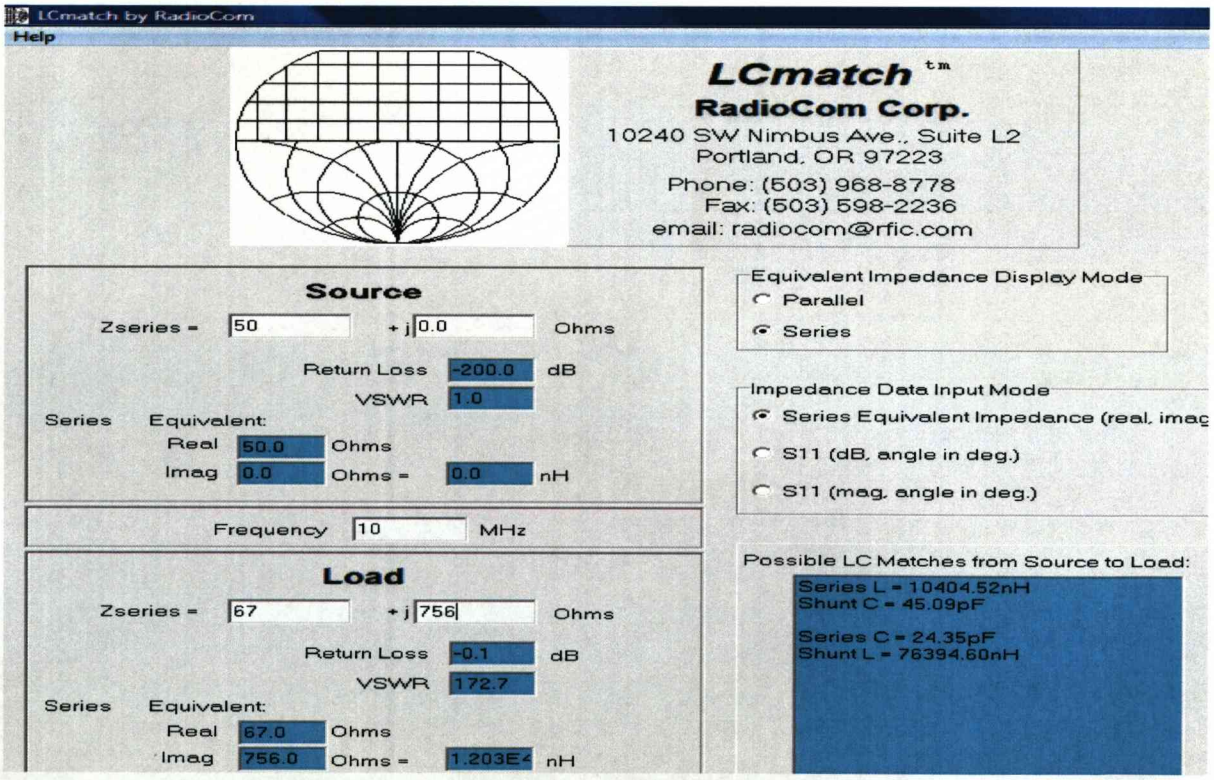

Figure 4.9 LC match by RadioCom

Once the appropriate value and connection is identified the matching is performed inside a BNC box shown below

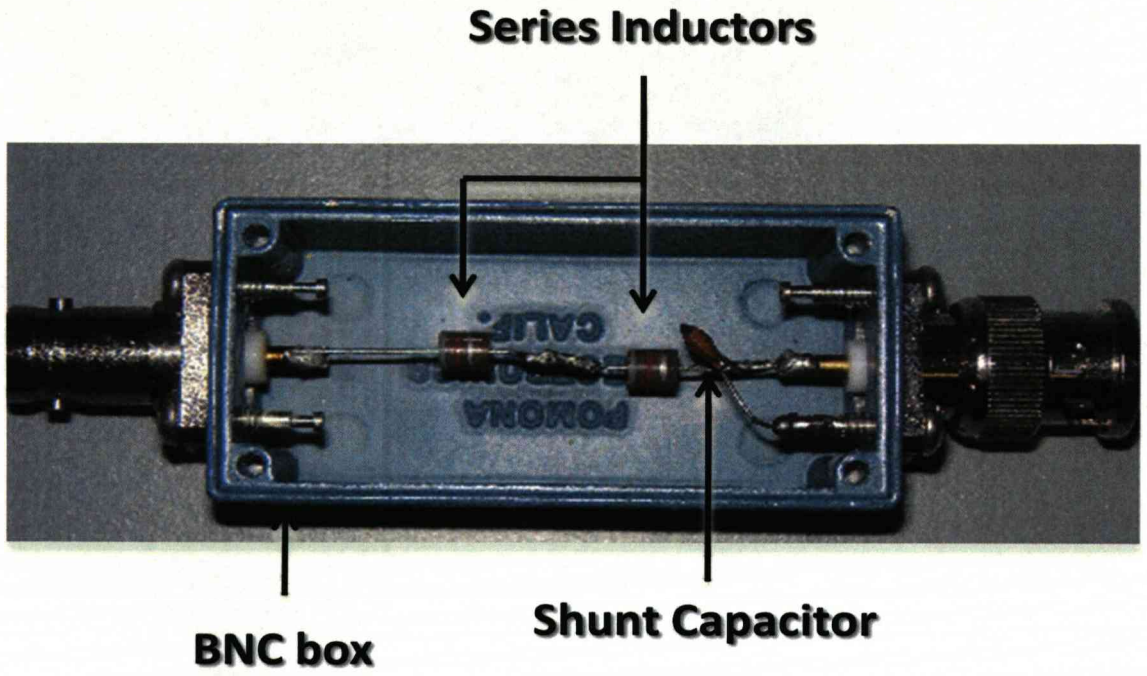

Figure 4.10 Typical matching Circuit

Once the match is performed the procedure is performed with the BNC box and the VSWR is measured again. It must be mentioned that the whole measurement is performed with the system as shown in figure 4.6 and place in the barrel of figure 4.7.

4.7 Coaxial Antenna construction

The antenna that was tested after the two rod antenna was a coaxial antenna that consisted of two rods of 16cm length has an inner copper conductor of radius 1.6cm while the radius of the inner part of the outer conductor is 1mm. The antenna is surrounded by liquid and that is kept in place by a cylinder of height and diameter of 20 cm and

Figure 4.11 Coaxial Antenna

CHAPTER 5 WATER ANTENNA DESIGN

5.1 Introduction

Studies of experiments performed show that EM waves can be propagated through seawater by conventional EM wave propagation [44] and by radiation generated from excitation of the dielectric dipoles in seawater caused by AC electric fields. The electric permittivity ε is complex while the conductivity σ is made up of two parts the one consisting the conductivity of the free ions in seawater mainly Na^+ and Cl^- (σ□) and the dielectric dipole loss term (σ□□). The real part of the conductivity has a value of 4S/m for seawater while the imaginary is much smaller and equals to

$$\sigma'' = \omega \cdot \varepsilon'' \quad (5.1)$$

The large attenuation associated with underwater EM communications is mainly caused by the conductivity. By applying Maxwell's equation the electric field strength E equals

$$E = E \cdot e^{-\alpha z} \sin(\omega t - \beta x) \quad (5.2)$$

$$\text{where } \alpha + j\beta = \sqrt{j\omega\mu(\sigma + \omega\varepsilon'' + j\omega\varepsilon')} \quad (5.3)$$

The table below shows that EM propagation is possible using standard loop and dipole antenna

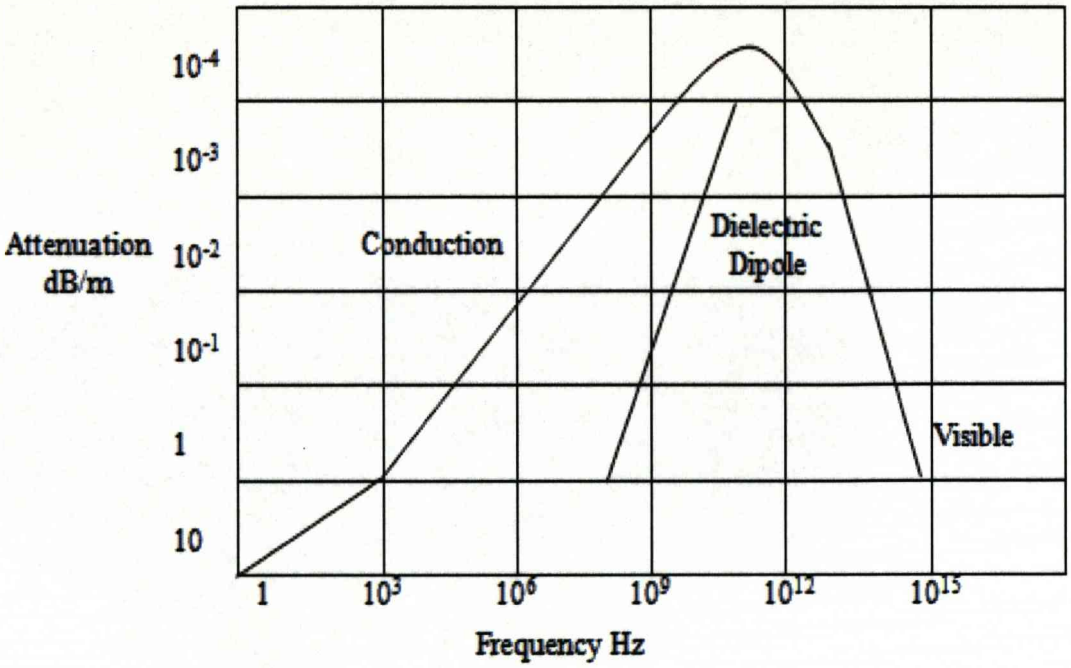

Figure 5.1 The attenuation of conduction and dielectric dipole EM waves

This chapter deals with the antenna design and its performance in seawater. It includes impedance measurements and a theoretical model of how the electric field and power is distributed in seawater. It also includes simulations based on the latter and comparisons with the recorded measurements. It must be noted that the model is based not only on current results but also on data obtained from previous studies [45], [46], [47].

5.2 Antenna Design

The aim of the design is to create an antenna that produces a strong electric field in the water. The antenna most suitable for this study is a simple copper 2-rod antenna that is surrounded by tap water in a PVC barrel shown in section 4.7, with dimensions 25cm height and diameter α=1mm while the distance between the two rods is at 7cm as shown below

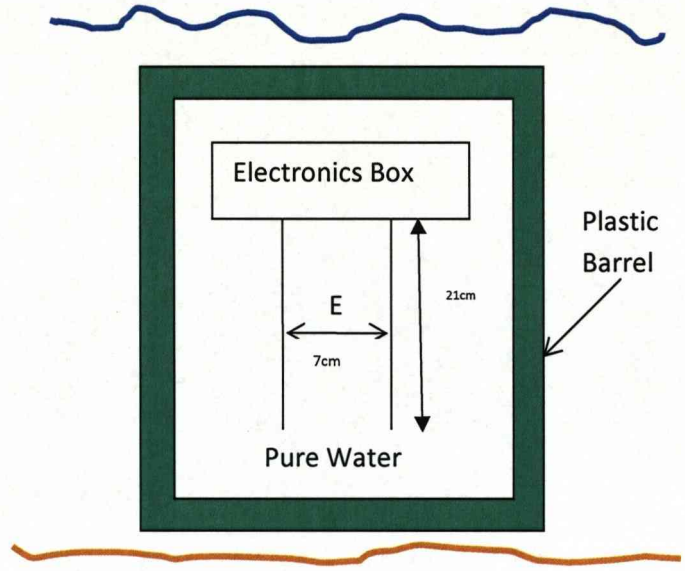

Figure 5.2 Two rod antenna

Essentially the antenna design is an open ended transmission line as shown in section 3.7.1. This antenna has a wide variety of uses in telegraphy, as on overhead power line operating at high voltages as well as in radio transmission. Its main characteristic is having resistance per unit length while the inductance and capacitance per unit length are usually quite small. It must be taken into account that there will be variations of the actual design shown above to accommodate higher frequencies. The variations are based on the fact that distance between the conductors is large compared to the antenna diameter but at high frequencies, radiation losses are minimised by bringing the two rods closer together.

From figure 5.1 the impedance of the transmission line of length l equals

$$Z = Z_0 coth(g) \quad (5.4)$$

where $g = \gamma \cdot l$ (5.5)

$$\gamma l = \sqrt{(j\omega L + r)(j\omega C + G)} \quad (5.6)$$

$$\text{and } Z_o = \sqrt{(j\omega L + r)/(j\omega C + G)} \quad (5.7)$$

where L is the inductance per meter (H/m).

C is the capacitance per meter (F/m).

G is the transconductance per meter (S/m).

The inductance and the capacitance are given by the following equations

$$L = \frac{\mu_o}{\pi} \ln d/\alpha \quad (5.7)$$

$$C = \frac{\pi \varepsilon_o \varepsilon_r}{\log_e(d/a)} \quad (5.8)$$

The resistances are given as follows

$$r = \frac{\rho l}{\pi \alpha \delta} \ (\Omega/m) \ (5.9)$$

$$where \ \delta = \sqrt{\frac{2}{\sigma \mu \omega}} \quad (5.10)$$

and ρ is the resistivity of copper=1.68×10^{-8}(Ω/m) and so by going back to equation (5.9)

$$r = \frac{1}{\pi \alpha} \sqrt{\frac{\mu \omega \rho}{2}} \leftrightarrow$$

$$r = 8.2 \times 10^{-5} \frac{\sqrt{f}}{a} \ (\Omega/m) \ with \ f \ in \ MHz \ (5.11)$$

G can be calculated by linking it to the dimensions of the capacitance

$$\frac{G}{C} = \frac{\sigma}{\varepsilon_o \varepsilon_r} \leftrightarrow$$

$$G = \frac{\pi\sigma}{\log(d/a)} \quad (5.12)$$

In order to obtain the equivalent circuit of the antenna we must return to equation 5.4 and using the expansion for coth(g) and assuming g is small

$$Z = Z_0 coth(g) \leftrightarrow$$

$$Z = Z_o\left(\frac{1}{g} + \frac{g}{3} - \frac{g^3}{45}\right) \leftrightarrow$$

$$Z \cong Z_o\left(\frac{1}{g} + \frac{g}{3}\right) \leftrightarrow$$

$$Z = \frac{1}{(j\omega C + G)l} + \left(\frac{j\omega L + r}{3}\right) l \quad (5.13)$$

The equivalent circuit is shown below

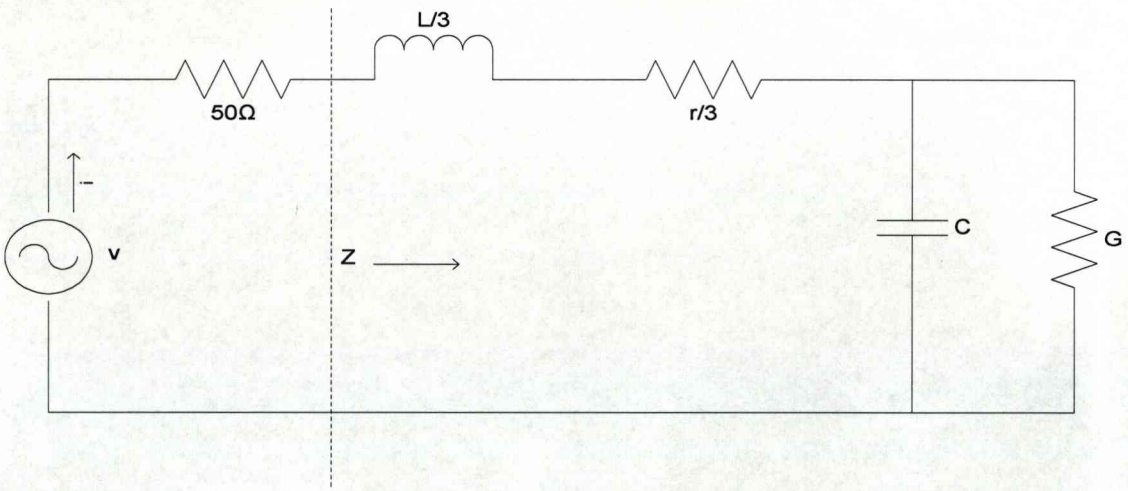

Figure 5.3 Antenna Equivalent Circuit

From figure 5.2 by calculating the power in the resistance (1/G) can be used to estimate the power used for dipole excitation

$$i = \frac{v}{50 + Z}$$

The voltage across the resistance is v^1.

$$v^1 = v - i(50 + j\omega L/3 + r/3)l \leftrightarrow$$

$$v^1 = v\left(\frac{Z - (j\omega L/3 + r/3)l}{50 + Z}\right) \leftrightarrow$$

$$v^1 = v\left(\frac{1}{(j\omega C + G)l}\frac{1}{(50 + Z)}\right) \quad (5.14)$$

$$P = v^1 Gl \quad (5.15)$$

5.3 Antenna in seawater

Once the insulated antenna is placed into seawater, by applying a voltage v_a between the rods, a smaller voltage v_s is generated within the seawater as shown below

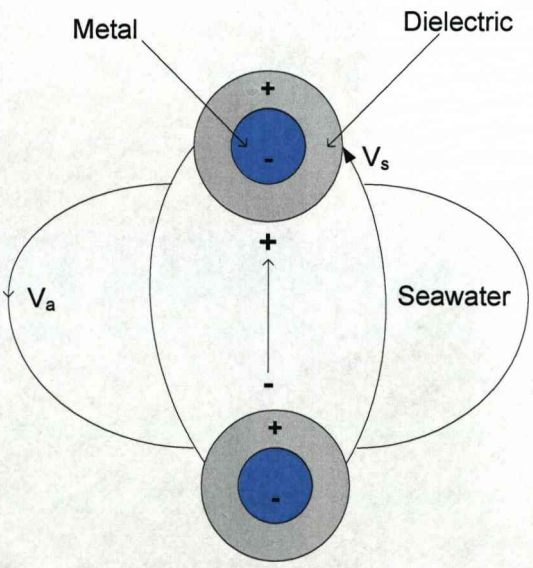

Figure 5.4 The Propagation Mechanism in Seawater [15]

The dipole radiation is circular around the antenna rods while EM propagation is transverse to the circle. The voltage v_s is greatly minimised by electric current conduction in the seawater due to the conductivity as well as the dielectric loss of the water molecules. The latter is associated with dipole oscillations within the water and leads to dipole radiation and EM propagation through the seawater.

5.3.1 The Effect of Water Conductivity

The voltage v_a is distributed across the insulator and the seawater. The equivalent circuit of the antenna in seawater can be shown by three capacitors and this leads to the creation of a voltage v_s

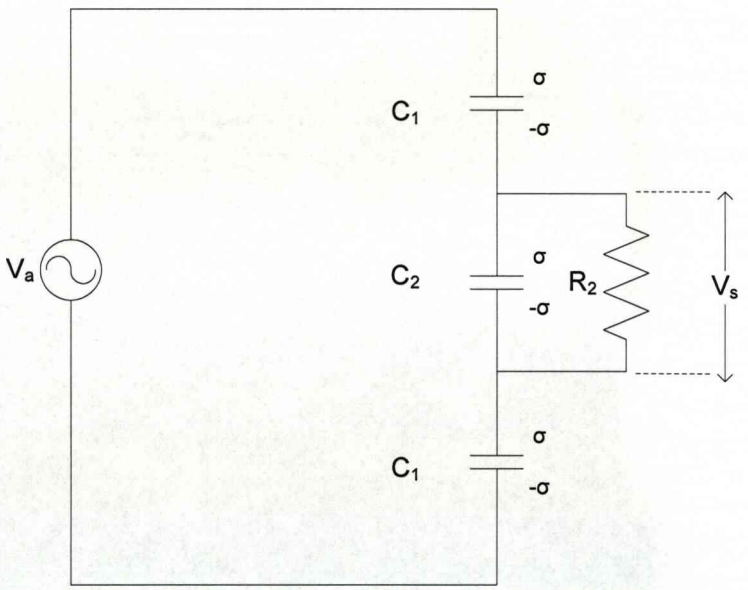

Figure 5.5 Antenna equivalent circuit in seawater

The voltages can be shown as

$$\frac{v_s}{v_a} = \frac{1}{2C_2/C_1 + 1} \quad (5.16)$$

The values of C_1 and C_2 can be estimated as

$$C_1 = \frac{2\pi\varepsilon_o\varepsilon_{r1}}{\log(b/\alpha)} \quad (5.17)$$

$$C_2 = \frac{\pi\varepsilon_o\varepsilon_{r2}}{\log(\alpha/b)} \quad (5.18)$$

where ε_{r1}=4.2

ε_{r2}=72

α=1mm is the diameter of the wire

b=1.8mm is the diameter with the insulation

d=170mm is the distance between the rods

So,

$$\frac{2C_2}{C_1} = \frac{\varepsilon_{r2}}{\varepsilon_{r1}}\frac{\log(b/\alpha)}{\log(d/b)} \approx 2.25$$

$$\frac{v_s}{v_a} = 0.29 \quad (5.19)$$

As it can be seen there is a 71% loss once the signal is generated inside the water. As it can be seen from the equations by bringing the two rods closer the losses are smaller. Additional losses are also produced due to capacitance C_2 that has a fast time constant caused by the conductivity of seawater.

5.3.2 Effect of time constant

The conductivity of the water leads capacitance C_2 to have a leakage resistance R_2. The time constant τ in which v_s decreases in the water is estimated as

$$v_t = v_s exp(-\tau/C_2R_2) \quad (5.20)$$

$$\text{where } \tau = C_2R_2 = \frac{\varepsilon_0\varepsilon_r}{\sigma} \quad (5.21)$$

The following table (2) shows the electrical properties of water and seawater

Table 2 Electrical properties of tap and salt water

	Dielectric Constant ε_r	Conductivity σ	Time Constant τ
Seawater	72	4S/m	159ps
Tap Water	81	0.02S/m	35.8ns

As it can be clearly be seen the time constant of tap water is much smaller than that for seawater and so the voltage v_s decreases slower in tap water and so there is more energy available to generate the transmitted EM wave.

5.3.3 Effect of Dielectric Loss

The resistance R_2 represents the conduction loss and dielectric dipole loss. The latter is of particular interest because it is the source of dipole radiation through the water.

The electrical power from the antenna can be obtained by comparing the electrical conductivities

$$P = P' + P'' = (\sigma' + \sigma'')E^2 \quad (5.22)$$

where P' is the radiation from the antenna

P'' is the dipole radiation

$$\frac{P''}{P} = \frac{\sigma''}{\sigma} = \frac{\omega\varepsilon''}{\sigma} \quad (5.23)$$

The fractional voltage is given as

$$\frac{v_i}{\hat{v}} = \sqrt{\frac{\omega\varepsilon''}{\sigma + \omega\varepsilon''}} \quad (5.24)$$

where $\hat{v}$ is the average signal voltage.

In order to calculate ε□′ we must apply the Debye equation introduced in section 3.6.2

$$\varepsilon'' = (\varepsilon' - \varepsilon'_\infty)\frac{\omega\tau}{1 + \omega^2\tau^2}$$

where ε□$_\infty$=3 at high frequencies

τ=8.20×10^{-3}ns

$$\text{so } \omega\varepsilon'' = 24.92 \cdot 10^{-9} f^2 \text{ with f in MHz} \quad (5.25)$$

5.3.4 Effect of Standing Waves

If there are no mismatches between the coaxial transmission line and the antenna so that the antenna impedance equals the characteristic there will be no loss of power P so that the voltage v developed across the antenna equals

$$v = \sqrt{2Z_o P} \quad (5.26)$$

If there is a mismatch then a standing wave is set up. The absorbed power P_A equals

$$P_A = \frac{4S}{((1+S)^2)} \quad (5.27)$$

where S is the VSWR

So the voltage generated at the transmitting antenna is

$$v_A = \sqrt{2Z_o P}\frac{(4S)^{1/2}}{(1+S)} \quad (5.28)$$

5.4 Antenna Power

As it can be seen the transmitted signal consisted of antenna radiation as well as radiation transmitted due to dipole oscillations. By applying equations (5.22) and (5.23) we get

$$\frac{P''}{P_o} = \frac{0.2 \times 10^{-6} f^2}{\sigma} \quad (5.29)$$

where P_o is the input energy

The equation shows that dipole radiation even at the MHz regions used in this study, is comparatively low. Furthermore additional losses are accumulated due to attenuation of the signal when it propagates as can be shown by the following equations

$$\gamma = \alpha + j\beta = \sqrt{j\omega^2\mu(\varepsilon' + j\varepsilon'')} \leftrightarrow$$

$$\gamma = j\omega\sqrt{\mu\varepsilon'}\left(1 - j\frac{\varepsilon''}{\varepsilon'}\right)^{1/2} \quad (5.30)$$

The attenuation coefficient α is

$$\alpha = \omega\sqrt{\mu\varepsilon'}\left(\frac{\varepsilon''}{2\varepsilon'}\right)^{1/2} \leftrightarrow$$

$$\alpha = 4.32 \times 10^{-6} f^2 \text{ with } f \text{ in MHz} \quad (5.31)$$

The attenuation loss is rather small for short distances and low frequencies. The most significant losses are due to diffraction and can be calculated as

$$\frac{P}{P_o} = \frac{A}{4\pi R^2} \quad (5.32)$$

where A is the receiving antenna area

If the receiving antenna has a diameter of λ/10 then

$$\frac{P}{P_o} = \frac{1}{400}\left(\frac{\lambda}{R}\right)^2 \quad (5.33)$$

$$\text{where } \lambda = \frac{c}{\sqrt{\varepsilon'} f} = \frac{35 \times 10^6}{f} \quad (5.34)$$

The theoretical results are shown in the following table (3)

Table 3 Signal Attenuation

f (MHz)	λ(m)	P/P_o R=100m	Diffraction Loss dB	Attenuation Parameter $2\alpha z$	Attenuation Loss dB	Total Loss dB
1	35	$3.06 \cdot 10^{-4}$	-35	$8.64 \cdot 10^{-4}$	-0	-35
10	3.5	$3.06 \cdot 10^{-6}$	-55	$8.64 \cdot 10^{-2}$	-0.4	-55
20	1.75	$7.66 \cdot 10^{-7}$	-61	$3.46 \cdot 10^{-1}$	-1.5	-63
30	1.17	$3.40 \cdot 10^{-7}$	-65	$7.78 \cdot 10^{-1}$	-3.4	-68
100	0.35	$3.06 \cdot 10^{-8}$	-75	8.64	-38	-113

From table 3 it can be seen that transmission of dipole radiation can be achieved at frequencies below 100MHz over a distance of 100m without being affected from diffraction loss.

In order to improve the generation of dipole radiation better coupling must be achieved between the antenna and the transmission medium. The relative power inserted into the dielectric water dipoles can be shown in terms of conductivity as

$$\frac{P}{P_o} = \frac{\sigma''}{\sigma' + \sigma''} \quad (5.35)$$

where $\sigma'' = \sigma' + \omega\varepsilon'' = 0.2 \times 10^{-6} f^2$ (5.36)

$$\sigma' = 4S/m$$

If we decrease the real part of the conductivity, the power transmitted will be much stronger due to dipole radiation. So we test the model by inserting tap (σ=2×10^{-2}S/m) and distilled (σ=2×10^{-4}S/m) water

Table 4 Emmited power by the antenna

***f* (MHz)**	**σ = 4S/m**		**σ = 2×10^{-2}S/m**	**σ = 2×10^{-4}S/m**
	P/P$_o$	**P/P$_o$ dB**	**P/P$_o$ dB**	**P/P$_o$ dB**
1	5·10^{-8}	-73	-50	-30
10	5·10^{-6}	-53	-30	-10.4
20	2·10^{-5}	-47	-24	-5.4
30	4.5·10^{-5}	-43	-20	-3.2

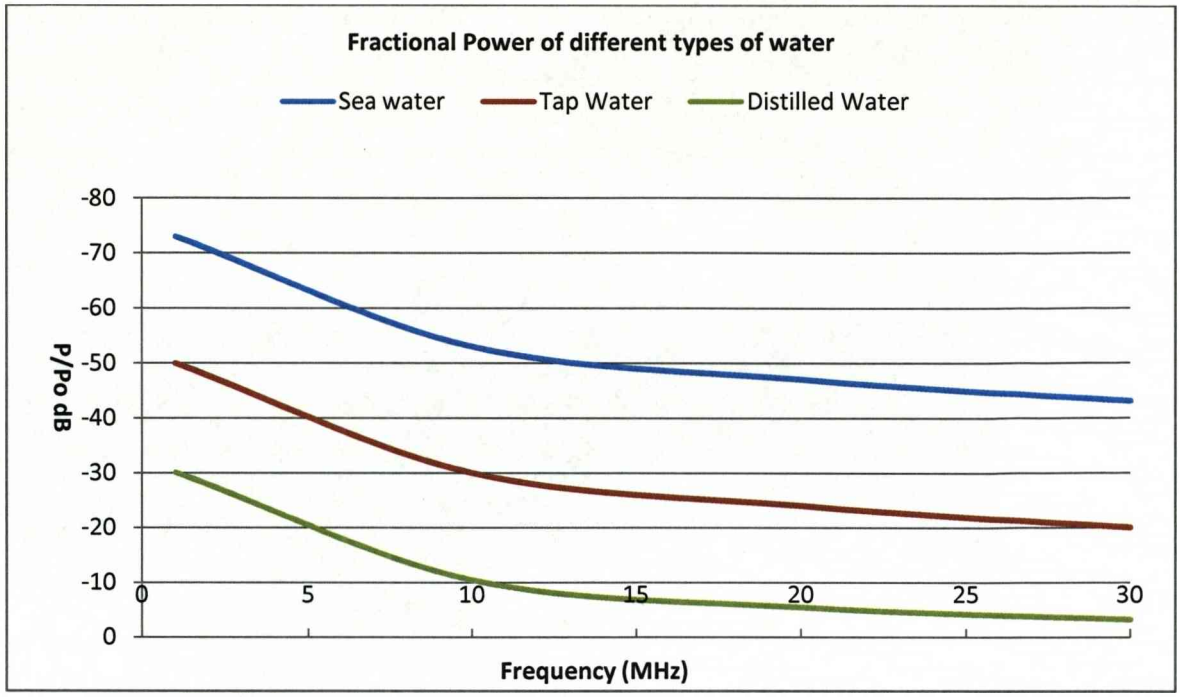

Figure 5.6 Emitted power for different conductivities of water

As it can be seen in tap water the signal is 23dB stronger than in salt water. If the medium is changed to distilled water then the signal is 40dB stronger with distilled water. The latter inconvenience especially when applying the latter is that it is easily contaminated in the air and so allows only a short time for any experiments to be performed.

5.5 Applying the model

The next step is to use all the above suggested theory in order to create a program that will validate the suggested model. The program was performed in MATLAB and contains most of the equations for the conductivity, power or impedance shown above. After the results are obtained they are tested against actual measurements undertaken.

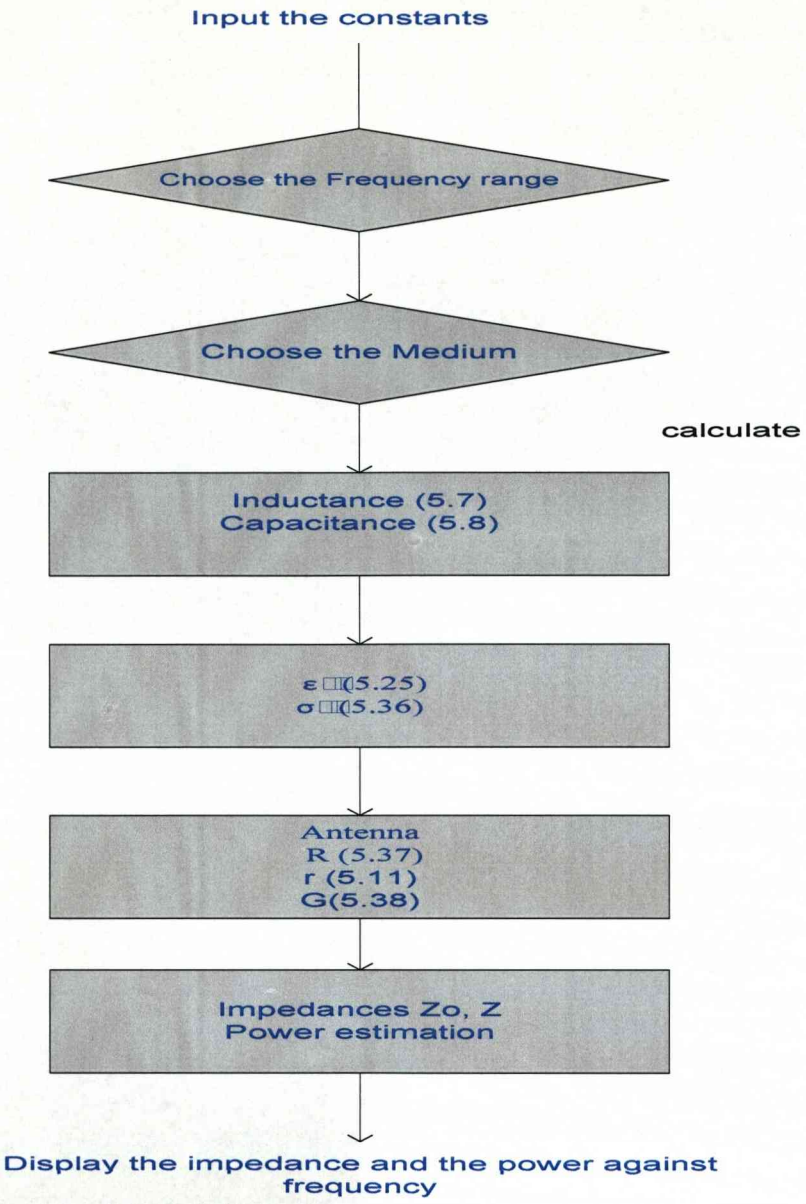

Figure 5.7 Steps in calculating power and impedance

The bracket in each parameter specifies the equation that is needed for the calculation. The impedance can be calculated from the equivalent circuit in fig 5.2. The additional equations used include the resitance of the antenna R and transconductance G shown below

$$R = \frac{\log(d/a)}{\sigma'' \pi l} \quad (5.37)$$

$$G = 1/R \quad (5.38)$$

The impedance and power calculations are performed from the equivalent circuit. The results were performed in MATLAB but were transferred to excel in order to compare them with the actual measurements. The full program used is in the appendices.

5.6 Impedance Measurements

This part of the study will show the impedances measured and compare them to theoretical simulations for the impedance. They include the current antenna as well as a shorter version of the one described.

5.6.1 Impedance in Tap Water

These measurements are performed with the antenna placed in tap water

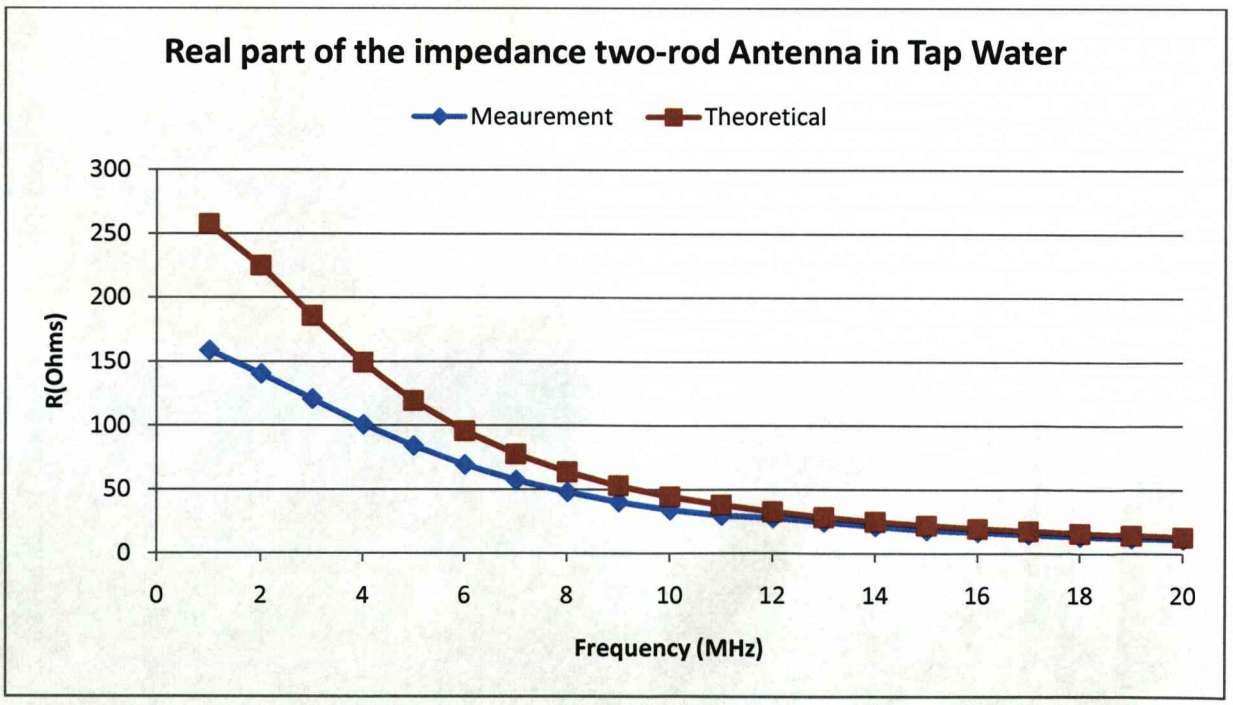

Figure 5.8 Real part of impedance in tap water

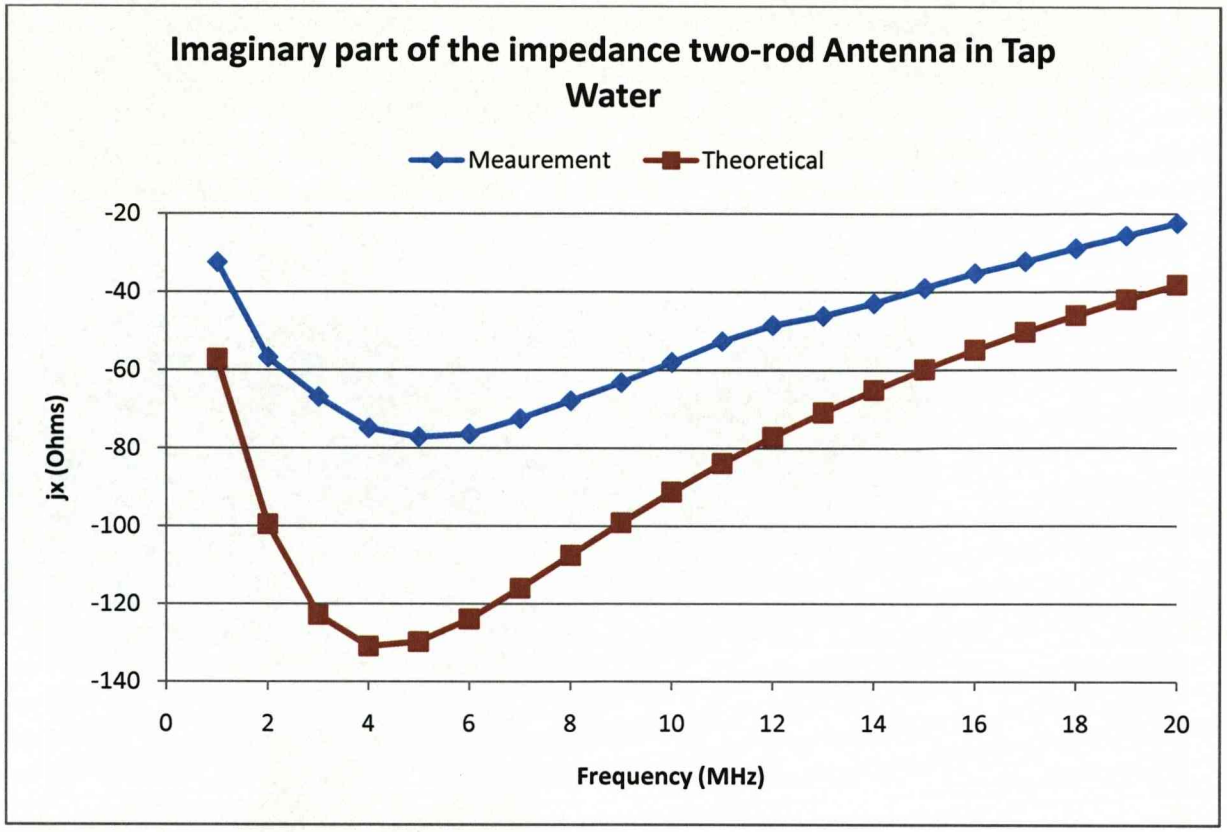

Figure 5.9 Imaginary part impedance in tap water

5.6.2 Impedance in Distilled water

These measurements are performed with the antenna surrounded with distilled water

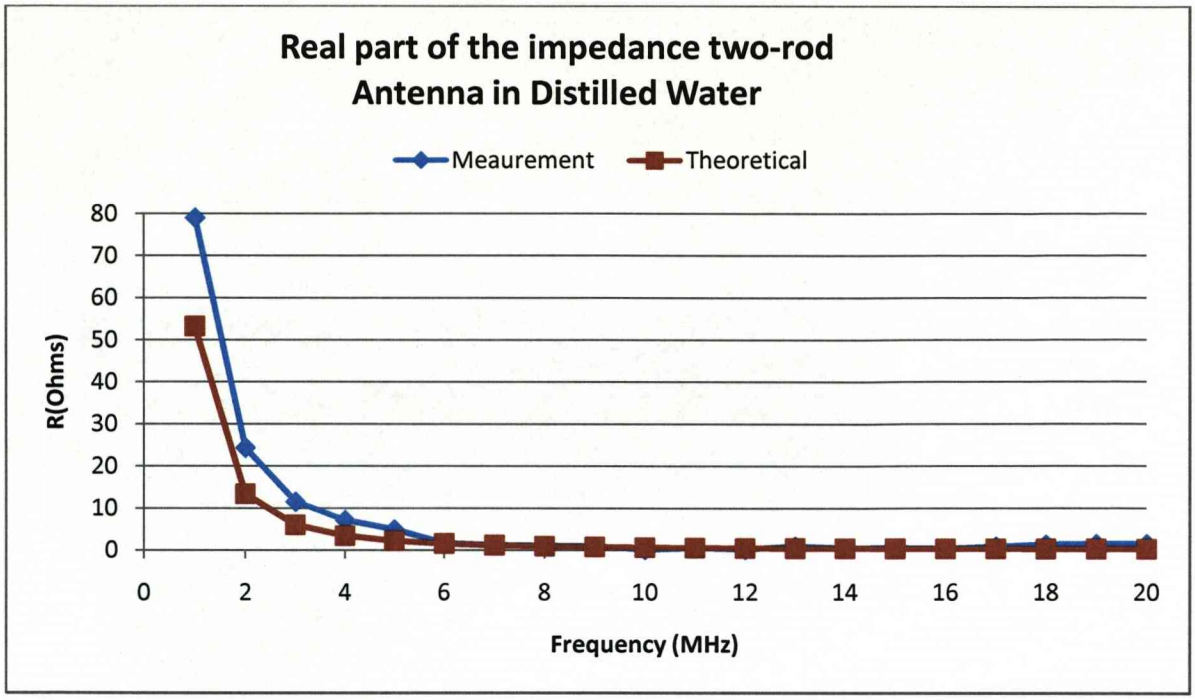

Figure 5.10 Real part of the impedance in distilled water

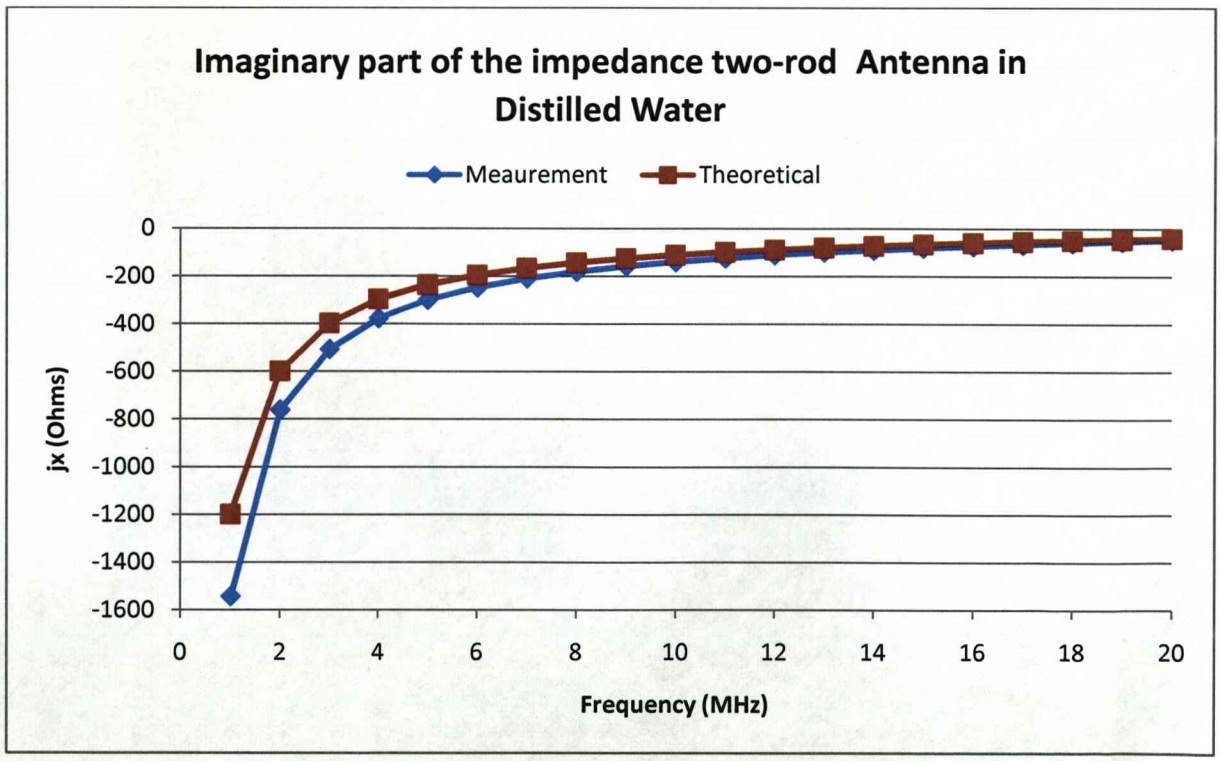

Figure 5.11 Imaginary part of the impedance in distilled water

5.6.3 Impedance in Salt Water

The antenna is placed inside a bucket filled with seawater and the measurements are performed

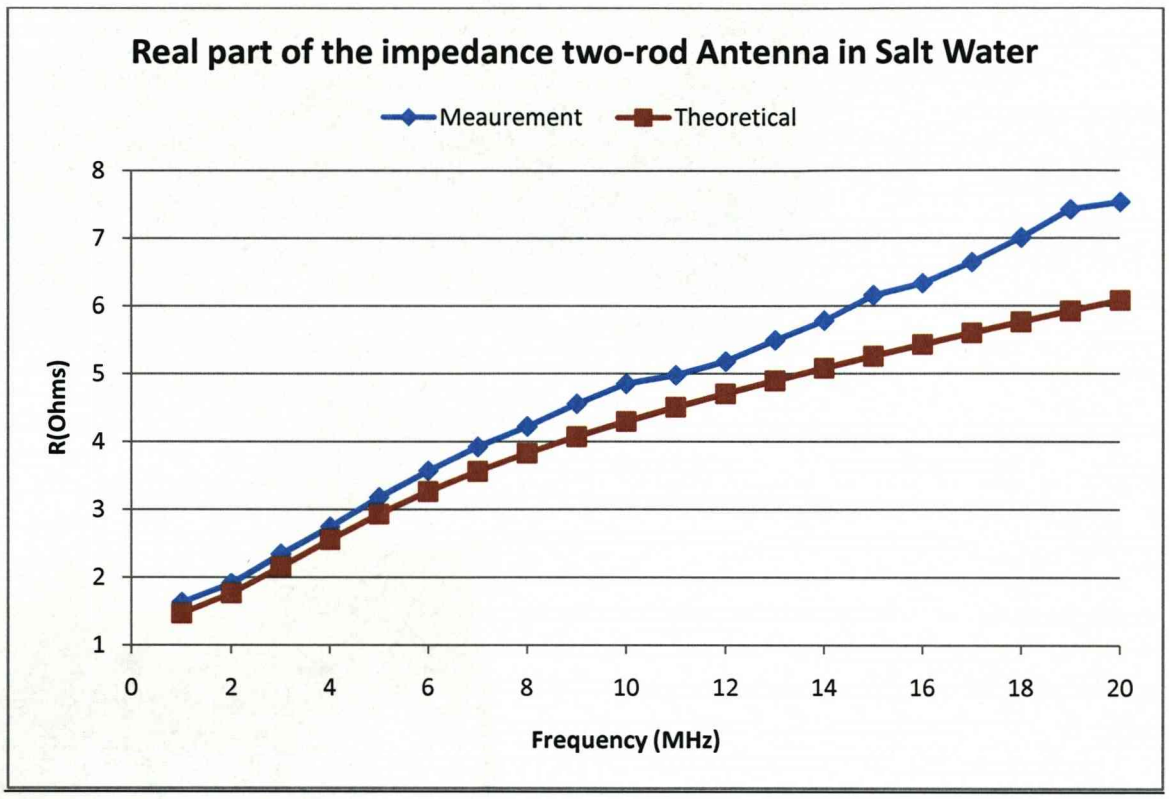

Figure 5.12 Real part of the impedance in salt water

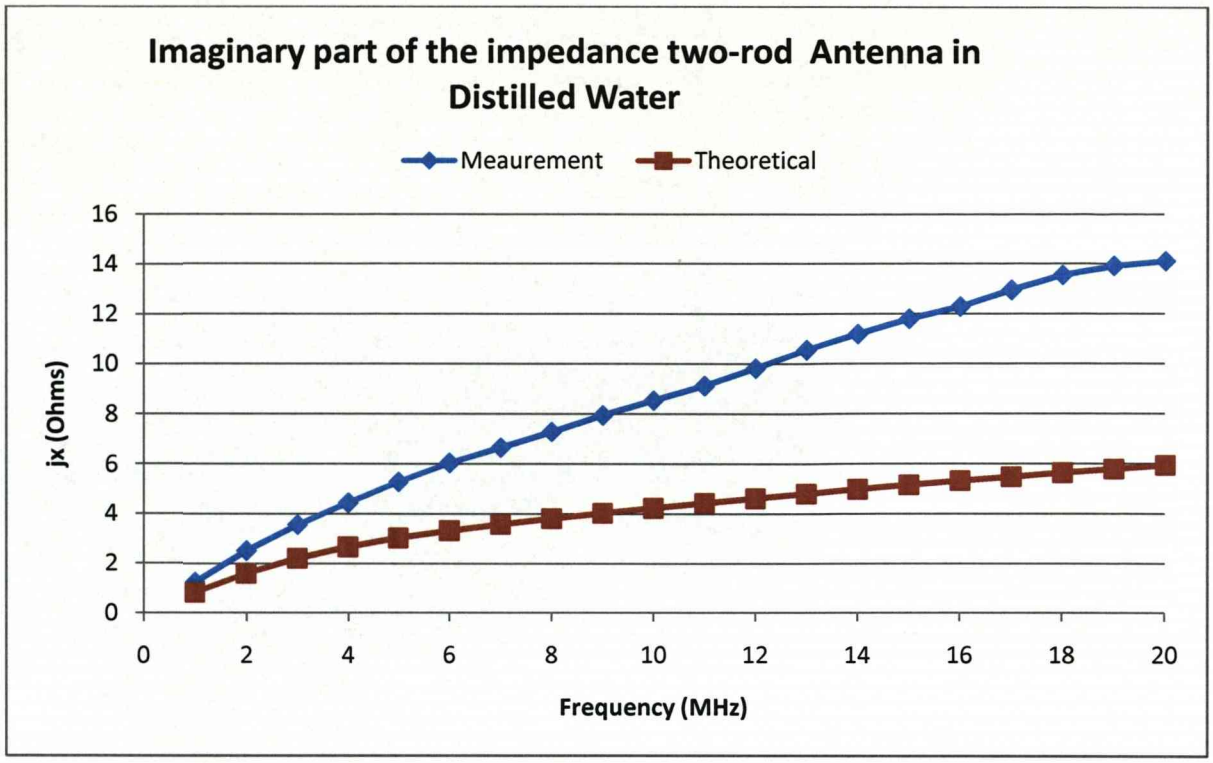

Figure 5.13 Imaginary part of the Impedance in salt water

As it can be seen the magnitude and variation with frequency for both the real and imaginary part show a good agreement between the measured and estimated values. The main discrepancies are due to the conductivity being slightly different compared to the theoretical value used.

5.7 Power Measurements

In a similar manner theoretical results were obtained for the power transmitted in the water

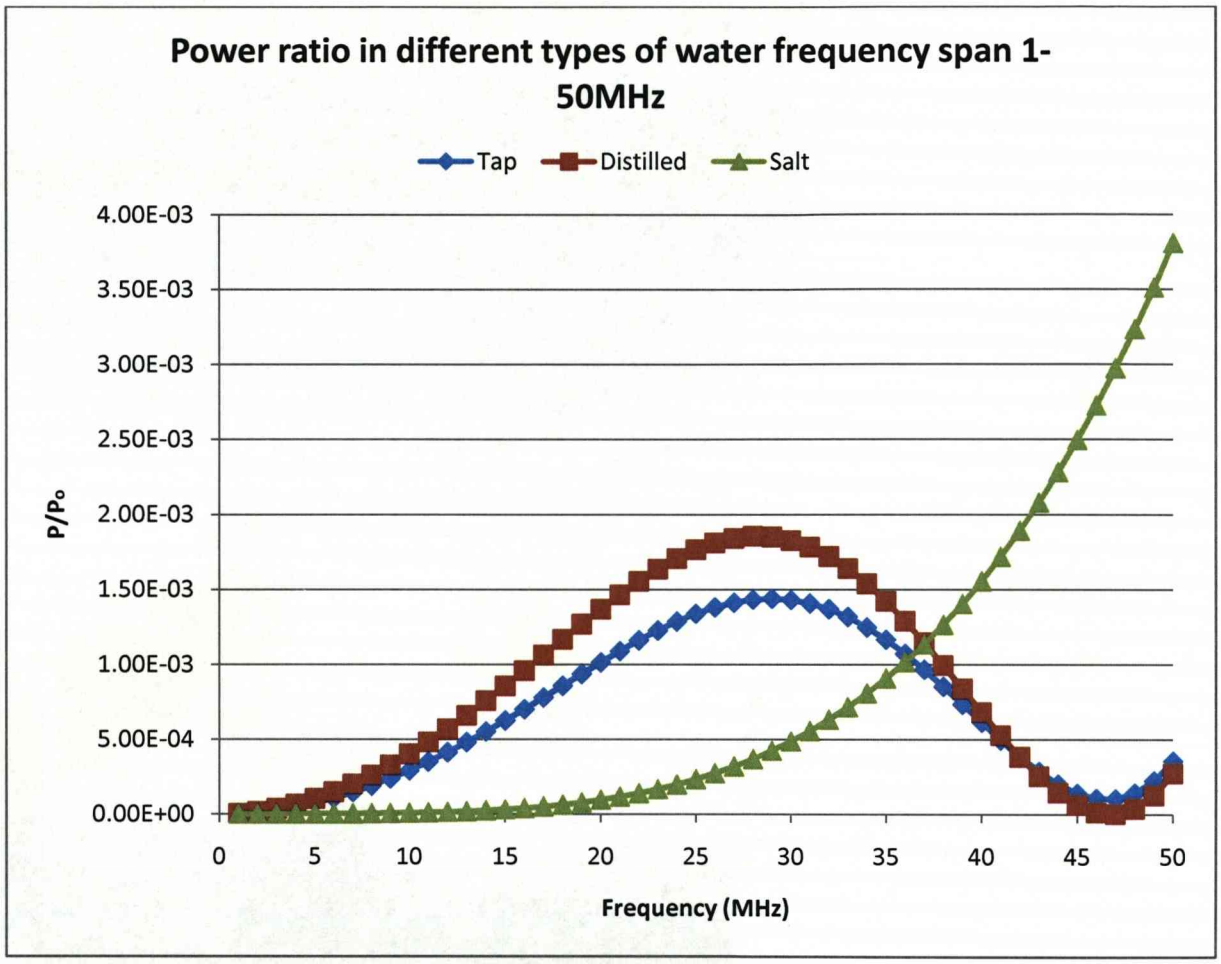

Figure 5.14 Theoretical power measurements in tap water

As it can be seen much more power can be passed through distilled and tap water compared to salt water. It is of particular interest that there are not many differences between distilled and tap water despite the large differences in conductivity. The loop that occurs for both the tap and distilled water is due to the antenna being too long for the higher frequencies and so reflections will occur. In section 5.9 the theoretical model is used for a shorter length antenna and this shows a similar pattern with the seawater as the power increases with frequency

5.8 Transmission Coefficients

The attenuation and propagation coefficients for the different types of antenna are shown in figure 5.15

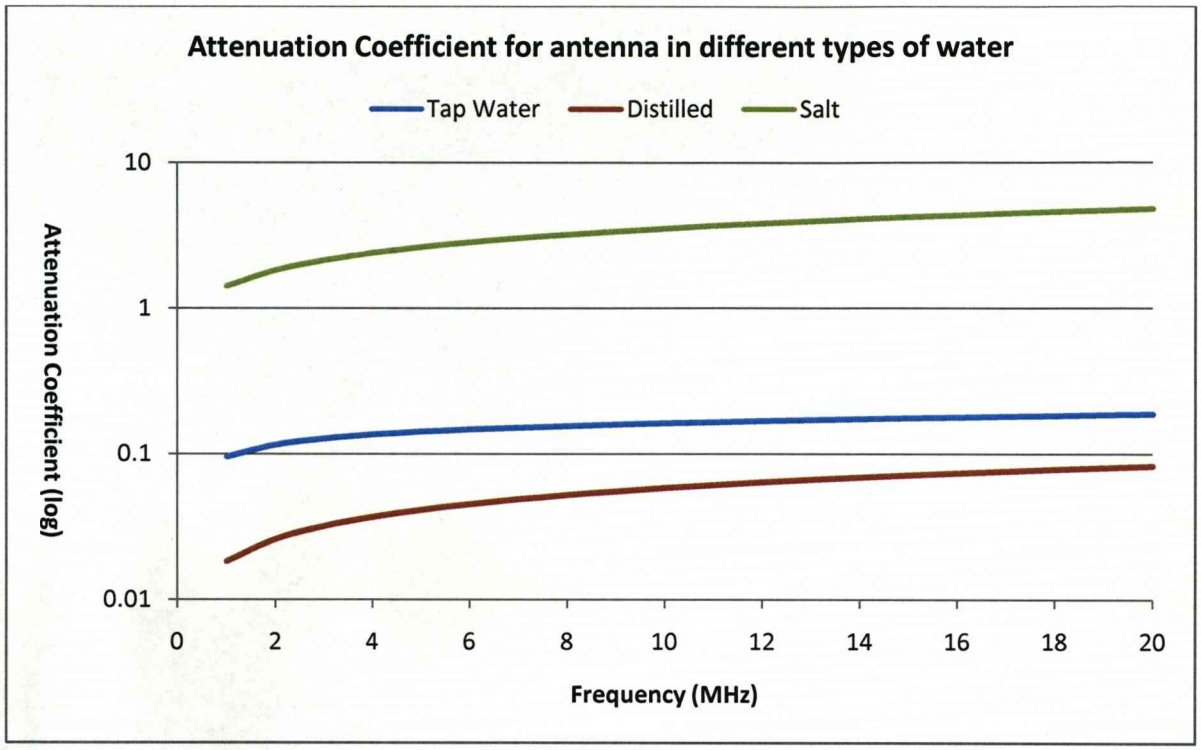

Figure 5.15 Attenuation coefficient

The results clearly show that a much higher loss occurs in higher conductivity liquids such as salt water compared to distilled water.

The propagation coefficient similarly becomes

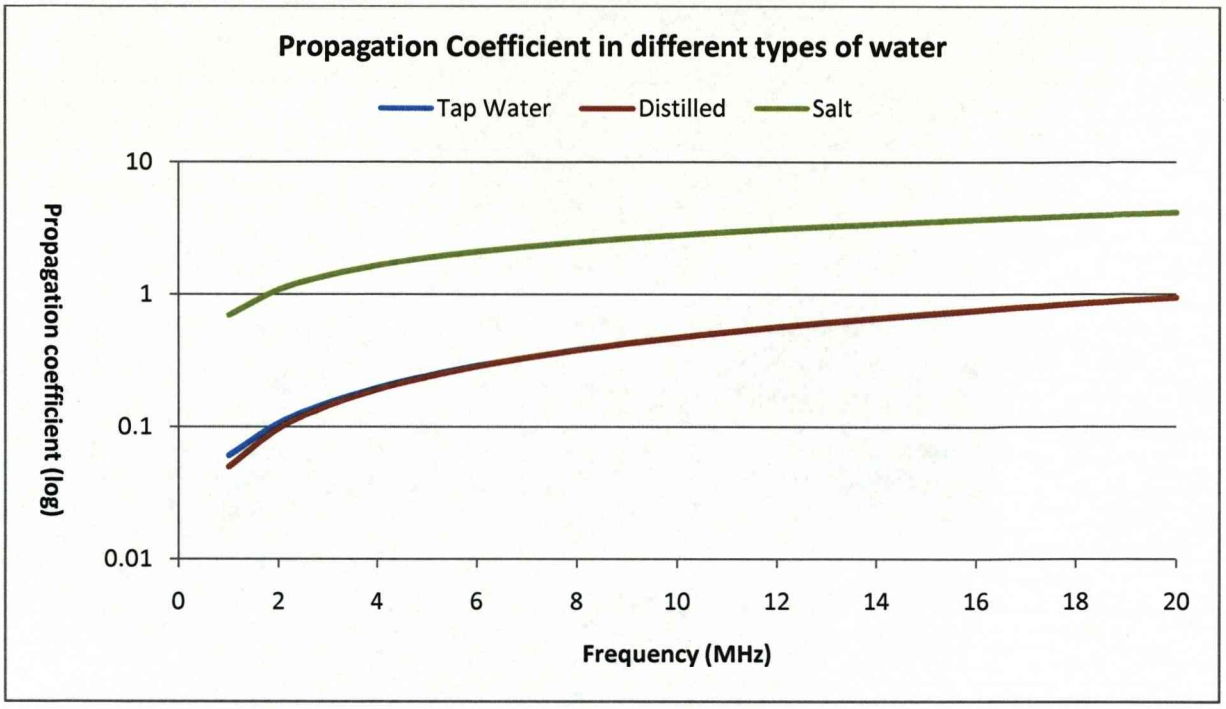

Figure 5.8 Propagation coefficient

5.9 Shorter length antenna

From the graphs shown above it can be seen that the only model in which power increases with frequency is the theoretical model for salt water. This lead to the realisation that a shorter length antenna (l=13cm), might be more suitable for higher frequencies

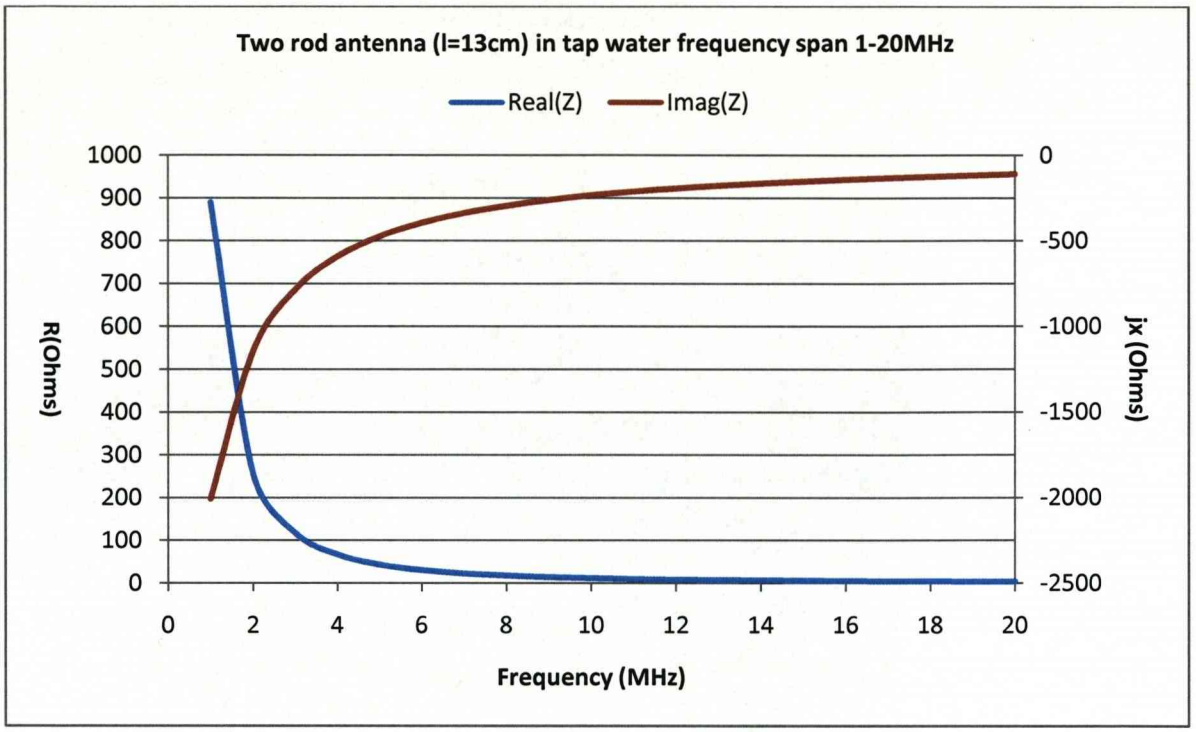

Figure 5.17 Theoretical impedance simulation with shorter length antenna in tap water

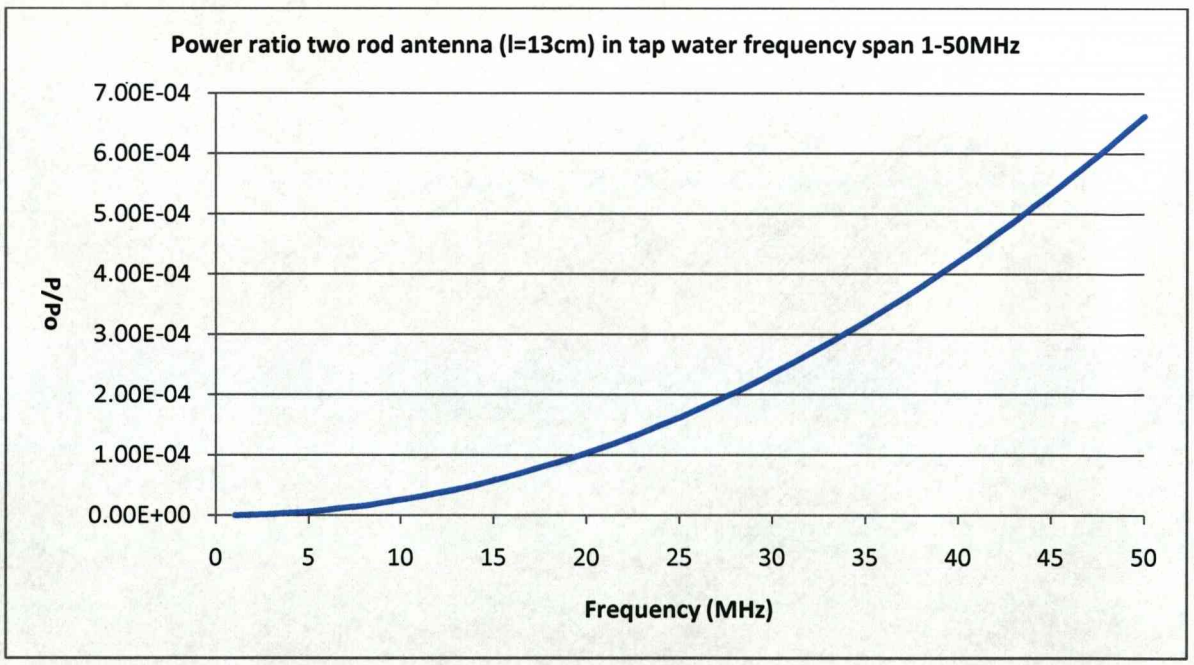

Figure 5.18 Theoretical power simulation with shorter length antenna in tap water

The last figure shows that in an antenna with shorter length the reflections at a higher frequency do not have much effect and that the power measurement follows the theoretical model as it increases with frequency.

5.10 The bucket as a resonant cavity

Since there is power inserted in the bucket and due to its shape it acts as a cylindrical resonant cavity. The occurrence of each mode depends on the dimensions of the barrel that acts as a resonant cavity. If the barrel dimensions and mode values are inserted into equation 3.102, the frequencies are expected to appear at the values shown at table 5

Table 5 Resonant modes inside the bucket

Mode	Resonant frequency
TE011	10.42MHz
TE012	11.34MHz
TE031	26.92MHz
TE111	5.5MHz
TE112	7.1MHz
TE131	22.63MHz
TM010	6.33MHz
TM021	18.66MHz
TM031	22.94MHz
TM111	10.42MHz
TM112	11.34MHz

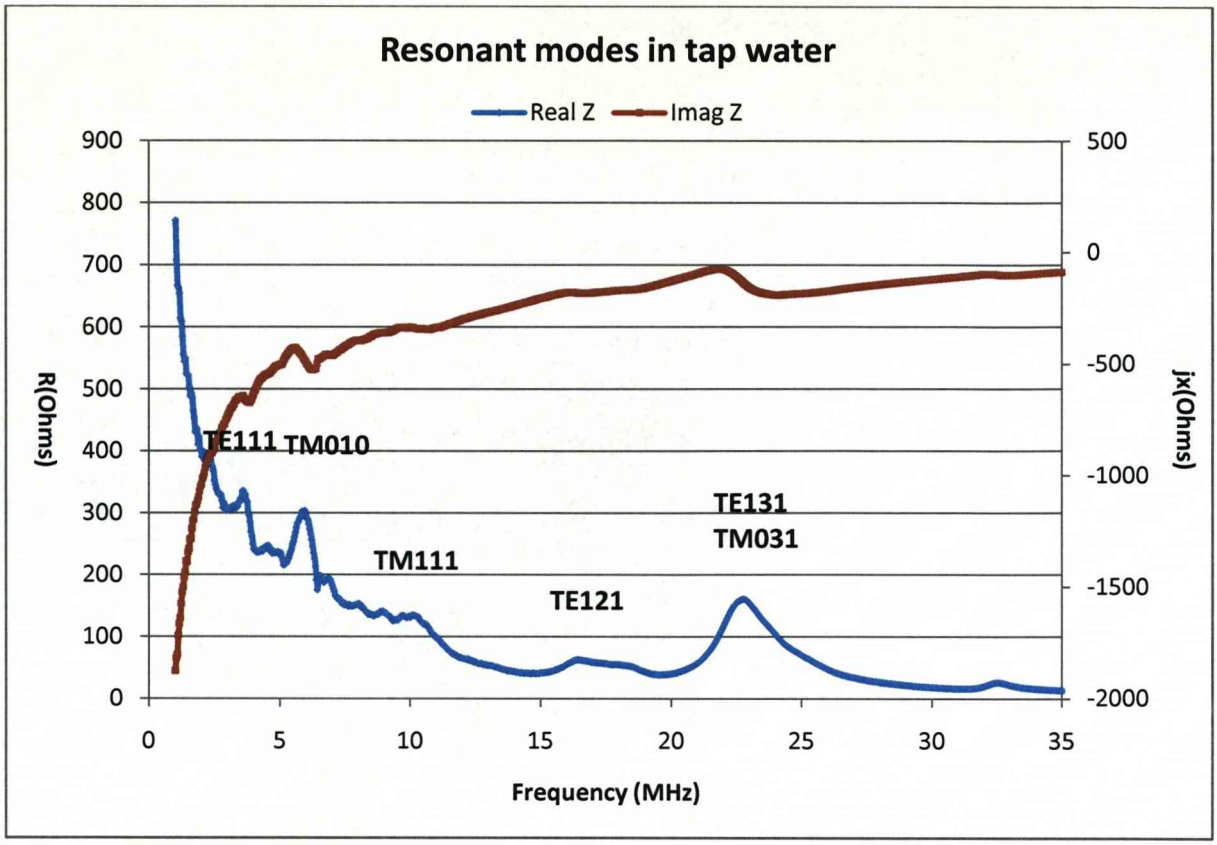

Figure 5.19 Measured resonant modes in tap water

These modes suggest that the electric and magnetic fields operate differently at different frequencies. The TE111 mode and TM010 are of particular interest since in the later the magnetic field is vertical and the waves move towards the top of the barrel. In the TE111 mode the electric field is directed in the x direction and forces the electric field towards the direction of propagation that is on the x direction outside of the barrel and so helps in the signal strength outside the barrel.

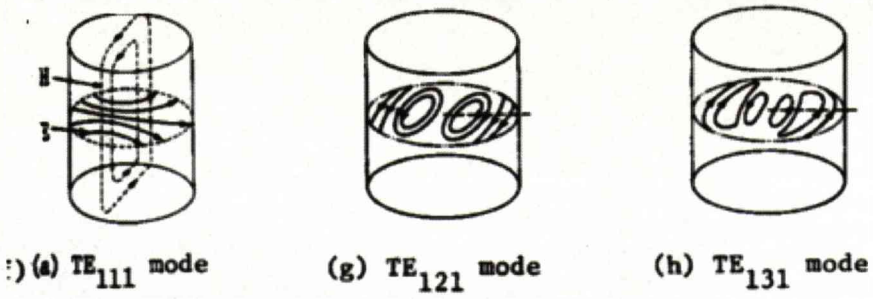

Figure 5.20 TE Modes in the barrel[48]

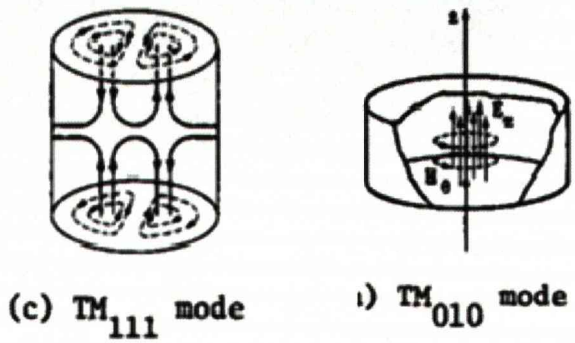

Figure 5.21 TM modes in the barrel [48]

5.11 Electric field of the antenna

Another simulation program was performed in order to observe the direction and strength of the electric field around the antenna. This was performed while assuming that there is no electric field in the y direction.

The coordinate plane used is shown below

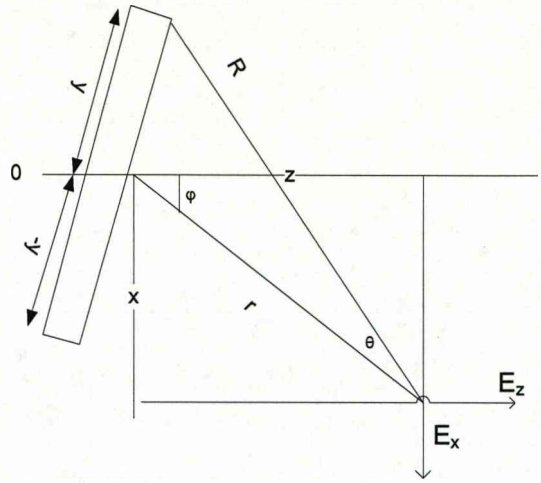

Figure 5.22 Coordinate plane along the z direction

The electric field along the z direction equals

$$E_z = \int \frac{q dy}{4\pi\varepsilon_o\varepsilon_r R^2} \cos\theta \cos\varphi \, d\theta \quad (5.39)$$

where $y = r\tan\theta$ (5.40)

$$dy = \frac{r}{cos^2\theta} d\theta \quad (5.41)$$

By integrating E_z becomes

$$E_z = \frac{q}{4\pi\varepsilon_o\varepsilon_r}(\sin\theta_2 - \sin\theta_1)\frac{z}{r^3} \quad (5.42)$$

From the geometry of the coordinate system these equations arise

$$\sin\theta = \frac{y}{R} = \frac{l}{2R} \quad (5.43)$$

$$r^2 = x^2 + z^2 \quad (5.44)$$

$$R^2 = r^2 + y^2 = r^2 + \left(\frac{l}{2}\right)^2 \quad (5.45)$$

The resulting field in the z direction becomes

$$E_z = \frac{q}{4\pi\varepsilon_o\varepsilon_r}\frac{l}{R}\frac{z}{r^3} \quad (5.46)$$

where q is the electron charge and equals 10^{-12}.

Similarly in the x direction the electric field equals

$$E_x = \frac{q}{4\pi\varepsilon_o\varepsilon_r}\frac{l}{R}\frac{x}{r^3} \quad (5.47)$$

There is also an electric field between the antenna rods, the coordinate plane in this case equals

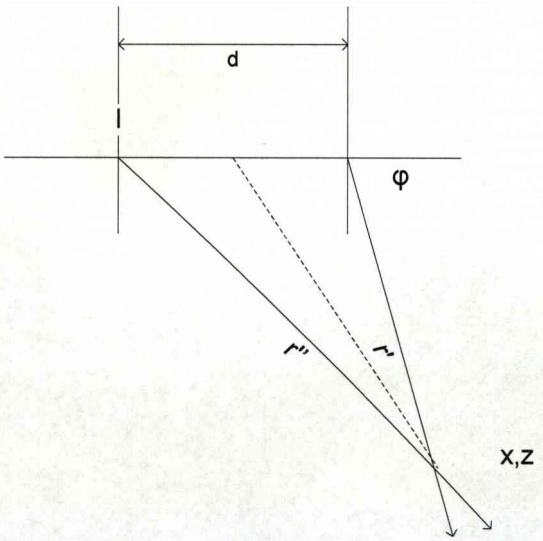

Figure 5.23 Coordinate plane of the field between the antenna rods

If we take the z coordinate again we can see that there are two directions that give rise to the field one in the positive (+l/2) while the other is in the negative (-l/2), so the geometry shows

$$z' = z - \frac{d}{2} \quad (5.48)$$

$$z'' = z + \frac{d}{2} \quad (5.49)$$

The same also occurs for r and so the fields in both the x and z directions have two components and equal

$$E_x = E'_x - E''_x \quad (5.50)$$

$$E_z = E'_z - E''_z \quad (5.51)$$

The total E field is then the vector sum

$$E = \sqrt{E_x^2 + E_z^2} \quad (5.52)$$

This program was run in MATLAB and the electric field at the middle of the rod (y/2) on the xz plane was

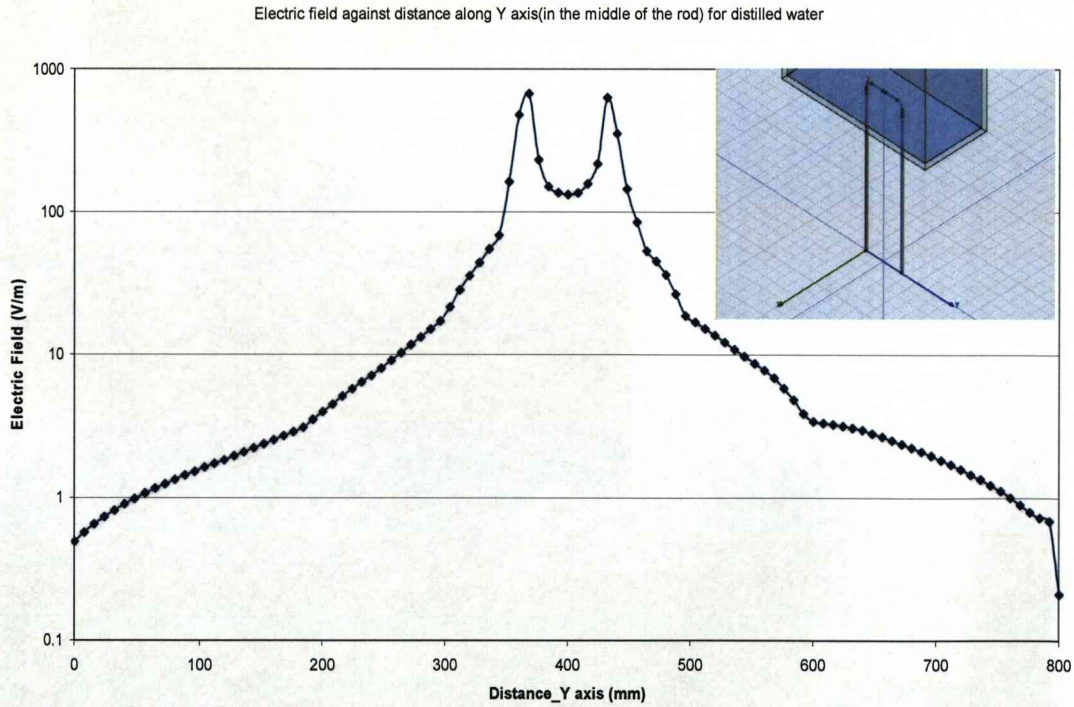

Figure 5.24 Electric field in the xz plane

As it can be seen the two peaks are around the antenna rods and the electric field is stronger around that area, assuming the centre is around 400mm. It is uniform in both directions and demonstrates that even a shorter amount of water can be used to improve transmission.

CHAPTER 6 Transmission Trials

6.1 Introduction

This chapter deals with the trials associated with the signal strength in the water as well as in the air. It also provides with a theoretical model and calculations around the propagation of the signal in the laboratory tank. In order to obtain an idea of how far the signal can reach some trials are performed with the antenna placed in the bucket and the receiver antenna in the air. This chapter deals with the transmitter and receiver antennas and their continuous improvement with better designs as well as impedance matching performed in the transmitter mainly for the two rod antenna as well as some optimisation trials of the environment using double loop antennas.

6.2 Signal Strength in the Tank

If a square wave voltage, similar to the one used in the experiments, is applied to the antenna having a time constant τ, an active signal is present only in the beginning of the signal period (T=1/f) and generates an average value over the rest

$$\hat{v} = \frac{\int_0^T v_t dt}{T} = \frac{\tau v_s}{T}\left(1 - \exp(-\mathrm{T}/\tau)\right) = v_s f\tau\left(1 - exp\left(-\frac{1}{f\tau}\right)\right) \quad (6.1)$$

In the previous section it could be seen that the signal strength from the antenna was affected by the effect of water conductivity, by the time constant, by dielectric loss as well as due to standing waves. The actual signal is a combination of the terms shown in equations 5.15, 5.24, 5.28 and 6.1 so that

$$v_i = \left(\frac{v_s}{v_a}\right) \times \left(\frac{\hat{v}}{v_s}\right) \times \left(\frac{v_i}{\hat{v}}\right) \times v_a \quad (6.2)$$

If we substitute the values obtained from the previous equations

$$v_i = 0.287 \times f\tau\left(1 - exp\left(-\frac{1}{f\tau}\right)\right) \times \sqrt{\frac{\omega\varepsilon''}{\sigma + \omega\varepsilon''}} \times \sqrt{2Z_o P} \times \left(\frac{\sqrt{4S}}{1+S}\right) \quad (6.3)$$

where P is the power supplied to the antenna and S is the VSWR. In order to improve the performance of the antenna the VSWR must be made equal to one and this occurs when the antenna impedance is matched to 50Ω.

6.2.1 Signal Propagation in tap water within the tank

If the laboratory tank is filled up with tap water we substitute the values from table 2 from section 5.2.2 into equation 6.3 we obtain the equation for the transmitted signal strength as

$$v_i = 0.287 \times \frac{f}{27.92}\left(1 - exp\left(\frac{-27.92}{f}\right)\right) \times \sqrt{\frac{24.92f^2}{20 + 24.92f^2}} \times \sqrt{754 \times P}\left(\frac{\sqrt{4S}}{1+S}\right) \quad (6.4)$$

The transmitted power (P) in tap water was 20mW (13dBm). The following table shows the variation of the signal strength released by the transmitting antenna as a function of frequency as well as the attenuation of the signal in tap water assuming that the VSWR is 1, which the antenna and transmission lines are perfectly matched.

Table 6 Signal Attenuation in tap water

Signal Frequency (MHz)	Signal Amplitude $\hat{v}/v_s \times 10^2$	Signal Attenuation (dB)	Emitted Signal (dBm)
0.5	1.8	-34.9	-42
1	3.6	-28.8	-32.2
5	17.9	-14.9	-15.8
10	33.6	-9.5	-10.3
20	53.9	-5.4	-6.2
40	72.0	-2.9	-3.7
60	78.0	-1.9	-2.7

The signal strength increases from -42dBm at 0.5MHz to -2.7dBm at 60MHz when VSWR=1.

6.2.2 Signal Propagation in sea water within the tank

In a similar manner if we substitute the dielectric properties for sea water the transmitted signal becomes

$$v_i = 0.287 \times \frac{f}{6289}\left(1 - exp\left(\frac{-27.92}{f}\right)\right) \times \sqrt{\frac{24.92f^2}{4000 + 24.92f^2}} \times \sqrt{754 \times P}\left(\frac{\sqrt{4S}}{1+S}\right) \quad (6.5)$$

The theoretical values for the transmitted signal strength in seawater become

Table 7 Signal Attenuation in salt water

Signal Frequency (MHz)	Signal Amplitude $\hat{v}/v_s \times 10^4$	Signal Attenuation (dB)	Emitted Signal (dBm)
0.5	0.79	-82	-111
1	1.59	-76	-99
5	7.95	-62	-72
10	14.9	-57	-62
20	23.9	-52	-54
40	40	-50	-51
60	35.5	-49	-50

The theoretical results for seawater follow the pattern from the previous section as the emitted signal strength increases with frequency. On the other hand in normal tap water the losses are smaller compared to sea water.

6.3 Signal Strength Water Antenna

The theoretical signal strength for the two rod antenna the receiver placed at a distance of 100m with a 10W transmitting amplifier is given below

Table 8 Two rod antenna Attenuation

f(MHz)	Emitted Signal Strength (dB)	Attenuation (dB)	Received dipole radiation (dB)
1	-20	-35	-55
10	0	-55	-55
20	5	-63	-58
30	7	-68	-61
100	9	-113	-104

6.4 Tank Optimisation

The first step in performing experiments in the laboratory tank was to be able to locate the signal and to remove any unwanted interference from any noise. This step was performed by using two loop antennas and comparing them with the theoretical values shown in figure 5.6. After the results matched the theoretical values the first test was performed by comparing the effects of the barrel as a resonant cavity as mentioned in section 5.8 in freshwater

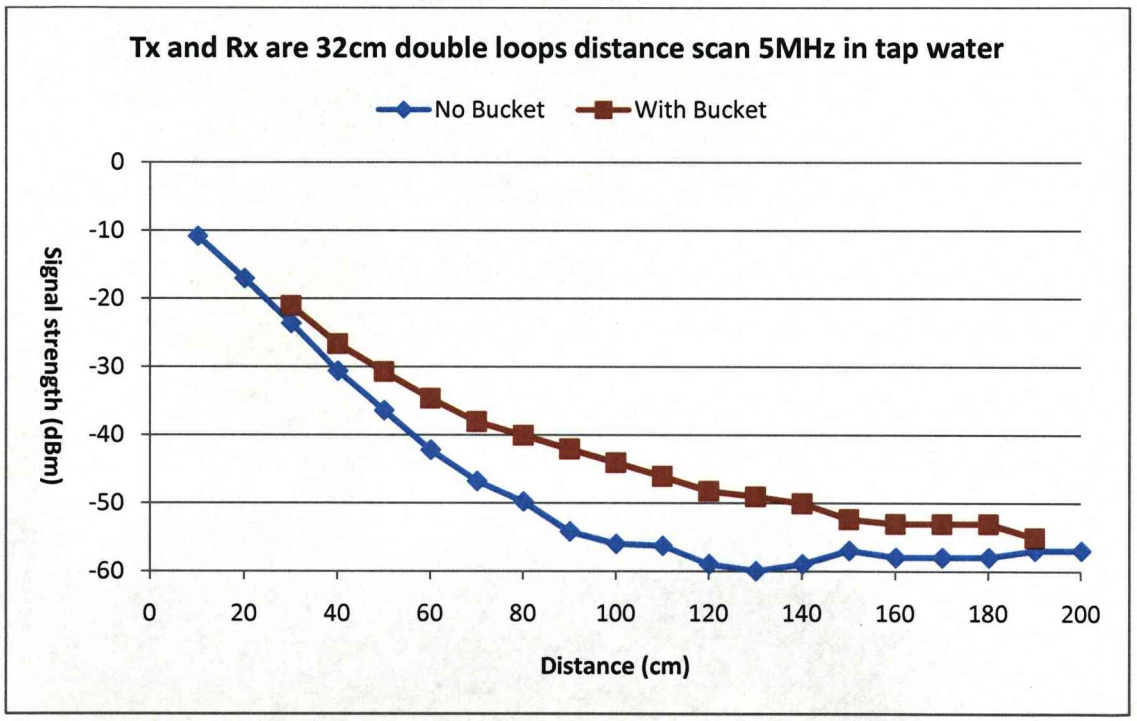

Figure 9.1 Distance scan at 5MHz in tap water

Despite the fact that both antennae are essentially in tap water so there are no matching losses between the antenna and its environment it can be seen that the bucket has a slight beneficial effect in this frequency range since at this mode the dipoles are oriented towards the transmission path and so are enhanced in moving towards the direction of propagation. This provides an advantage of this design at this particular frequency range. Besides the dipole simulation seems to be enhanced in the area inside the bucket and so provide an added stimulus for propagation.

This test was also repeated using double loops placed inside the bucket while the rest of the tank was full with seawater. The results are shown below

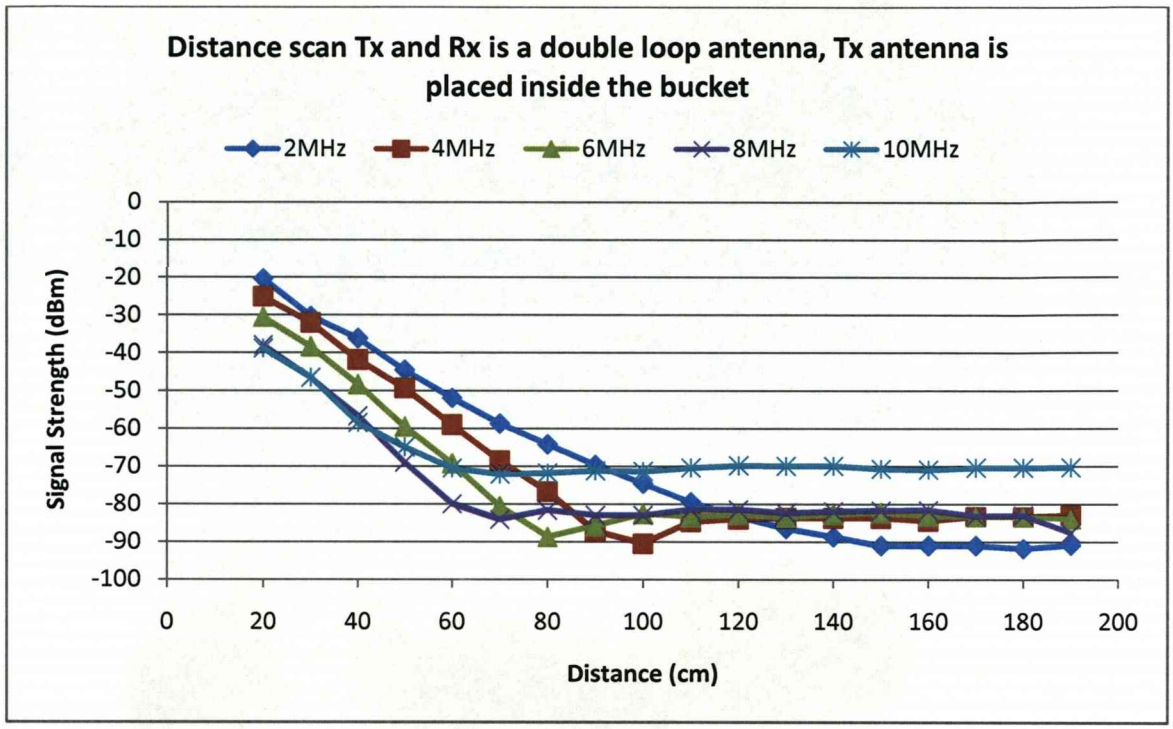

Figure 6.2 Distance scan for 2 double loop antenna 32cm diameter

6.5 Water Antenna Trials

As mentioned in the previous chapter the main advantage of this antenna is that matching losses are minimised since the antenna is directly launched into tap water. The trials were performed at a variety of frequencies while matching was also performed as well as the use of different type of receivers.

The distance scans in the frequency range between 1-10MHz were performed using the DDS based transmitter while in the higher frequencies the crystal based oscillator transmitter was used.

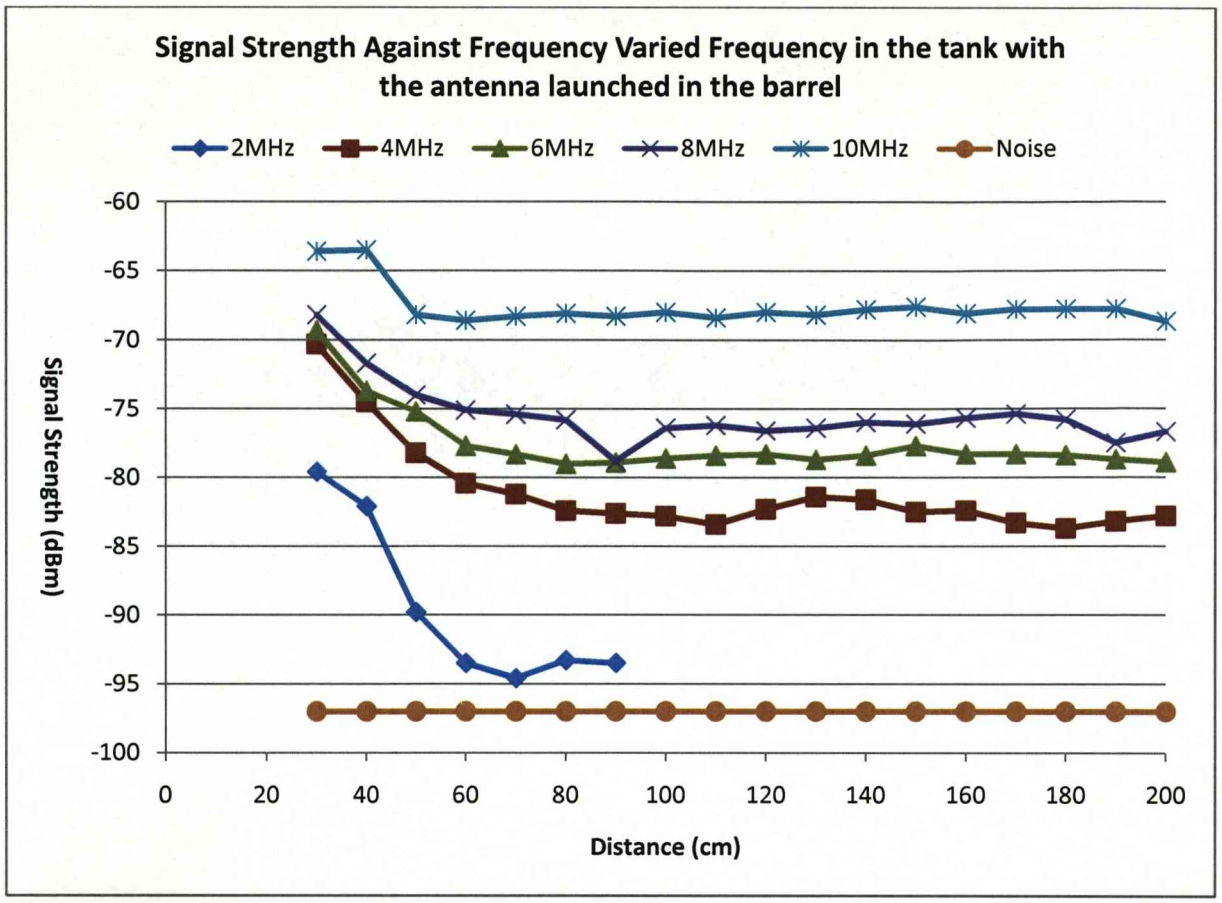

Figure 6.3 Signal strength in the tank

The graph follows the theory in chapter 5 since as the frequency increases so does the signal strength due to increased power transmitted through the antenna. Besides if the antenna is directly launched into salt water, without being placed in the bucket full of tap water the results are rather different and the signal quickly dies away as shown below

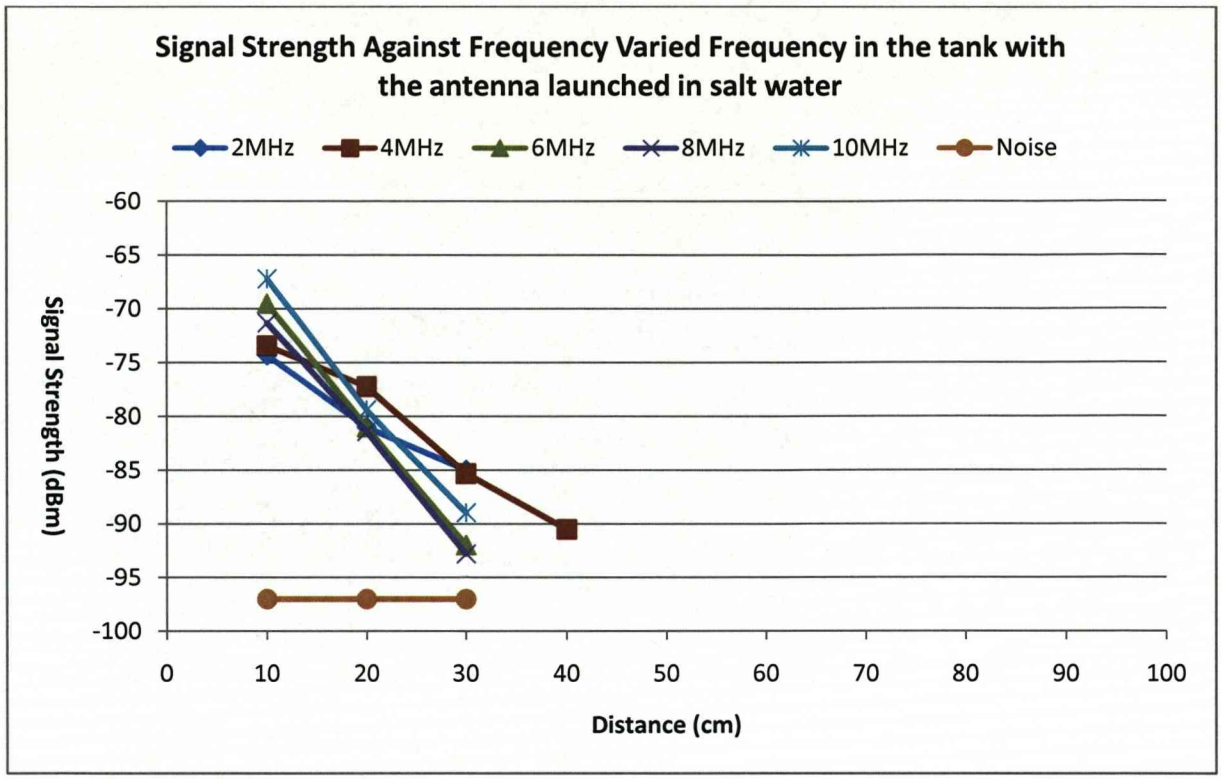

Figure 6.4 Distance scan with the antenna launched in sea water

As it can be clearly be seen the tap water offers an improved match to the antenna so much more power is transmitted to the medium

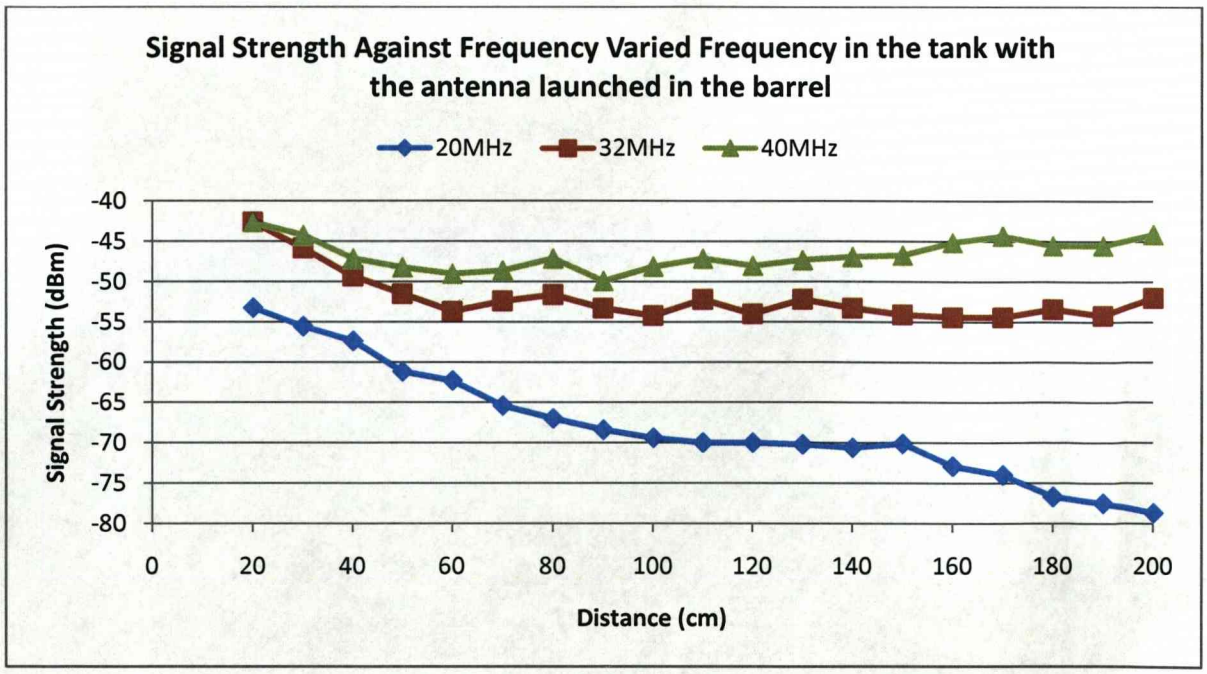

Figure 6.5 Signal Strength at higher frequencies

Even at higher frequencies it is clearly shown that the signal strength increases with frequency. At higher frequency levels there is a limitation within the lab tank as there are reflections in the latter stages as it can be seen for the 40MHz crystal with the signal becoming actually stronger in the far field region.

6.6 Receiver trials

The next phase of this study was to apply different receiver antennas to observe whether there is any improved effect. The double loop antenna is a rather effective antenna that offers a large area for the receiving signal but is more susceptible to pick-up noise as well as receiving reflections especially at higher frequencies. The first receiver trial included a 2-rod antenna that is similar to the transmitter

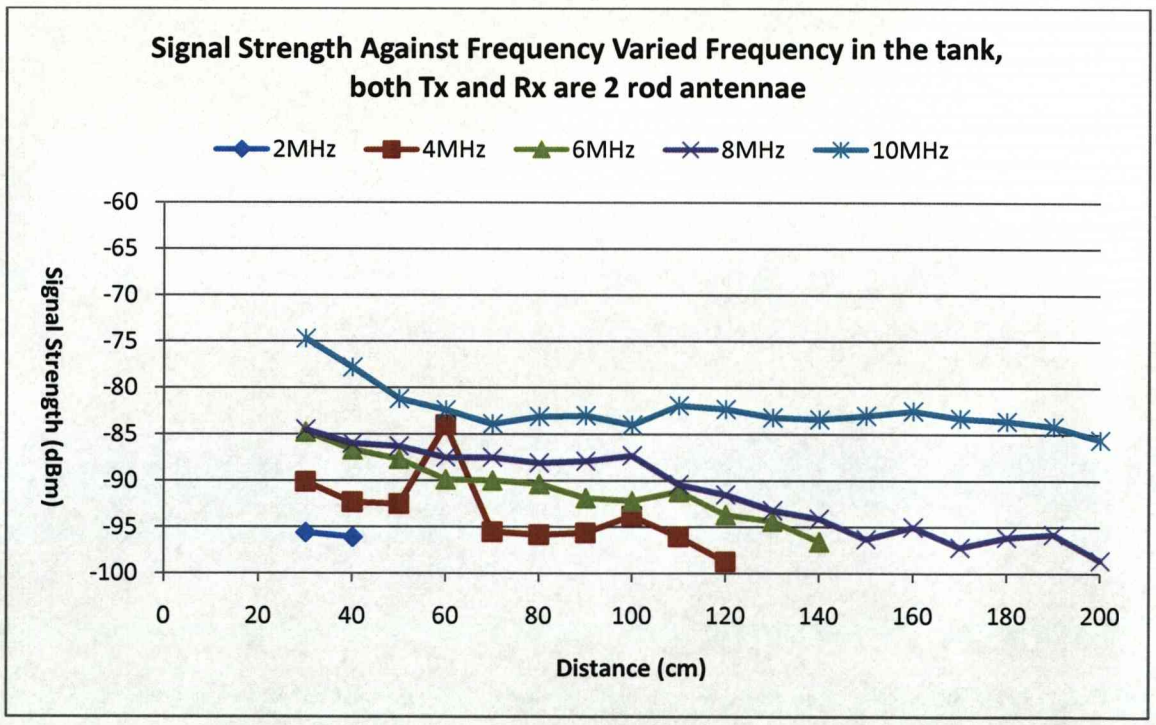

Figure 6.6 Distance scan for Rx 2 rod antenna

The main reason behind this trial was that since the antennae of the transmitter and the receiver are the same, it would lead to improved performance from the system as a whole. Although the signal strength follows the general pattern of the previous trials, it is not as strong as when the double loop receiver is applied.

The next test was performed using a folded dipole antenna as the receiver. This test was performed at high frequencies to observe whether it is more accurate at collecting the signal without the reflections that are observed in the far field of the tank.

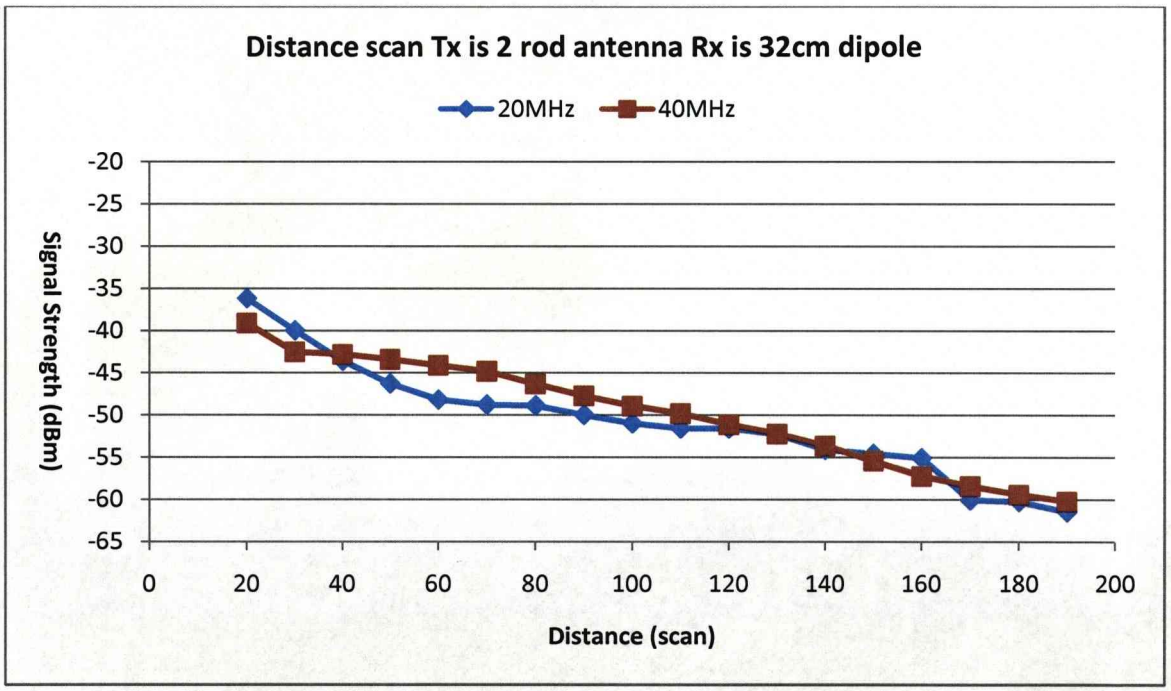

Figure 6.7 Distance scan for 32cm dipole receiver antenna

The main advantage as can be seen by using a dipole receiver especially at high frequencies is that at the 40MHz range the signal strength continues to decline so there are no reflection signals received compared to the same trials with the double loop receiver. This might indicate that for higher frequencies the receiving antenna can be reduced in area and will be able to receive the signal without reflections.

6.7 Matching trials

The next step in this study is to observe whether the signal strength can be improved by appropriate matching between the transmitter and the antenna. The previous trials all include the antenna unmatched to the transmission line so there is significant loss of power during transmission. The matching was performed by using the antenna box connected to an impedance analyser, while the box is immersed in the bucket. The unmatched antenna smith chart and VSWR ratio are shown below

Two wire rod with sheath and box in tap water span 1MHz to 60MHz.

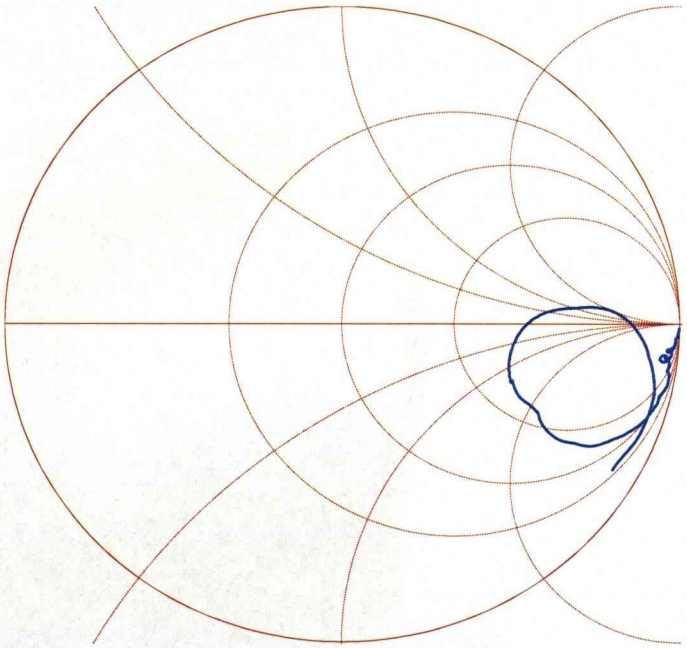

Figure 6.8 Smith Chart for unmatched antenna 1-60MHz

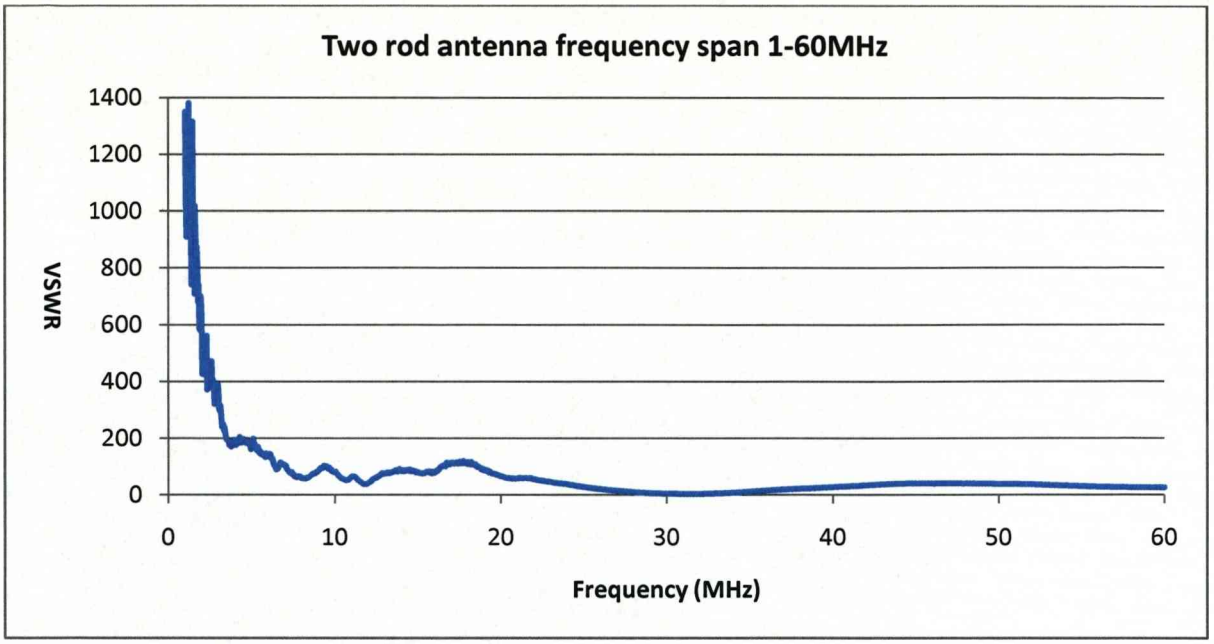

Figure 6.9 VSWR scan for unmatched antenna

6.7.1 Matching at 10MHz

The next step was to apply the matching at the required frequency in this case was 10MHz. The matching was performed below and did improve the signal strength as shown by figure the plots become as shown

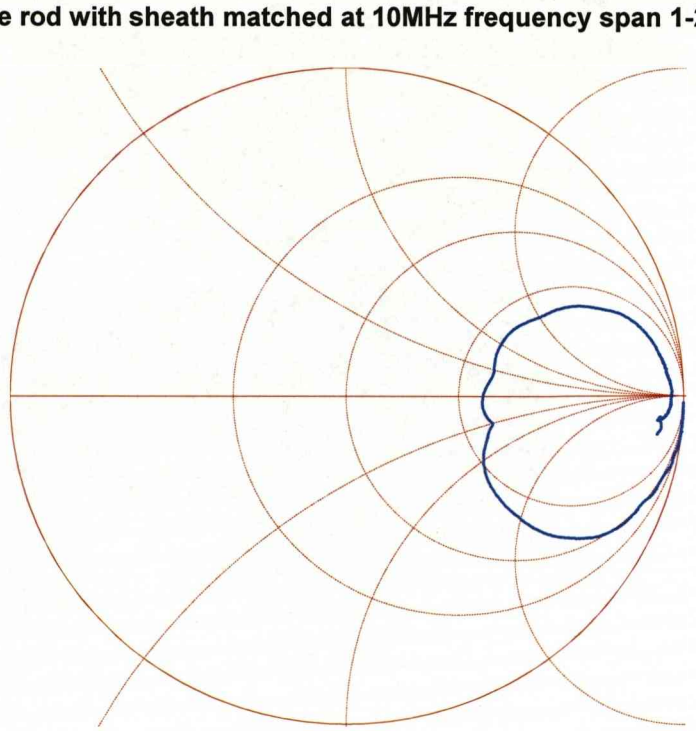

Figure 6.10 Smith chart for Antenna Matched at 10MHz

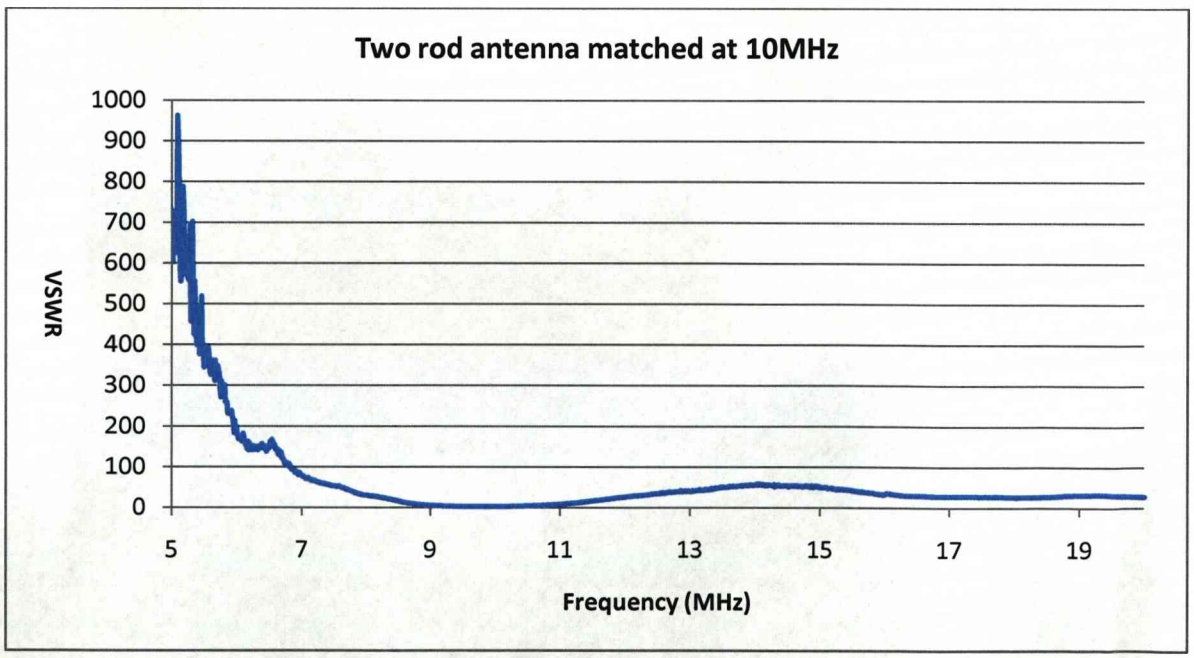

Figure 6.11 VSWR signal matched at 10MHz

The matching was performed to 50Ω. The next step was to perform a distance scan of the matched antenna and compare it to the unmatched antenna

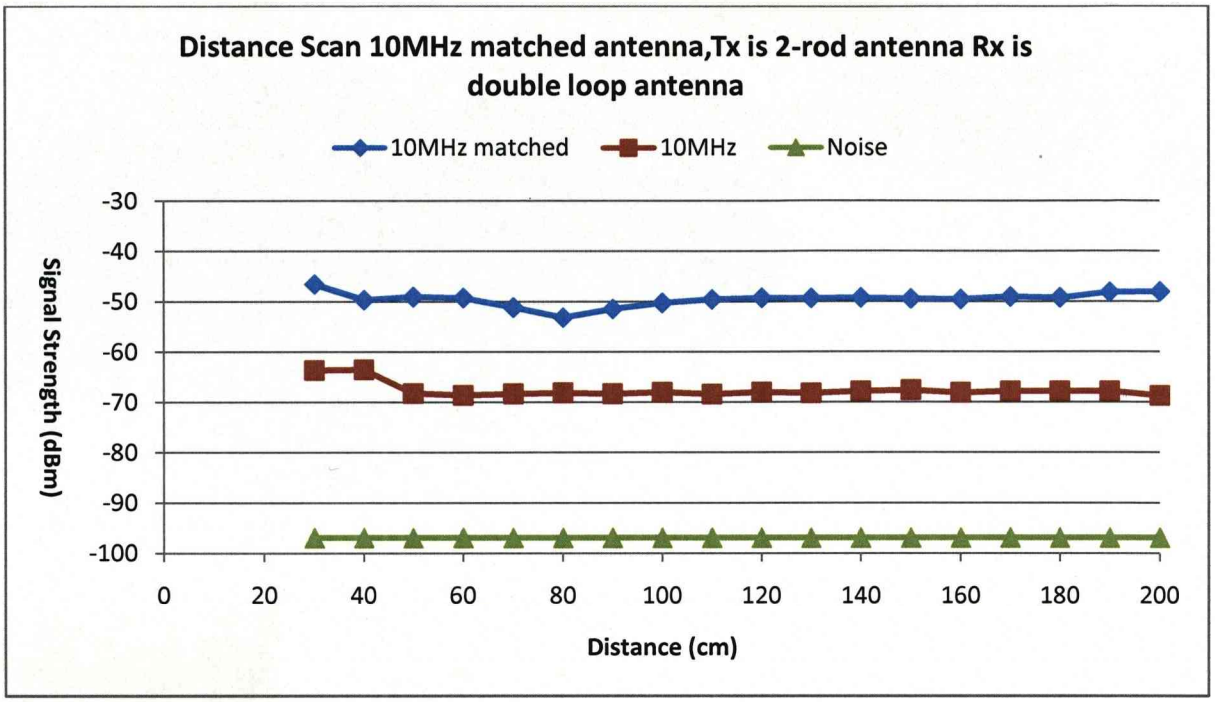

Figure 6.12 Distance scan for 10MHz matched antenna

As it can be seen from the graph there is a 10dBm improvement on the signal strength as the matching is applied.

6.7.2 Matching at 20MHz

The next successful match was performed at 20MHz and the graphs are shown below

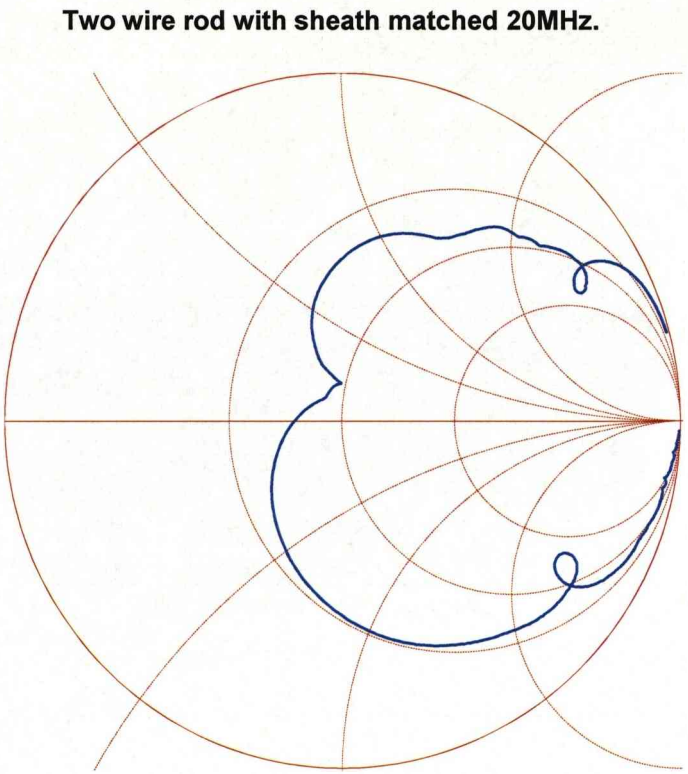

Figure 6.13 Smith Chart for Antenna Matched at 20MHz

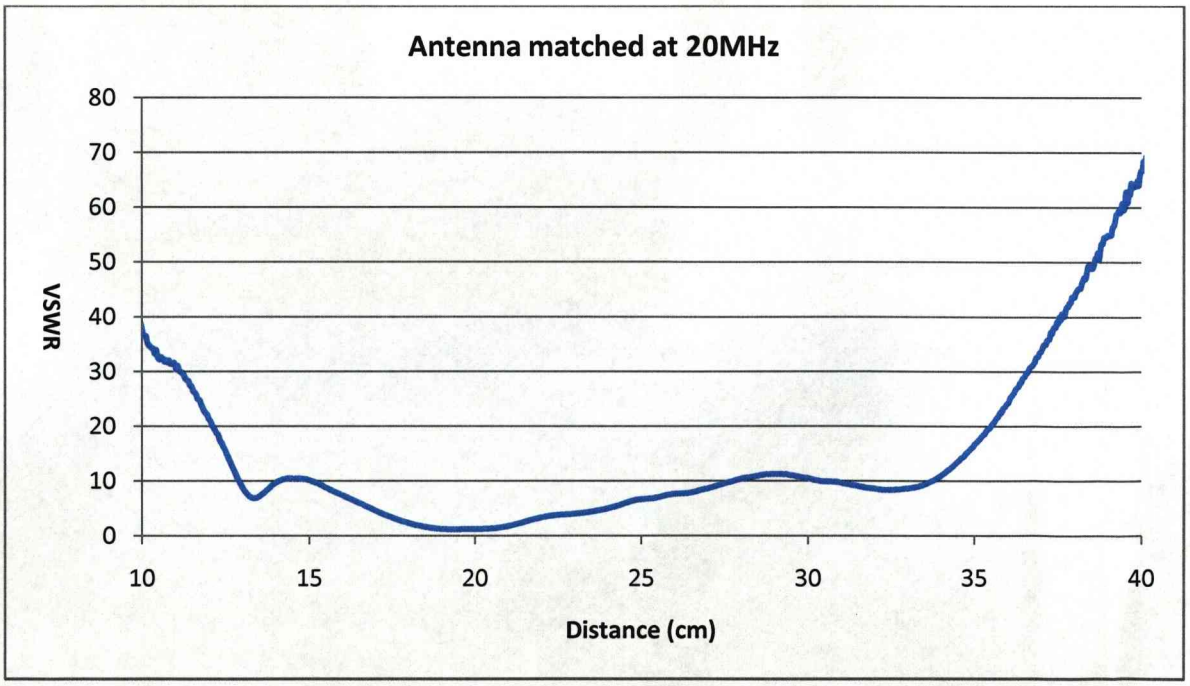

Figure 6.14 VSWR for antenna matched at 20MHz

The distance scan shows the effect of the matching on the signal strength

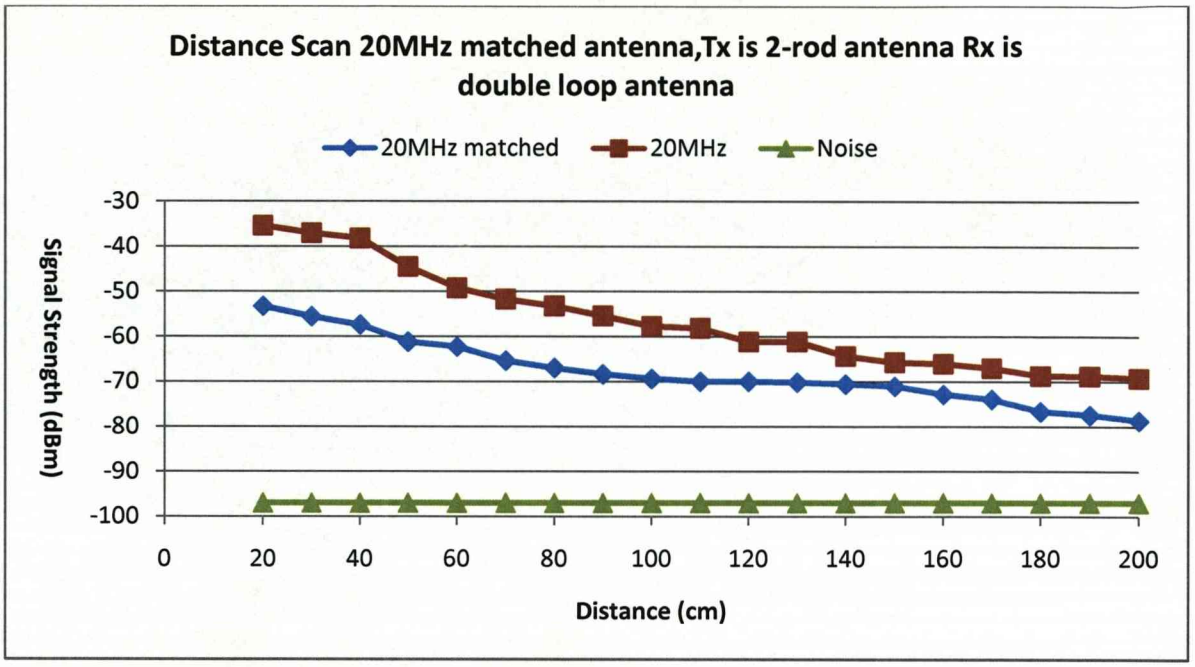

Figure 6.15 Distance scan for 20MHz matched antenna

6.7.3 Matching Overview

The table below summarises the matching parameters

Table 9 Matching properties

Frequency (MHz)	Impedance (Ω)	VSWR	VSWR (matched)
10	118-24.5j	81	2.45
20	185-358j	17.8	1.11
32	308-59.1j	6.4	1.18
40	125-369j	24.6	3.2

The matching as can be seen was also performed for the 32 and 40MHz but despite the improvement in the VSWR it did not seem to have any improved effect on the transmission. In the case of the 32MHz crystal it seems that the VSWR is relatively low and despite the six fold improvement, there is no significant improvement in the amount of power transferred

from the transmitter to the antenna so there is no difference in the distance scan. Since the VSWR is relatively low without the matching it might indicate that the length of the antenna is the most suitable for this frequency range. Similarly the 40MHz crystal did not provide any difference in the distance scan.

The improvement in matching can be shown below. The VSWR for the unmatched antenna is 89 so the reflection coefficient equals

$$\Gamma = \frac{VSWR + 1}{VSWR - 1} = \frac{81 - 1}{81 + 1} = 0.9705$$

The power transmitted to the antenna before matching equals

$$P_{A1} = (1 - |\Gamma|^2)P_T \quad (6.6)$$

where P_T is the power from the signal generator in Watts and equals

$$P_{A1} = (1 - 0.9705^2)P_T = 0.058P_T$$

Once the antenna is matched

$$\Gamma = \frac{2.45 - 1}{2.45 + 1} = 0.42$$

The power transmitted to the antenna equals

$$P_{A2} = (1 - 0.42^2)P_T = 0.823P_T$$

The power gain in dB can be found as

$$P_A = 10 \log\left(\frac{P_{A2}}{P_{A1}}\right) \quad (6.7)$$

$$P_A = 10 \log\left(\frac{0.823}{0.058}\right) = 11.5\ dB$$

This shows that when the match is applied the power passed to the antenna increases by 11.5dB as is shown in the distance scan in figure 6.12

If the match is ideal then Γ=0 and the power gain becomes

$$P_A = 10\log\left(\frac{1}{0.058}\right) = 12.3\ dB$$

For the 20 MHz the reflection coefficient and the power becomes when the antenna is unmatched equal

$$\Gamma = \frac{16.8}{18.8} = 0.893$$

$$P_{A1} = (1 - 0.893^2)P_T = 0.202P_T$$

Once the antenna is matched the values become

$$\Gamma = \frac{0.11}{2.11} = 0.052$$

$$P_{A2} = (1 - 0.052^2)P_T = 0.99P_T$$

The improvement of the power gain equals

$$P_A = 10\log\left(\frac{P_{A2}}{P_{A1}}\right) = 6.9dB$$

This match is shown to improve the signal by approximately the above amount.

Theoretically in the case of the 32MHz and 40MHz the signal should increase by

$$P_{32} = 3.2dB$$

$$P_{40} = 9.6dB$$

In the case of the 32MHz the signal improvement is too small to be observed while in the case of the 40MHz despite the increased amount that should cause a marked effect on the signal. This effect is not being observed and could be down to reflections in the tank when the signal is unmatched leading to increased signal strength. This shows that the laboratory tank is not ideal for measurements at high frequencies or with increased transmitter power as the signal will bounce back from the walls.

6.8 Trials in the air

Another test performed was a distance scan with the transmitter antenna left in the air and placed in the bucket while the receiver is in the atmosphere. The receiver in both cases is a 20cm dipole and the frequency used was 20 MHz and is unmatched in both cases

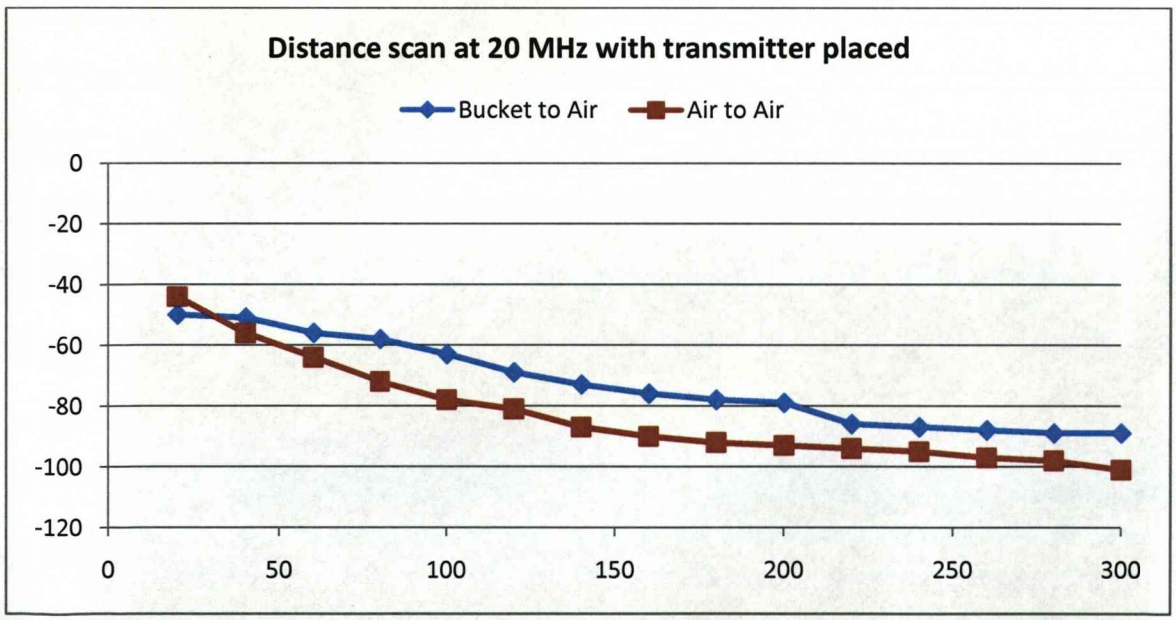

Figure 6.16 Antenna trials with receiver in the air

As the graph shows the antenna design is perfectly matched for use in the water. Despite the losses due to the water to air interface the signal when both transmitter and receiver are placed in the air the signal decreases faster.

6.9 Antenna Realisation

The design of the antenna consists of a parallel transmission line placed inside a bucket which was filled with tap water separated by a thin PVC wall that prohibits it from coming into touch with the seawater inside the tank. At the PVC boundary there is only a net weak reflection coefficient because of phase cancelling since the wall thickness is very much smaller than the radiation wavelength. The formula for the reflection coefficient is a direct result by using the wave impedance in the three media as shown in figure 6.19

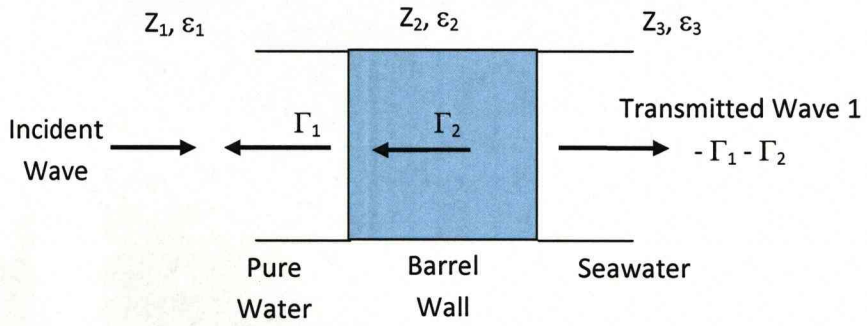

Figure 6.17 EM wave transmission through PVC wall

The reflection coefficient is estimated as

$$\Gamma = \left(\frac{Z_1 - Z_2}{Z_1 + Z_2}\right) + \left(\frac{Z_2 - Z_3}{Z_2 + Z_3}\right) \leftrightarrow$$

$$\Gamma = \left(\frac{\sqrt{\varepsilon_2} - \sqrt{\varepsilon_1}}{\sqrt{\varepsilon_2} + \sqrt{\varepsilon_1}}\right) + \left(\frac{\sqrt{\varepsilon_3} - \sqrt{\varepsilon_2}}{\sqrt{\varepsilon_3} + \sqrt{\varepsilon_2}}\right) \quad (6.6)$$

Since ε_1 is the permittivity of fresh water = 81

ε_2 is the permittivity of the PVC barrel=3

ε_3 is the permittivity of salt water=72

The reflection coefficient becomes

Γ=–0.677+0.660=0.016

An additional advantage of using the curved barrel in that it will produce a lens focussing action as shown in figure 6.17

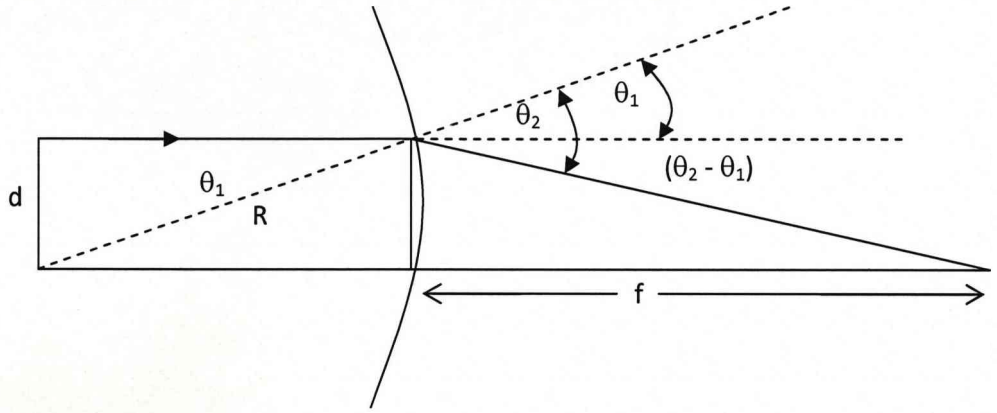

Figure 6.18 Focussing Action of PVC Wall

Snell's law gives [48]

$$\sqrt{\varepsilon_1}\sin\theta_1 = \sqrt{\varepsilon_3}\sin\theta_2 \Leftrightarrow$$

$$\sin\theta_2 = \frac{\sqrt{\varepsilon_1}}{\sqrt{\varepsilon_3}}\sin\theta_1 \quad (6.7)$$

The relative lower dielectric of the seawater will produce a focussing action with a focal length f

$$f = {}^{d}/_{\tan(\theta_2-\theta_1)} = d\left(\frac{1+\tan\theta_1\tan\theta_2}{\tan\theta_2-\tan\theta_1}\right) \quad (6.8)$$

For R = 25cm and d =3.5cm then $\theta_1 = 8.942^\circ$ and $\theta_2 = 9.488^\circ$ so that

f=4.07m

This shows that the bucket antenna enhances the transmission of the dipoles through the medium. As mentioned above in section 5.9 the frequency can also affect the strength of propagation since the bucket acts as a resonant cavity. This allows the antenna design to be modified according to the requirements of the application since the antenna will require a larger length but a smaller amount of water to produce dipole radiation at lower frequencies.

CHAPTER 7 Coaxial Antenna

7.1 Introduction

The next step was to design another antenna to observe whether the theory mentioned in chapter 5 will also apply to a different design. The antenna used is the coaxial antenna which is useful mainly in the low frequencies up to 100MHz but its use is limited in the higher frequencies due to skin effect in conductors. Similarly the new antenna will be tested surrounded by different liquids to observe whether better power transmission can be achieved between the antenna and the medium.

7.2 Coaxial Antenna theory

A typical air-cored cable has an inner copper conductor of radius α held in position by an outer conductor of polyethylene discs of inside radius b which in turn is surrounded by one or more layers of steel tape for screening. Coaxial cables usually apply the TEM mode of propagation as shown below

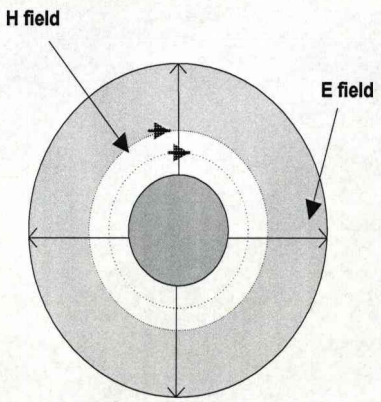

Figure 7.1 TEM mode in the coaxial cable

Similarly to the two rod antenna the coaxial cable can be characterised in terms of R, r (skin effect), L, G and C per unit length and the equations are shown below

The radiation resistance (skin depth) is

$$r = \frac{1}{2\pi}\sqrt{\left(\frac{\omega\mu\rho}{2}\right)} \cdot \left[\frac{1}{a} + \frac{1}{b}\right] (7.1)\ \Omega/m$$

The inductance along the coaxial cable

$$L = \frac{\mu_o \mu_r}{2\pi} \ln b/a\ (7.2)\ H/m$$

The transconductance is

$$G = \omega C \tan\delta\ (7.3)\ S/m$$

The capacitance equals

$$C = \frac{2\pi\varepsilon_o\varepsilon_r}{\ln b/a}\ (7.4)\ F/m$$

The intrinsic impedance

$$Z_o = \sqrt{L/C} = \frac{138}{\sqrt{\varepsilon_r}} \log b/a\ (7.5)\ \Omega$$

The velocity thus becomes

$$v = \frac{1}{\sqrt{\mu\varepsilon}} = \frac{3 \times 10^8}{\sqrt{\mu_r\varepsilon_r}}\ (7.6)\ m/sec$$

These equations will be used to formulate a theoretical model for the antenna impedance inside each liquid. In this case the diameter of the inner conductor α is 1.6cm while the radius of the inner part of the outer conductor b is 1mm. The length of the antenna is 16cm.

7.3 Dielectric Properties of materials

In order to test the model different liquids were considered which are similar in conductivity with distilled water ($\sigma \approx 0$). This is done in order to improve the matching between the antenna and the medium so a limited amount of liquid is required in order to provide dipole radiation. The barrel antenna required quite a large amount of water and is not suitable for some applications like communications between divers. In trials with the two rod antenna by limiting the amount of water surrounding the antenna there was a decrease in the signal strength transmitted.

The dielectric behaviour of liquids is defined by the Debye equation described in section 3.6 and the loss factor is shown below

$$\varepsilon'' = \frac{(\varepsilon_s - \varepsilon_\infty)\omega\tau}{1 + \omega^2\tau^2} \quad (3.53)$$

The low-frequency or static value of the real permittivity ε_s equals the value of the dielectric constant. The optical-frequency value of the real permittivity ε_∞ equals the square of the refraction index. The refractive index of a medium is a measure for how much the speed of light is reduced inside the medium; it is defined as the ratio of the phase velocity of a wave phenomenon such as light over the mediums phase velocity

$$n = \frac{c}{v_p} \quad (7.7)$$

It can also be defined with respect to the permittivity and the permeability of the medium

$$n = \sqrt{\varepsilon\mu_r} \quad (8.8)$$

In this case the permeability is 1so the refractive index is generally taken to be equal to the square root of the permittivity ε_∞.

The dielectric properties of the materials considered are shown below

Table 10 Dielectric Properties of Materials [49], [50]

Material	Dielectric constant (ε_s)	Refractive Index	Time constant (ps)
Acetone	37.4	1.36	3.4
Chlorobenzene	5.6	1.5	1.51
Cyclohexanone	16.8	1.462	10.5
Ethyl Benzoate	6	1.5	17.6
Methyl Acetate	6.7	1.35	3.7
Methanol	19.9	1.483	11.3
Nitrobenzene	39.4	1.55	13.4
Toluene	2.4	1.497	7.6

These materials are very suitable for this type of experiments since their conductivity is extremely low and that would allow improved matching between them and the antenna without the losses associated with the complex conductivity.

7.4 Impedance Measurements

Similarly to the 2-rod antenna, a model was created for the coaxial antenna which is rather similar to the one described in section 5.4. The only major difference is that the equations that describe the electrical properties of the antenna are different. The equivalent circuit of the antenna is similar to the one for the two-rod antenna. A major difference in these simulations is that since different liquids are used, the estimation of the complex part of the permittivity is performed by using Debye's equation. Similarly the actual impedance measurements were performed by using the impedance analyser.

7.4.1 Water trials

The first liquid to be tested was water in order to be able to compare the results to the two rod antenna the actual impedance measurements for tap and distilled water were found to be

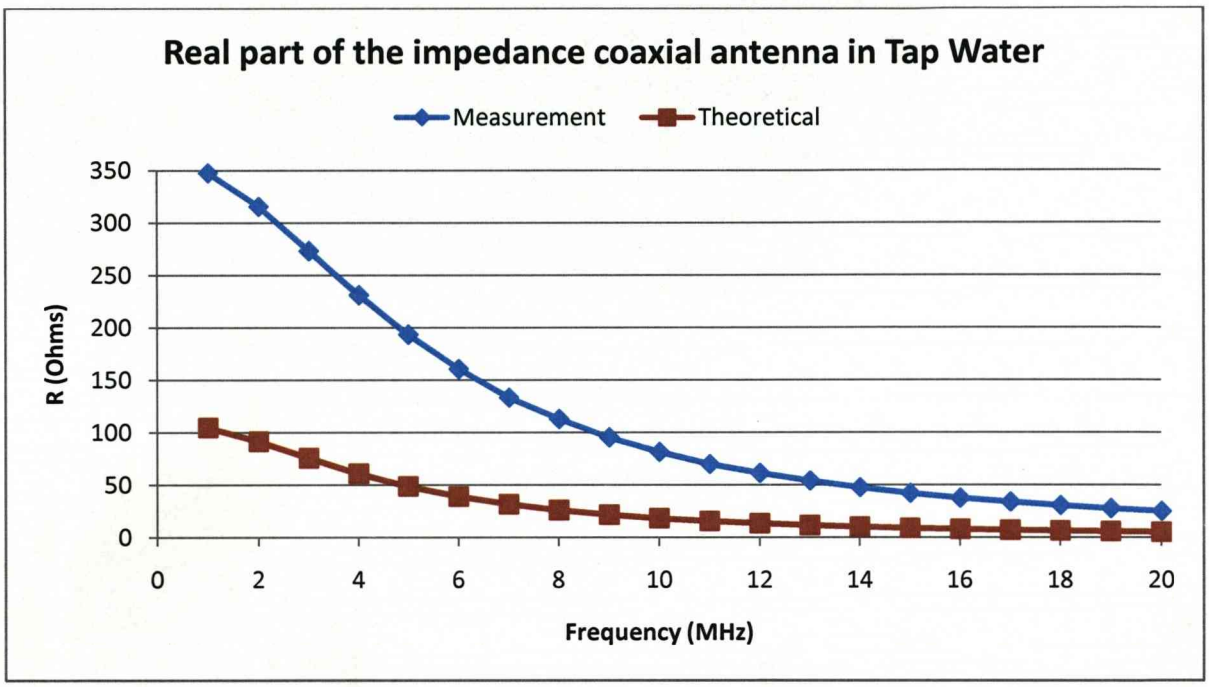

Figure 7.2 Real part of the Impedance in Tap Water

In the case of the imaginary part of the impedance in tap water the measured value of the impedance is

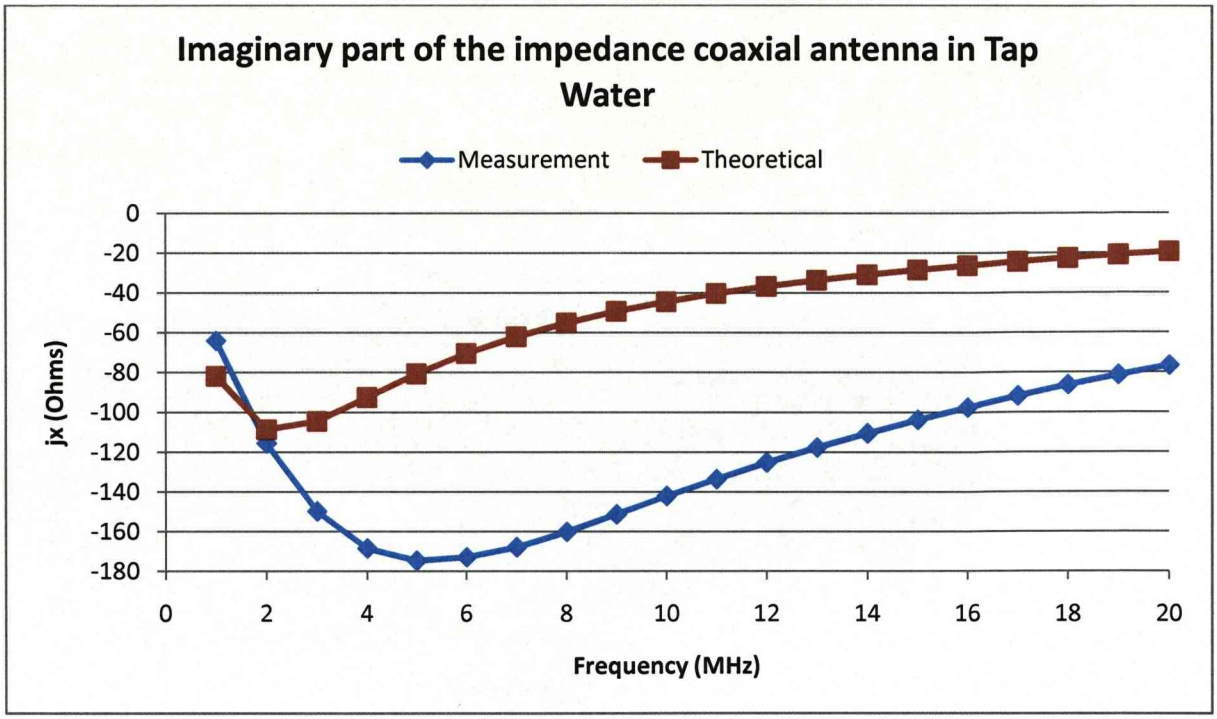

Figure 7.3 Imaginary part of the Impedance in tap water

The impedance values for distilled water are shown in figures 7.4 and 7.5

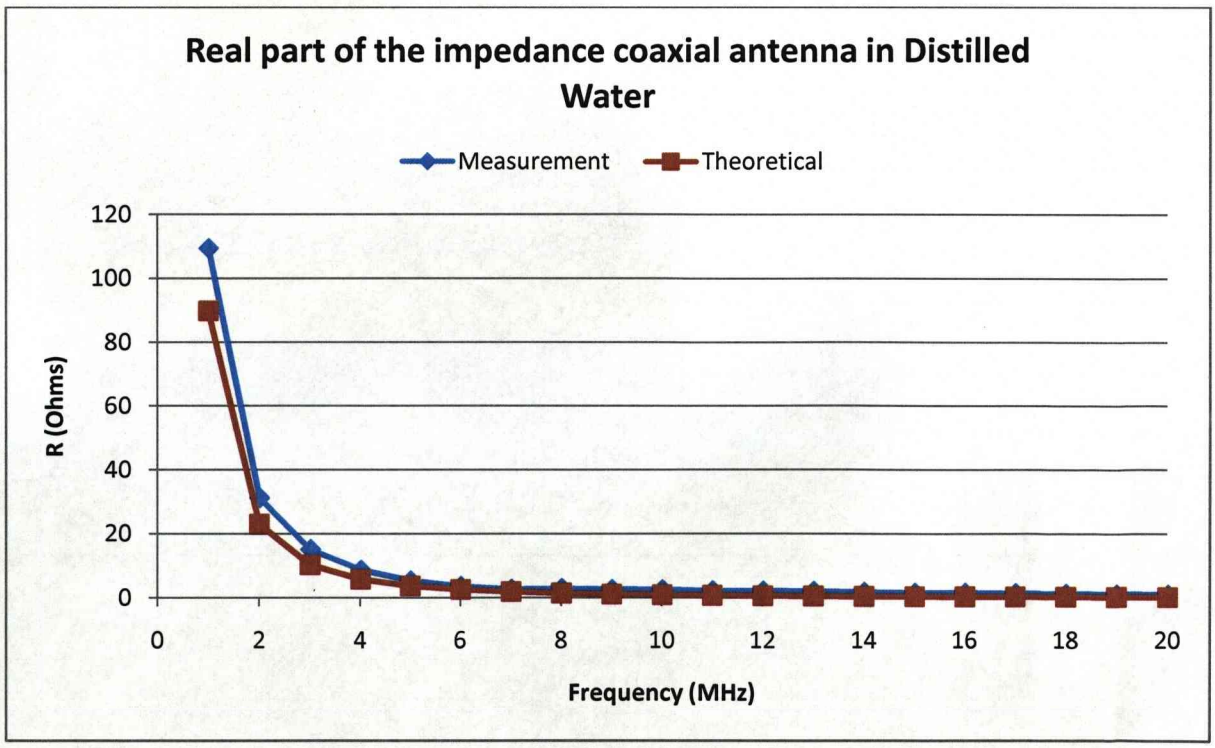

Figure 7.4 Real part of the Impedance in Distilled Water

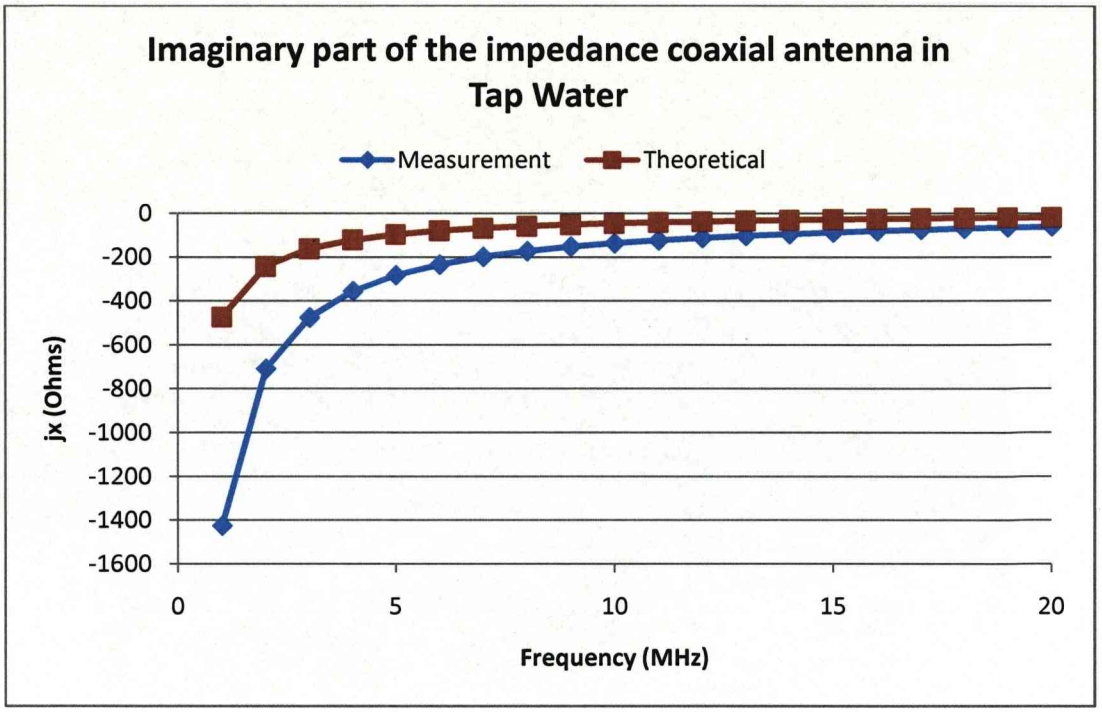

Figure 7.5 Imaginary part of the Impedance in Distilled Water

There are slight differences with the theoretical model possibly due to the actual conductivity of the water used in the impedance scan being slightly different to the value used in the model. The main difference with the two rod antenna is that the real part of the antenna impedance at high frequencies is very low and that will have an effect on the actual antenna strength. This will also lead to problems with the matching between the antenna and the transmitter because the resistance needs to be lifted by a high amount in order to reach the required 50Ω.

7.4.2 Acetone Trials

The next liquid in which the antenna was tested was acetone. The latter is the simplest ketone and is commonly used as a solvent.

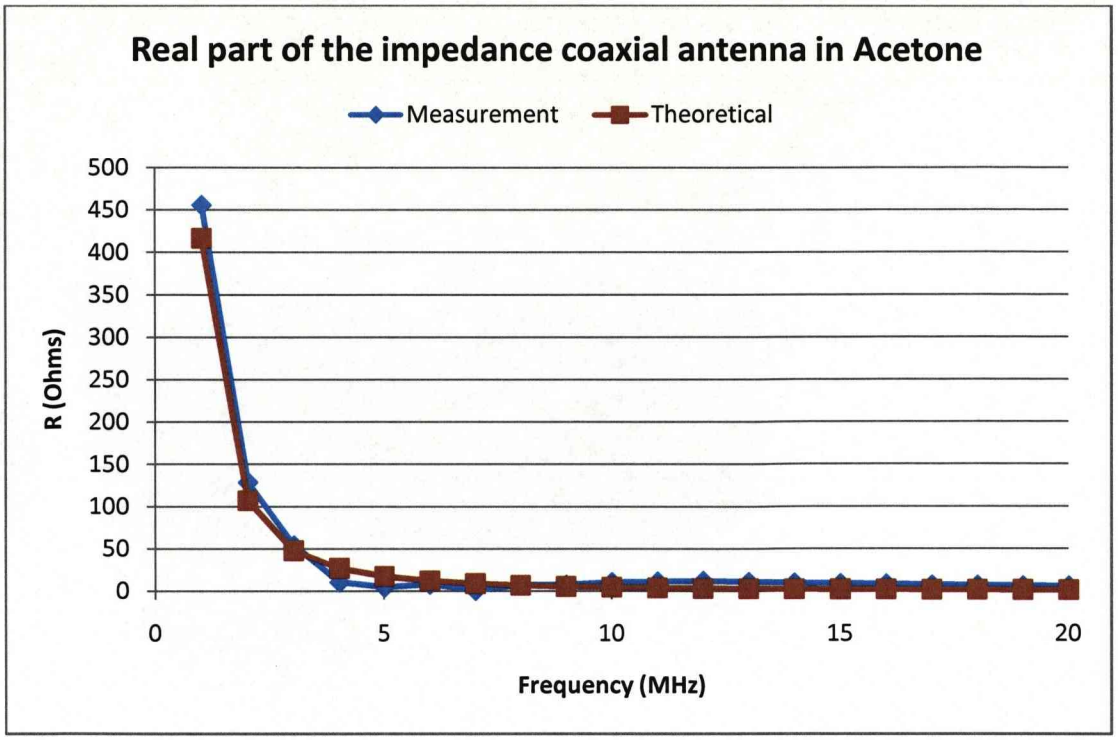

Figure 7.6 Real part of the Impedance in Acetone

The imaginary part of the impedance equals to

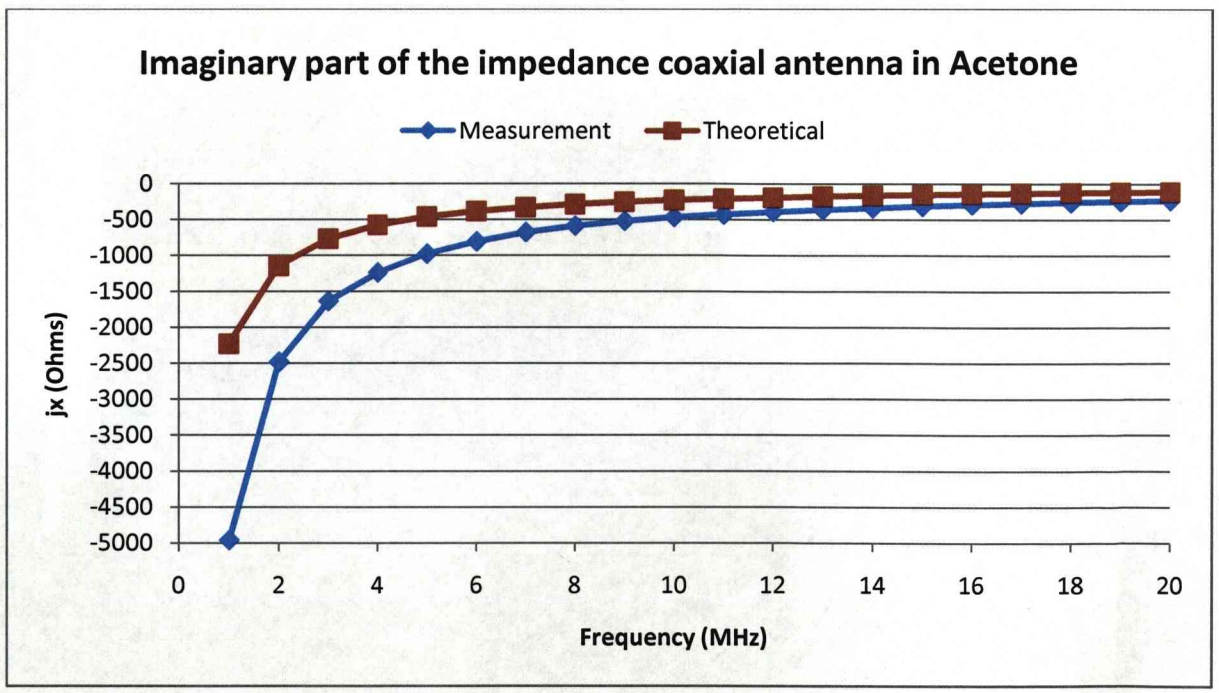

Figure 7.7 Imaginary part of the Impedance in Acetone

The main advantage of coupling the antenna with acetone is that it provides a higher resistance value than water. As expected though the results of acetone are rather similar to distilled water minimising the coupling losses associated with higher conductive materials.

7.4.3 Methanol Trials

Methanol is a light, volatile, colourless, flammable, poisonous liquid which has very low conductivity. The real part of the impedance is shown below

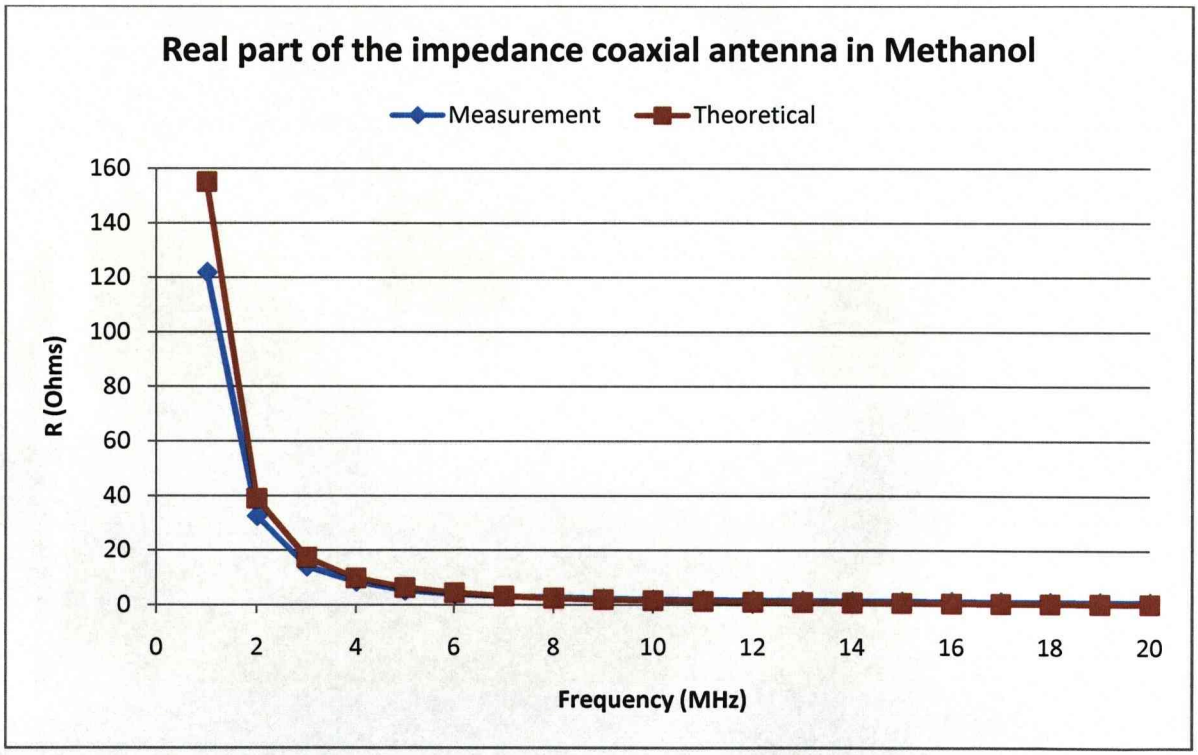

Figure 7.8 Real part of the Impedance in Methanol

The imaginary part of the impedance is shown in figure 7.9

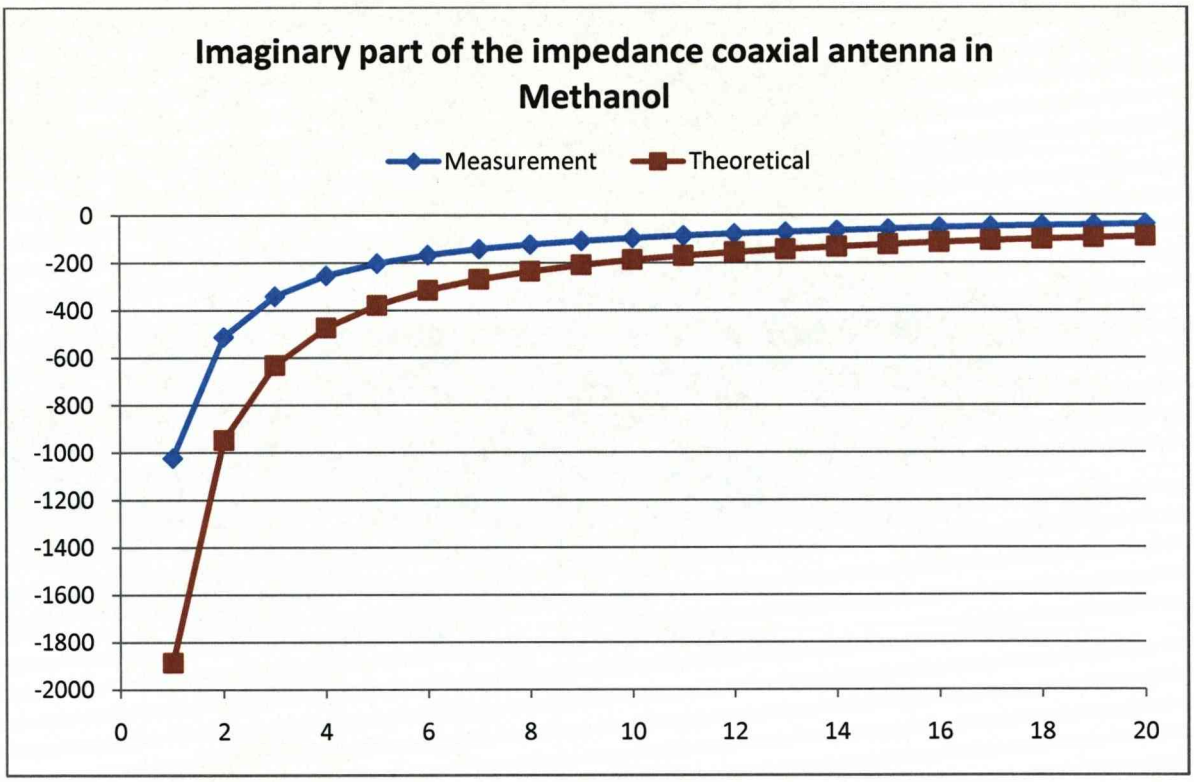

Figure 7.9 Imaginary part of the Impedance in Methanol

The theoretical model seems to match the impedance measured. Similarly to the other liquids the impedance of the antenna is relatively low.

7.5 Power Measurements

The next simulation is to observe the power transmitted through each liquid. This ideally should follow the pattern in chapter 5 and signal power should increase with frequency

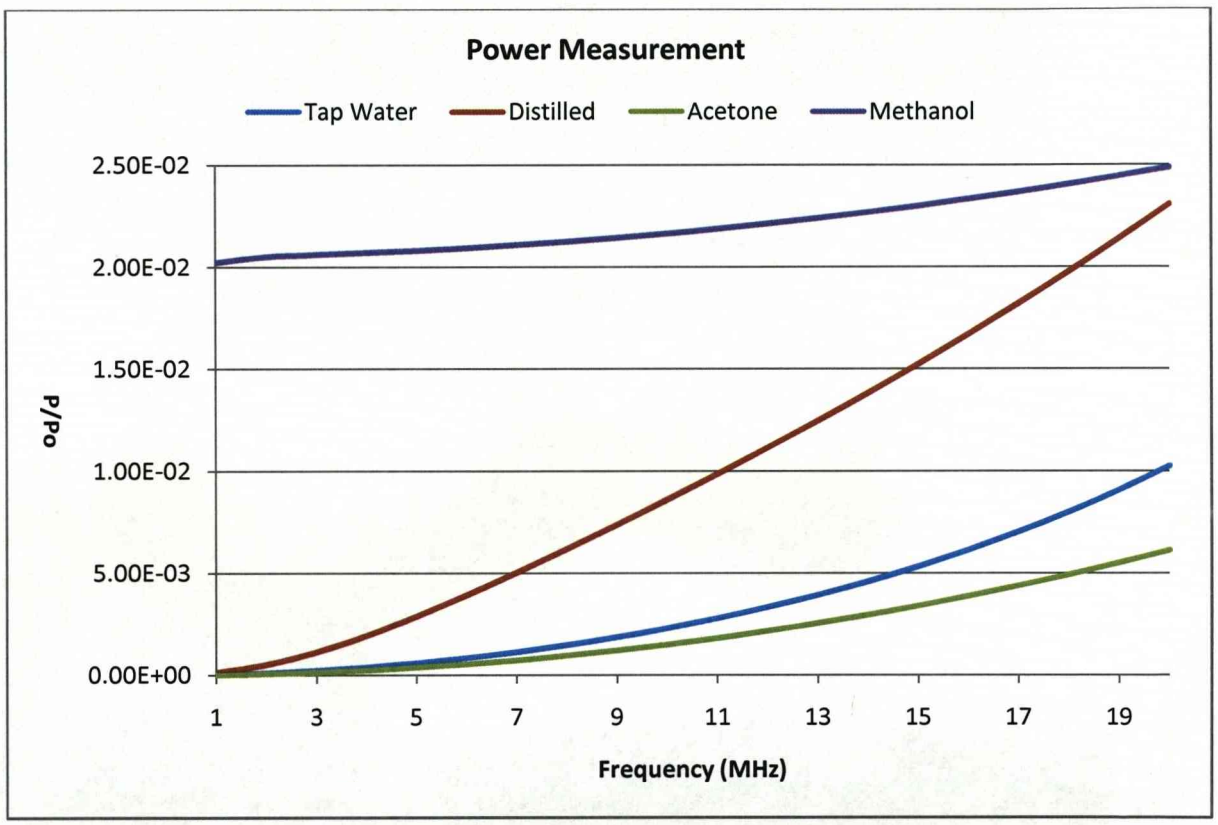

Figure 7.10 Power Transmitted in different media

As the figure shows at low frequencies Methanol provides a slightly higher power transfer between the antenna and the medium. At higher frequencies distilled water provides a similar and even better match than all the rest of the liquids. This is expected since the conductivity is inversely proportional to the power ratio and the lower conductivity of distilled water provides an improved power ratio compared to tap water.

7.6 Transmission Coefficients

The theoretical measurements of the attenuation and propagation coefficients are shown in fig 7.11

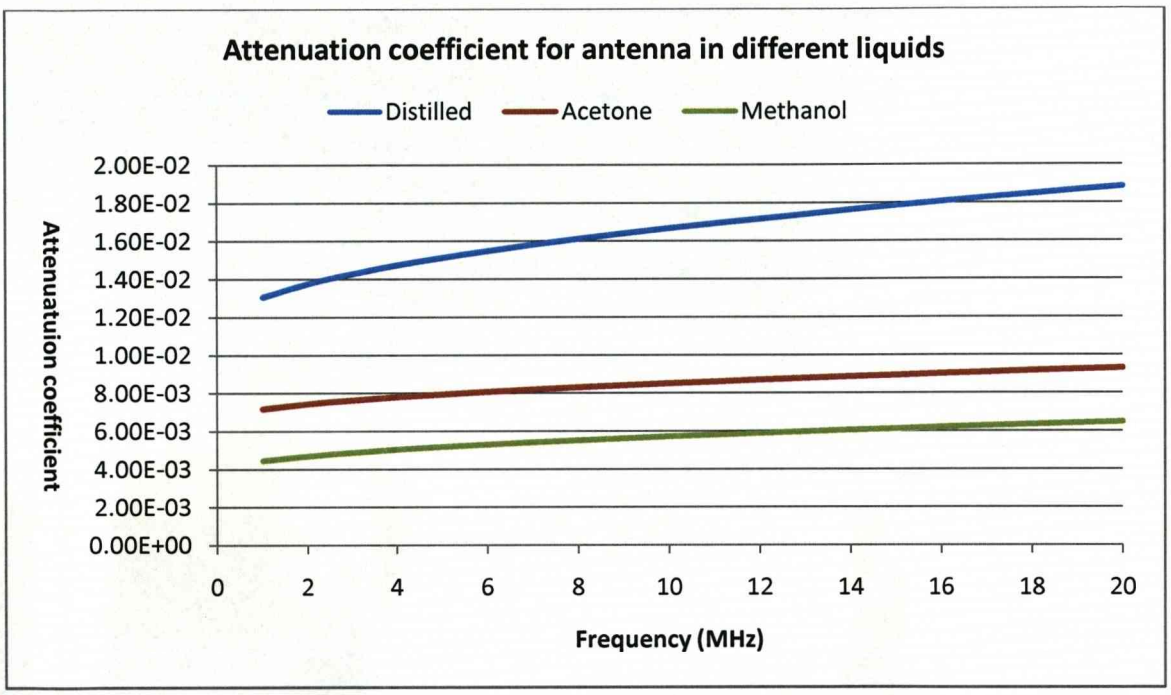

Figure 7.11 Attenuation coefficients in different mediums

The attenuation coefficients shows that the higher attenuation loss is for distilled water compared to the other materials but the differences are rather small and do not seem to increase significantly with higher frequencies. Tap water has a much higher attenuation loss that is expected due to the large difference in conductivity compared to the other materials.

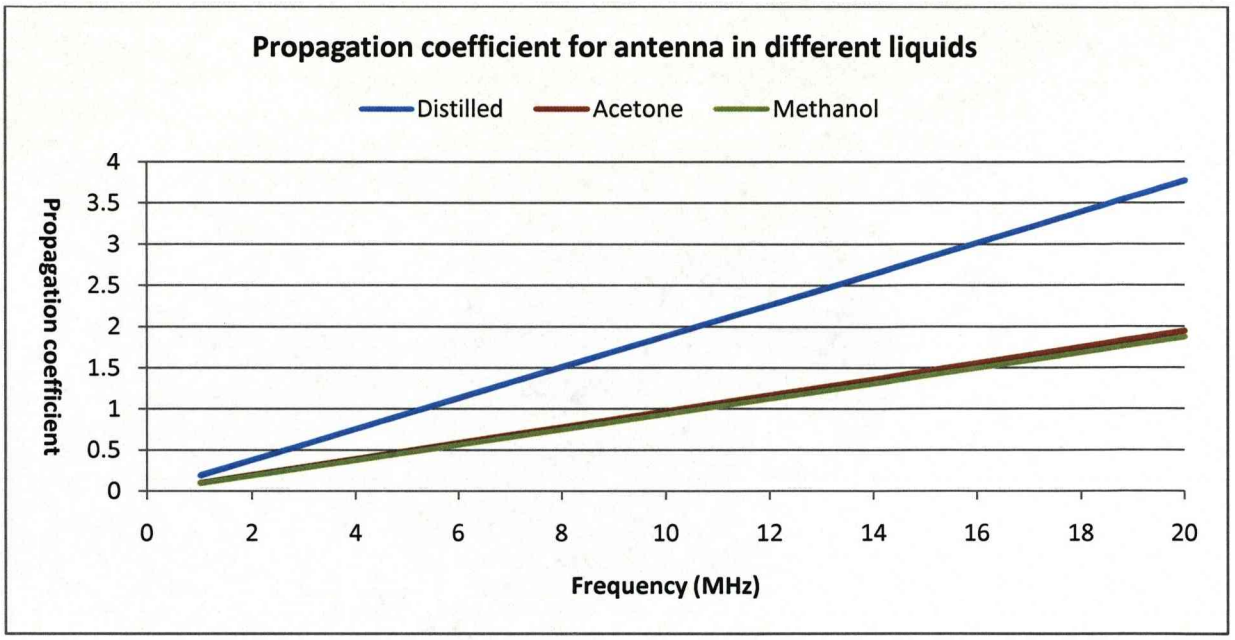

Figure 7.12 Propagation coefficient in different medium

As expected the propagation coefficient is higher for distilled water due to the slightly higher conductivity compared to the other two materials.

7.7 Antenna Overview

The main aim of the construction of this antenna is to observe whether the antenna model formulated in chapter 5 will work for a different type of antenna. The only change the model has as shown in appendix is the properties of the antenna like inductance and capacitance due to the differences in the antenna properties. The main advantage of this design is that it is much smaller than the two-rod antenna design and could be used for applications like diver to diver communications where the size of the water antenna is not suitable. The plastic coating of the tube also removes resonances from the impedance measurements.

This antenna as mentioned above has a limited size so there will be an effective decrease in the area for dipole radiation and so will lead to a decrease in the signal strength of the antenna. This lead to the requirement of placing the antenna inside a medium with minimal

conductivity and so the dielectric losses are small. This on the other hand led to a major disadvantage with the antenna performance since the impedance is very low compared to the one from the transmitter and so the losses are considerable higher unless a rather strong matching circuit is applied. The other major disadvantage with this design is that the liquids must be sealed properly because if they come into contact with air will lead to problems due to evaporation and will lead to problems with the results.

CHAPTER 8 Conclusions and Further Research

8.1 Conclusions

The main aim of this study is to improve the antenna design in order to provide a stronger signal for underwater transmission. The main aim was to improve the power flow between the antenna and the medium. In the case of seawater the strong electric field produced is greatly reduced by the resistance and so most of the input energy is removed from the dipoles. This lead to the antenna being placed inside of barrel with tap water that leads to improved energy transfer and increased signal strength.

The main theoretical approach to the propagation of EM waves in seawater was shown as consisting of the effect of water conductivity that in turn consists of the conductivity of seawater and the dielectric loss of the water molecules. As it was shown in chapter 5 if the antenna is placed directly into seawater there is a 71% loss. This loss is also enhanced due to the capacitance of seawater that has a fast time constant due to the high conductivity so that the voltage generated in seawater is greatly reduced and this minimises the energy available to generate the transmitted EM wave. The resistance of seawater consists of terms representing the conduction loss, the conductivity σ, and the dielectric dipole loss,$\omega\varepsilon''$, that provides the dipole radiation for the propagation trough the water.

The antenna is placed into tap and distilled water in order to remove the conductivity losses associated with salt water. The time constant for tap water is much larger than seawater and a larger amount of dipole radiation can be generated since the voltage reduces with a smaller time constant. This led to the design of the two rod antenna as well as the coaxial antenna. The large volume of the barrel offers an advantage as it allows an increased amount of dipole radiation to be generated since the signal strength increases with frequency even with relatively low power transmitters. On the other hand it is not suitable the size of the design is

not suitable for applications like diver to diver communications. So, in order to minimise the size of the antenna the surrounding liquid must have minimal conductivity so the losses are reduced in order to observe that the signal strength is similar to the barrel antenna.

The results have shown that by placing the antenna in tap water it is able to produce a dielectric dipole signal approximately 23dB stronger than in seawater. For distilled water with conductivity $\sigma = 2\times10^{-4}$S/m then the water dipole signal strength is approximately 40dB stronger than the signal generated in seawater. This frequency is suitable for sub-sea video signal propagation at 25 frames per second, according to the results obtained in this study. This also demonstrates a marked improvement on previous results. The barrel antenna is a good emitter of dipole radiation when distilled water is used. The output is strong at the desired frequency (32MHz) for underwater propagation because of the small amount of attenuation loss of -3.4dB per 100m, as shown in chapter 5. For optimum emitted power the dielectric dipole conductivity equals the water conductivity ($\sigma_w = \omega\varepsilon''$) at a frequency f_E given by

$$f_E = \sqrt{\frac{\omega\varepsilon''}{0.225}} = 10^3\ MHz$$

In the case of distilled water f_E=30MHz.

In the case of tap water f_E=300MHz.

In the case of salt water f_E=4.2GHz.

This clearly demonstrates that in order to obtain the required dipole radiation the use of extremely low conductivity materials is preferential as the amount of energy saved is enormous. Besides the optimal frequency for distilled water is much lower and thus leads to a decrease in the attenuation that the signal suffers when the signal frequency increases.

Another major advantage by applying this design is that the barrel offers some structural advantages. The barrel can act as a resonant cavity that in the correct mode can enhance

dipole orientation towards the direction of propagation. The mode can be adjusted for each frequency by altering the dimensions of the barrel to accommodate each frequency. Besides the barrel offers a focusing effect on the direction of propagation and also enhance the signal strength. There is also minimal loss at the tap to salt water interface.

The distance scans in the laboratory tank clearly demonstrated that by placing the antenna in tap water instead of directly placing it into salt water. In the latter case the signal disappeared before reaching the end of the tank. The signals generally followed the theoretical results. There was a decrease in the beginning due to the near field effect while in the far field there was minimal loss allowing the signal to propagate to large distances. Impedance matching between the antenna and the transmitter offered an improvement in the signal strength as expected. The only major limitation is that at high frequencies in the far field there were some reflections and so they restrict the use of even higher frequencies in the laboratory tank although in actual field measurements this might not be a disadvantage.

The theoretical model for the antenna was tested and compared for both antennas. In both cases it showed to be close to the actual measurements. Although the impedance graphs followed the general patterns there were some small differences in the actual values especially in the case of evaporating liquids since the slightest air interference can lead to changes in the dielectric properties. Despite this the model clearly demonstrated antenna behaviour in the water in relation to dielectric losses mentioned above.

The coaxial antenna was designed in order to limit the effective area of the water antenna. The only major problem with the practicality of this antenna is that at high frequencies it offers a very bad match between the antenna and the transmitter. The resistance value is below 1Ω and so will require extremely good matching in order to be used in distance scans.

8.2 Future Work

This section represents a number of guidelines for potentially improving and extending the work proposed in this thesis:

1) The water antenna design mention in chapter 5 could be modified in relation to its size and distance between the antenna rods in order to be modified for each specific frequency and liquid.
2) There could be more liquids instead of water placed inside the bucket at considerable cost like distilled water or acetone and distance scans can be formulated.
3) The bucket design could be modified and altered for each specific frequency in order to act as a resonant cavity in the required mode that is more beneficial for this application.
4) The model could be expanded to explain propagation through different media.
5) The receiver design could be modified even better with the addition of matching in order to improve signal pickup.
6) Noise cancellation technique could be applied to remove low noise signals.
7) The whole apparatus needs to be tested at remote locations and in real time environment.
8) The coaxial antenna could be matched properly to the antenna and distance scans could be performed.
9) The apparatus for permittivity measurement is quite similar to the coaxial antenna setup and this method could be used for obtaining permittivity values at the required frequency.
10) Instead of liquids, some solids instead could be used that have extremely low conductivity like perovskites could be used.
11) The design can be modified in order to include the lowest amount of liquid required possible.

REFERENCES

1. B.P. Lathi *Modern Digital and Analogue Communications Systems*, 3rd Ed. Oxford. University Press Inc, USA.

2. Ifiok Otung *Communication Engineering Principles*, Palgrave Macmillan 2001.

3. Coaxial Cable available at http://images.google.com/imgres?imgurl.

4. J. Dunlop and D.G. Smith, *Telecommunications Engineering*, 3rd Ed. CRC press 2004.

5. J.R. Smith, *Modern Communication Circuits* 2nd Ed. McGraw-Hill 1998.

6. Giles, J.W. Bankman, I.N. "*Underwater optical communications systems. Part 2: basic design considerations*" Military Communications Conference, 2005. MILCOM 2005. IEEE. Vol. 3. pp 1700- 1705, 2005.

7. D. F. Rivera and R. Bansal, "*Towed Antennas for US submarine communications: A Historical Perspective*," IEEE Antennas and Propagation Magazine, vol. 46, no. 1, pp. 23-36, February 2004.

8. R. E. Collin, "*Antennas and Radio Wave Propagation*" New York: McGraw Hill, 1985.

9. R.Bansal, "*ELF communications an obituary*" *IEEE* Antennas and Propagation Magazine, vol. 46, no. 6, pp. 124, December 2004.

10. Mark Rhodes, Underwater Electromagnetic Propagation: Re-evaluating Wireless Capabilities. available at http://www.wirelessfibre.co.uk/Content/press/articles/Hydro%20International%20Dec%2006.pdf

11. S.Boogie, "*Conduction and Magnetic Signalling in the Sea*", The radio and electrical engineer, vol. 42, pp 447-452, 1972.

12. M. Siegel and R.W.P King, "*Electromagnetic Propagation between antennas submerged in the ocean*", IEEE Transactions on Antennas and Propagation magazine, Vol. AP-21, No 4 July 1973.

13. Underwater Radio Communication by Lloyd Butler VK5BR (Originally published in Amateur Radio, April 1987) available at http://www.qsl.net/vk5br/UwaterComms.htm

14. A.I Al-Shammaa, A. Shaw and S. Saman *"Propagation of electromagnetic waves at MHz frequencies through seawater"*. IEEE Transactions on Antennas and Propagation magazine, vol 52, 11, 2843-2849, Nov. 2004.

15. Lucas J and Yip CK, "*A determination of the propagation of electromagnetic waves through seawater*". Underwater Technology,27(1), 1-9, April 2007.

16. Electromagnetic (EM) waves available at http://electron9.phys.utk.edu/optics421/modules/m1/emwaves.htm

17. EM spectrum available at http://kingfish.coastal.edu/marine/Animations/Images/Electromagnetic-Spectrum-2.png

18. R. Bartnikas and R. M. Eichhorn (eds.), "*Engineering Dielectrics,* Vol. II A, *Electrical Properties of Solid Insulating Materials: Molecular Structure and Electrical Behavior",* STP 783, Philadelphia: ASTM, 1983.

19. Polarization of molecules available at http://hyperphysics.phy-astr.gsu.edu/hbase/electric/dielec.html

20. Richard C. Dorf (ed), "*The Electrical Engineering Handbook*", Second Edition (Hardcover) by 2nd edition CRC press LLC 2000.

21. William H. Hayt and John A. Buck, "*Engineering Electromagnetics*". 7th edition. McGraw Hill 2005.

22. J. Thuéry, "*Microwaves: Industrial, Scientific and Medical Applications*" Boston, MA: Artech House, 1992.

23. P.Debye, "*Polar Molecules*", Dover 1929.

24. A.Chelkovsky, "*Dielectric Physics*", Amsterdam, Elsevier Scientific Publishing 1980.

25. R. Somaraju and J. Trumpf , "*Frequency, Temperature and Salinity Variation of the Permittivity of Seawater*" IEEE Transactions on Antennas and Propagation magazine, vol 54, 11, pp.3441-3448, Nov.2006.

26. K.S Cole and R.H.Cole, "*Dispersion and Absorption in Dielectrics*", J. Chem. Physics, vol , pp.341-351,Apr 1941.

27. L.Klein and T.Swift, "*An improved model for the dielectric constant of sea water at microwave frequencies*", IEEE Transactions on Antennas and Propagation magazine, vol 21, no 1, pp.104-111, Jan.1977

28. H. J. Liebe, G. A. Hufford, and T. Manabe, "*A model for. the complex permittivity of water at frequencies below 1thz*", Int. J. Infrared and Millimeter Waves, vol 12, no 7, pp659-675, 1991

29. T.Meissner and F.J.Wentz, "*The complex dielectric constant of pure and sea water from microwave satellite observations*", IEEE Transactions on Geoscience and Remote Sensing, vol 42, no 9, pp.1836-1849, Sept 2004.

30. J.D. Kraus and D.Fleisch, "*Electromagnetics*", 5th edition, McGraw-Hill Series in Electrical & Computer Engineering, 1999

31. J.Kraus and R.Marhefka, "*Antennas*",3rd edition, McGraw-Hill Series in Electrical & Computer Engineering, 2007.

32. C. A. Balanis, "*Antenna Theory Analysis and Design*", 2nd ed. John Wiley & Sons, 1996.

33. C.A. Balanis, "*Antenna theory: a review*", Proceedings of the IEEE, vol 80, no 1, pp.7-23, Sept 2004

34. M. Ghavami, "*Ultra Wideband Signals and Systems in Communication Engineering*", John Wiley and Sons 2004.

35. W. L.Stutzman and G.A.Thiele," *Antenna theory and design"*, Thiele 2nd edition New York J. Wiley, 1998.

36. F. A. Connor, "*Introductory Topics in Electronics and Telecommunications: Antennas v. 4"*, Hodder Arnold 1972.

37. David M. Pozar, "*Microwave Engineering"*, 2nd Ed, John Wiley & Sons 1997.

38. Reinhold Ludwig and Pavel Bretchko, "*RF Circuit Design Theory and Applications"*, Prentice Hall.

39. The ideal transformer for impedance matching available at http://en.wikipedia.org/wiki/Transformer

40. J.Rogers, "*Radio Frequency Integrated Circuit Design"*, Artech House 2003.

41. A Technical Tutorial on DDS available at http://www.analog.com/UploadedFiles/Tutorials/450968421DDS_Tutorial_rev12-2-99.pdf

42. Fundamentals of Quartz Oscillators available at http://home.agilent.com/agilent/redirector.jspx?action=ref&cname=AGILENT_EDITORIAL&ckey=1000000356%3

43. D. Scott and G. S. Smith, "*Measurement techniques for antennas in dissipative media*", IEEE Trans. Antennas Propagation, vol. 4, pp. 499-506, 1973.

44. C. K. Yip, A. Goudevenos and J.Lucas, "*Antenna Design for the propagation of EM waves in seawater*", Submitted in the journal of underwater technology.

45. S.Gerasimidis "*Optical Fibres EM waves Through and Wireless Systems for Underwater Communications*", The University of Liverpool, MSc Thesis September 2002.

46. S.Saher, "*EM waves propagation in Seawater*", M.Phil Thesis, The University of Liverpool, May 2003.

47. C. K. Yip, *"Underwater Communications using EM waves"*, Ph.D thesis, The University of Liverpool, May 2007.

48. Leserf, J. "*Millimetre-wave Optics, Devices and Systems*", IOP Publishing Ltd, 1990.

49. Dielectric Constant of Materials available at: http://www.clippercontrols.com/info/dielectric_constants.html.

50. 3D Millennium, index of refraction values available at: http://www.m3corp.com/a/tutorials/refraction.htm.

APPENDIX

This part of the thesis gives the MATLAB codes for impedance calculation

1.Two rod antenna in water

```
%11/10/2006 This Program is to analyse a dielectric antenna

%Define the variables

e_r=81; %water permittivity
e_o=8.8542*10^-12; %permittivity of free space
m_o=1.2566*10^-6;%permeability of free space
d=0.07; %distance between the rods
l=0.25; %length of the rods
a=1*10^-3; %rod diameter
A=d*l; %area of radiation

%Perform the calculations

s=0.02;  %the conductivity of the medium
f=1:1:20;  %range of frequencies and step between them
w=2*f.*pi*10^6;  %calculate the angular frequency
e_2=(24.92*10^-9*(f.^2))./w;  %calculate the complex pemittivity
L=m_o*log(d/a)*l/pi;  %calculate the inductance of the rods
c=pi*e_o*e_r*l/log(d/a); %calculate the capacitance of the rods
s_2=s+w.*e_2;  %calculate the complex conductivity
R=log(d/a)./(s_2*pi*l);  %calculate the resistance of the rod
G=1./R;  %calculate the transconductance
r=0.00829*sqrt(f)*l/a;  %calculate the resistance due to radiation
Z_l=j*w*L;  %calculate the inductive impedance
Z_c=1./(j*w*c);  %calculate the capacitive inductance
g=sqrt((r+j*w*L).*(G+j*w*c)); %calculate the propagation coefficient
Z_o=sqrt((r+j*w*L)./(G+j*w*c));%calculate the characteristic impedance
Z=Z_o.*coth(g); %calculate the impedance (the circuit is assumed o/c)
P_I=100*G.*((Z-Z_l/3-r/3)./(50+Z)).^2.*((w.*e_2)./(s+w.*e_2)); %Power ratio
plot(f,real(Z),'b'); %plot the real part of P
hold on;
plot(f,imag(Z),'r--');
```

2. Antenna Electric field

```
%Calculate the electric field strength E
e_r=81; %water permittivity
e_o=8.8542*10^-12; %permittivity of free space
l=0.25; %length of the rods
q=10^-12; %Charge value
d=0.07; %distance between the rods
clf;
%Assuming the antenna is placed exactly at the center of the barrel

z=-0.25:0.01:0.25;%distance in the z axis
r=-0.5:0.02:0.5; %radius of radiation
x=-0.25:0.01:0.25; %distance in the x-axis

%Geometry modifications
z_1=z-d/2;
z_2=z+d/2;
y=0;
r_1=sqrt(x.^2+z_1.^2);
r_2=sqrt(x.^2+z_2.^2);
y_1=l/2-y;
y_2=-l/2-y;
R_1=sqrt(r_1.^2+y_1.^2);
R_2=sqrt(r_2.^2+y_2.^2);
t_1=asin(y_1./R_1);
t_2=asin(y_2./R_2);

%Electric field calculations for the fields in the x and z axes
E_x1=q/(4*pi*e_o*e_r).*((sin(t_2)+sin(t_1))./(2*R_1)).*x./((r_1.^2).*r_1);
E_x2=q/(4*pi*e_o*e_r).*((sin(t_2)+sin(t_1))./(2*R_2)).*x./((r_2.^2).*r_2);
E_z1=q/(4*pi*e_o*e_r).*((sin(t_2)+sin(t_1))./(2*R_1)).*z_1./((r_1.^2).*r_1)
;
E_z2=q/(4*pi*e_o*e_r).*((sin(t_2)+sin(t_1))./(2*R_2)).*z_2./((r_2.^2).*r_2)
;
E_x=E_x1-E_x2; %Total electric field in the x direction
E_z=E_z1-E_z2; %Total electric field in the z direction

E=sqrt(E_x.^2+E_z.^2); %Total Electric field

plot(x,E)
%[X,Y] = meshgrid(E_x,E_z);
%n=sqrt(x.^2+z.^2);
%meshc(E,X,Y);

%xlabel('Distance in the x axis (m)')
ylabel('Electric field strength (V/m)')
xlabel('Distance in the z axis ')
Title('Electric field strength 2 rod antenna (y=0.6,x=0) 1/11/06');
```

3.Coaxial Antenna in Water

```
%8-10-07 Coaxial antenna in water

e_r=81;
e_o=8.8542*10^-12; %permittivity of free space
m_o=1.2566*10^-6;%permeability of free space
b=0.016; %inner radius
a=0.001; %outer radius

l=0.16; %length of the antenna

%Perform the calculations

s=0.0002; %the conductivity of the medium
f=1:1:50; %range of frequencies and step between them
w=2*f.*pi*10^6; %calculate the angular frequency
e_2=(225*10^-9*(f.^2))./w;
L=m_o*log(b/a)/(2*pi); %calculate the inductance of the rods
c=2*pi*e_o*e_r/log(b/a); %calculate the capacitance of the rods
s_2=s+w.*e_2; %calculate the complex conductivity
G=c.*w.*(s_2)/(w.*e_r*e_o); %calculate the transconductance
R=1./G;
r=sqrt(w.*m_o*1.682*10^-8)*(1/a+1/b)/(2*pi); %calculate skin effect
Z_l=j*w*L; %calculate the inductive impedance
Z_c=1./(j*w*c); %calculate the capacitive inductance
g=sqrt((r+j*w*L).*(G+j*w*c)); %calculate the propagation coefficient
Z_o=sqrt((r+j*w*L)./(G+j*w*c));%calculate the characteristic impedance
Z=Z_o.*coth(g*l); %calculate the impedance (the circuit is assumed o/c)
P_I=100*G.*((Z-Z_l/3-r/3)./(50+Z)).^2.*((w.*e_2)./(s+w.*e_2)); %Power ratio
P=abs(P_I);
l_1=2*pi./imag(g);
y=w.*e_2;
%R_1=80*pi^2*(l./l_1).^2.*sin(pi*d./l_1);

plot(f,real(Z),'b'); %plot the real part of P
hold on;
plot(f,imag(Z),'r--');
```

4. Coaxial Antenna in Acetone

```
%09-11-07 Coaxial antenna in acetone

e_r=21.5;
e_o=8.8542*10^-12; %permittivity of free space
m_o=1.2566*10^-6;%permeability of free space
b=0.016; %inner radius
a=0.001; %outer radius
t=7.6*10^-12; %time constant
l=0.21; %length of the antenna

%Perform the calculations

s=10^-4; %the conductivity of the medium
f=1:1:50; %range of frequencies and step between them
w=2*f.*pi*10^6; %calculate the angular frequency
e_2=15.25*w.*t*e_o;
L=m_o*log(b/a)/(2*pi); %calculate the inductance of the rods
c=2*pi*e_o*e_r/log(b/a); %calculate the capacitance of the rods
s_2=s+w.*e_2; %calculate the complex conductivity
G=c.*w.*(s_2)/(w.*e_r*e_o); %calculate the transconductance
y=w.*e_2;
R=1./G;
r=sqrt(w.*m_o*1.682*10^-8*0.5)*(1/a+1/b)/(2*pi); %calculate skin effect
Z_l=j*w*L; %calculate the inductive impedance
Z_c=1./(j*w*c); %calculate the capacitive inductance
g=sqrt((r+j*w*L).*(G+j*w*c)); %calculate the propagation coefficient
Z_o=sqrt((r+j*w*L)./(G+j*w*c));%calculate the characteristic impedance
Z=Z_o.*coth(g*l); %calculate the impedance (the circuit is assumed o/c)
P_I=100*G.*((Z-Z_l/3-r/3)./(50+Z)).^2.*((w.*e_2)./(s+w.*e_2)); %Power ratio
P=abs(P_I);
l_1=2*pi./imag(g);
%R_1=80*pi^2*(l./l_1).^2.*sin(pi*d./l_1);

plot(f,real(Z),'b'); %plot the real part of P
hold on;
plot(f,imag(Z),'r--');
```